Heterobimetallic Lewis Acid Catalyst Development for Polyesterification and Depolymerization

by
Jacob H. Jansen

A dissertation submitted in partial fulfillment of
the requirements for the degree of

Doctor of Philosophy
(Chemistry)

at the
UNIVERSITY OF WISCONSIN-MADISON
2024

Date of final oral examination: 8/12/2024

The dissertation is approved by the following members of the Final Oral Committee:

Ive Hermans, Professor, Chemistry & Chemical and Biological Engineering
Shannon Stahl, Professor, Chemistry
John F. Berry, Professor, Chemistry
Eszter Boros, Associate Professor, Chemistry

Abstract

Polyesters made through the use of a homogeneous catalyst are integral to many areas of life and the chemical or materials industries. Titanate catalysts such as titanium tetrabutoxide (TBT) have long been known to be effective polyesterification catalysts. However, their use on an industrial scale has been hindered by their sensitivity to moisture. Previously, this challenge has been addressed by using mixtures of titanate catalysts with tin-based catalysts such as stannous octoate (SnOct), showing a synergistic effect for hydrolytic stability. The structure of this mixed metal catalyst has been defined for the first time since its discovery as a heterobimetallic dimer using a suite of nuclear magnetic spectroscopy (NMR) techniques and mass spectrometry. Unfortunately, due to toxicity concerns around tin catalysts, this efficient catalyst mixture is not a long-term viable solution. To address this issue, a mixed metal catalyst of TBT and bismuth neodecanoate (BiNeo) is first reported on and possesses little toxicity concerns while have as good of or better stability or reactivity as mixtures of titanium and tin. A key set of discoveries allowed for the understanding that mixed metal catalysts possess greater stability but not necessarily greater activity.

The mixed metal catalysts were studied for the strength of their Lewis acidity and for any interactions arising from proximal metal centers. A series of different measurements of the effective Lewis acidity gave varied results but agreed with respect to the metals being generally isolated active sites for reactant binding.

Finally, the novel mixed metal Lewis acid catalysts were tested in the glycolysis of polyethylene terephthalate waste plastic. The mixed metal catalysts outperformed the unmixed precursors but did not outperform an industrial catalyst under most reaction conditions.

Acknowledgements

I would like to begin by thanking Professor Ive Hermans for being my advisor for the last six years. Thank you for taking a chance on me when I knew so little about heterogeneous catalysts and finding ways to get back to working with homogeneous catalysts. It's been a wild and fun ride between all of the building shutdowns, floods, possibilities of moving continents, parental leaves, deadlines, struggles, but also discoveries, successes, and just joking about the news. Thank you for pushing me through the highs and lows but also trusting me with making my own decisions. I know I am a better scientist because of your influence. Thank you to my committee members, Professors Shannon Stahl, John Berry, and Associate Professor Eszter Boros. Your guidance through the stages of reaching this point has been very much appreciated. I would also like to thank Dr. Adam Powell, who I have come to think of as nearly a second advisor through our time collaborating and talking science and careers. You have demonstrated what it means to have high standards and resilience in the face of frustration. In addition to Adam, Dr. Will Keown joined the collaborative fun and immediately helped us and built me up. I would also like to acknowledge my funding sources: PPG Industries, and the University of Wisconsin-Madison

It has been a huge privilege to be in a the scientific family of the Hermans group. The people I got to work with on a daily basis had a huge impact on my ability to keep going. I could write many pages of thank yous to each group member that has been around in the last 6 years, but I want to highlight a few of the most impactful group members for me. Dr. Sarah Specht, it's really hard to put into words the appreciation I have for all the investment you have put into me professionally and personally. You made me feel welcome to the Hermans group when I felt lost. I feel lucky to have a super star friend that cares so much. Dr. Son Dong, what a fun time we got to share. I'd drive across the country with you anytime. Dr. Abdullah Al Abdullghani, I so much enjoyed sitting across from you in the office the last couple of years. Thank you for believing that people can be kinder. To the former members, Dr. Natalie Altvater, Dr. Theo Agbi, Dr. Melissa Cendejas, Dr. Shao-Chun Wang, Dr. Will McDermott, Dr. Juan Venegas, (Master) Ryan Hagmann, (Master) Connor Huntwork, Dr. Lesli Mark, Dr. TK Ryu, Dr. Victor Lo, Dr. Zoey Zhang, you have made me a catalysis scientist. I would not be where I am today without you all's help. To my current colleagues - Dr. Matias Alvear, Unni Kurumbail, Edgard Lebron, Faysal Ibrahim, Zahra Alikhani, Sudipta Ganguly, Jadiel Lopez, Kitty Ma, Collin Oi, Yamil Adorno, Sebastián Rivera, Harsh Darji, Fillipp Salvador – Thank you for continuing to make the group a place to continue enjoy coming to and pushing ourselves towards higher heights.

I have also had the opportunity to have some excellent mentees that have helped me grow, not only scientifically, but as a person. Thank you to Jalianet Román-Matías, Alex Marrione, Destiny Mathews, Oscar Li, Arianna Alirez, and Yamil. Your scientific contributions were helpful but your presence and enthusiasm were real drivers for my growth.

My previous mentors got me into chemistry and to Wisconsin and continue to be lights that I look for in times of uncertainty. Professor Jeff B. Johnson, you were an excellent mentor to me in my introduction to catalysis research and inspired my current self. Thank you also to my high school chemistry teacher, Mrs. Beguhn for making chemistry fun and interesting to start me down this whole path.

Finally, I need to thank my family and friends who have given so much support in the last 6 years but also throughout my whole life. Thank you to the volleyball crew, and my church group, they kept my head on straight. To my parents, your unhesitating belief and love has been a rock for me. To Anna, thank you for being such a force for good in my life. So much looking forward to where we head next. To Elizabeth, you have only been with us a year at this point, but the joy you bring me every day is unspeakable. To my other friends throughout graduate school, you have been such inspirations in your successes and humanity, thank you.

From the depths of myself, thank you to all those who have helped me accomplish this!

Table of Contents

List of Figures

List of Tables

List of Schemes

Chapter 1. Introduction (for my family)

The work presented here investigates a class of catalysts made up of two different metal complexes where the reaction being studied is esterification in general which gets applied either to the synthesis of polyesters or the depolymerization of polyesters. I used a series of complex spectroscopic and spectrometric to determine the molecular structure of the catalysts, studied how they work together to enhance reactivity, then applied the catalyst to address a problem not originally part of the goal in developing the catalyst. One of the main goals of this work was to improve the sustainability of the processes that might employ this type of catalyst both in terms of the toxicity of the produced polymer and in terms of being able to efficiently recycle the polymer. There are a lot of questions that somebody without a background in this area would have to ask to understand what all that means. The purpose of this introduction is to answer some of those questions and give a brief overview of the contents of this thesis.

1.1 Polyesters

A polyester is a polymer meaning it is a substance or material made up of repeating units of smaller molecules called monomers. Polyesters are a specific class of polymer where the monomers are connected using esters (see Figure 1.1). The specific structure of the monomer can be changed to change the properties of the polyester to be useful for different purposes. Through their varied usefulness polyesters have become an integral part of everyday life and in ways that we do not commonly recognize.[1] For example, Chapter 5 will discuss polyethylene terephthalate (A.K.A. PET), the most used polyester. It is used to make fibers that are the “polyester” you see on the tag of your clothing; it is what plastic water bottles are made from and you can recognize them as the plastic with #1 recycling code. Changing the molecular structure of the monomers to be bulkier around the ester linkers makes the polymer more robust to

degrading and so when a coatings company like PPG Industries paints a polyester onto a material, they modify the molecular structure to hold up to weathering, for example.[2]

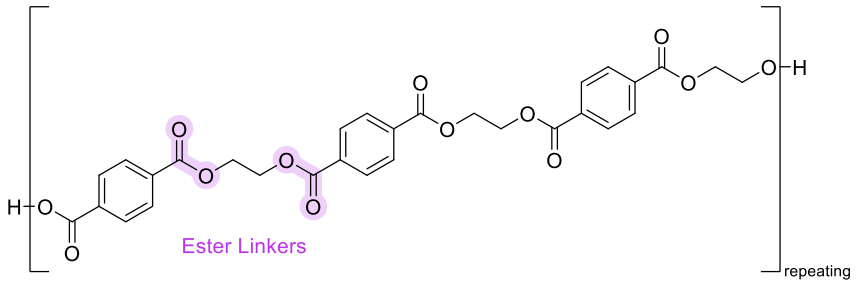

Figure 1.1. Example segment of polyethylene terephthalate polymer. Notice the repeating units and specific type of linker.

1.2 Catalysts

The reactions to make polyesters (polyesterification) are run at relatively high temperatures (>180 °C) but would struggle to reach high conversion to the polymer without the addition of a catalyst. A catalyst is simply a material that gets added to the reaction to speed it up without being consumed itself and ideally it is unchanged throughout the reaction.[3] As you will see in this thesis, that ideal is not always met, and the catalyst can degrade under certain conditions. The way that a catalyst speeds up the rate of a reaction is through lowering the amount of energy that it takes for the chemistry to happen. In the case of this work, the catalysts are made up of a mixture of two different metal complexes. The complexes are liquids and dissolve in the reaction solutions, so are termed homogeneous catalysts as they are the same phase (liquid) as the reactants.

1.2.1 Metal complexes

Metal complexes are also not thought about by many people in day-to-day life but have a rich history of being able to catalyze the chemical reactions that build the world around us.[4] Most people think of metal as that stuff that their cars are made of or that the kitchen sink is made of. However, most metals can, for instance, be dissolved by acids where the solid metal reacts down to even single atoms that are

often positively charged ions and the metal ion or atom gets decorated with water or a counterion, and the decorations can be switched out using different reactions. This grouping of metal and decoration is called a metal complex or coordination complex.[3,4] The decorations are called ligands and can have a huge influence on the chemistry of the metal complex depending on how big they are (sterics), if they can bind to the metal just once or multiple times (denticity), if they can bind to multiple metals at the same time (hapticity), and how strongly they bind to name a few of the important factors.[3] There are even a few ways a ligand can interact with the metal depending on how the quantum mechanical wave functions interact geometrically in space. Both the metal and ligand have their chemistry effected by their interaction with each other. These interactions are important for the catalysis, and there is a whole chapter (chapter 4) of this thesis dedicated to measuring and understanding those (Lewis acidic) interactions. Once one of these metal complexes takes on a reactive molecule as a ligand, that reactive molecule can be made more reactive due to that interaction. In the case of the polyesterification reaction, one of the oxygens in the ester linking group becomes ligated to a metal, making the adjacent carbon more reactive toward the alcohol reactant, and lowering the energy required for the reactants to react and, on the larger scale, for the polymer to be made.[1] Sometimes there are molecules that can become ligands on a metal that inhibit how well they can be catalysts. This can be either by blocking it from reacting with the molecules you want it to (e.g., binding to all the available spots and too strongly for anything else to find a spot) or by causing the metals to clump up (agglomerate) where the metals on the inside of the agglomerate do not have the opportunity to react with anything among other deactivation pathways.[3,5] The metal complexes studied in this thesis tend to get deactivated in the second of these ways by reacting with water and forming agglomerates. However, we explore a way to prevent the catalysts from reacting too much with water while still being able to react with what we want them to, namely the ester linkers. The main method used within this thesis is to mix two different metal complexes with different metals and ligands, which gives interesting properties elaborated upon within the following chapters.

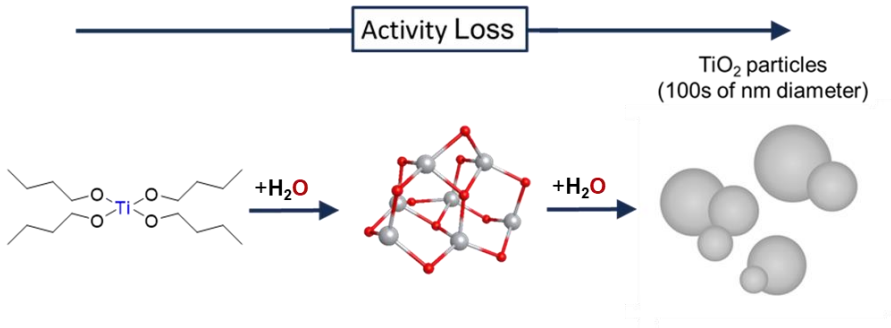

Figure 1.2. Example scheme of titanium complex agglomeration with reaction with water. Silver spheres represent titanium and red sphere represent oxygen in middle structure.

1.3 Nuclear Magnetic Spectroscopy

It is important for our ability to improve a catalyst to know what it looks like, but how can we look at things so small as single metals? We use the spectrum of light/electromagnetic waves and how they interact with the material of interest. The large set of techniques that do this are collectively called spectroscopy. The type of spectroscopy that was most used and was most useful within this thesis was nuclear magnetic spectroscopy (or NMR for short).[6] As the name suggests, NMR spectroscopy looks at how the nuclei of atoms behave in a magnetic field. In fact, it works on the same principles as an MRI machine. To collect NMR data, a sample of dissolved catalyst or material is put within a powerful magnet and a small majority of the nuclei become aligned with the magnetic field over a small minority that become anti-aligned. The energy between the aligned and anti-aligned state can be measured. Then a radio frequency is pulsed at the sample which knocks them off the axis of the magnetic field where they begin to spin about the axis in a manner like a gyroscope spinning about an axis. The frequency the nuclei spin at is picked up by a radio receiver and all the different frequencies are deconvoluted and plotted on a spectrum plot. What becomes fun is that within the strong magnetic field, each effected nucleus generates a small magnetic field that interacts with nearby nuclei and the patterns of those interactions can be identified and interpreted to tell what type and how many neighboring nuclei are present. NMR works great for many types of atoms like hydrogen, carbon, and tin atoms, but not as well for others such

as titanium and bismuth. Combining the analysis of the different types of atoms/nuclei that NMR gives high quality data for can allow for the stitching together of whole molecular structures. There are many additional specialized methods that look specifically at different aspects of the interactions between nuclei such as what hydrogen atoms are near carbon or tin atoms or even just other nearby hydrogen atoms. We take advantage of a couple of specialized NMR techniques throughout our study. One that shows how quickly the dissolved molecules diffuse through the solvent and gives approximate molecular weights (diffusion-ordered spectroscopy, A.K.A. DOSY), another that show how quickly parts of a molecule move from one geometric location to another (exchange spectroscopy, A.K.A. EXSY).[6,7] All of these come together to allow the determination of the molecular structures and reactivity of the metal complexes that are generated in this thesis.

1.4 Scope of this Thesis

Chapter 2 is the first foray into homogeneous polyester catalysts for me and for the Hermans group in general. This was also the start of a highly enjoyable, and productive collaborative effort with scientists at PPG Industries. It is a story of molecular detective work or reverse engineering of an old technology patented by BASF in 1977 on mixtures of specific metal compounds, namely titanium alkoxides and tin carboxylates, that are better at speeding up a polyester forming reaction than either of those compounds when they are not mixed. We identify that the structure of the mixture gives small clusters of one titanium with one tin that have greater stability to water than the unmixed compounds. During this study we developed a suite of characterization techniques including 1D and 2D NMR, diffusion measurements of the catalyst in solution using DOSY NMR, and non-fragmenting mass spectrometry that gave the structural insights needed to find the compound's structure.[8]

In Chapter 3, a new mixed metal polyester catalyst is described. We use what we learned in our studies on mixtures of titanium and tin compounds and the stability of the small clusters formed to find a mixture that does not contain tin, as it is known to be toxic to humans and animals. After a bounded search

of alternative metals, we discovered that mixing titanium alkoxides with bismuth carboxylates leads to a similar increase in the ability to catalyze polyester formation as titanium/tin mixes and even gave better stability to water. We were able to decouple the rate of reaction that the catalyst can supply with its stability to water to show that catalyst stability is the most important improvement for these types of mixed metal catalysts. In addition, we confirmed that, like in Chapter 2, small clusters are made in these mixtures.[2]

Chapter 4 presents a series of techniques that were used to find the underlying characteristics of the mixed metal catalysts discussed in Chapters 2 and 3, namely how Lewis acidity they were. These techniques used probe molecules that change measurably when they interact with Lewis acids and ideally the magnitude of that change modulates with the strength of the acid. We find that not all published techniques will give great results for every catalyst but are able to pull out interesting takeaways about how the metals interact, or rather, don't interact with each other.

Finally, Chapter 5 takes the mixed metal catalysts from Chapters 2 and 3 and redirects their use to a pressing sustainability issue in recent years, recycling of polyester plastics. In this chapter, the techniques necessary to analyze the breakdown of plastic over time in a reactor are developed and our mixed metal catalysts are compared to industrially known catalysts.

1.5 References

(1) Otera, J.; Nishikido, J. *Esterification: Methods, Reactions, and Applications, Second Addition*, 2nd ed.; Wiley-VCH Verlag, 2009. https://doi.org/10.1002/9783527627622.

(2) Jansen, J. H.; Mathews, D.; Marrione, A.; Román-Matías, J.; Al Abdulghani, A.; Powell, A. B.; Gerislioglu, S.; Keown, W.; Specht, S. E.; Hermans, I. Sustainable and Stable Esterification Catalysts Made from Titanium-Bismuth Clusters. *ACS Sustain Chem Eng* **2024**, No. 12, 9612–9619. https://doi.org/10.1021/acssuschemeng.4c00561.

(3) Hartwig, J. F. *Organotransition Metal Chemistry: From Bonding to Catalysis*; University Science Books, 2010.

(4) Crabtree, R. H. *The Organometallic Chemistry of the Transition Metals*, 6th ed.; John Wiley & Sons, Inc: Hoboken, NJ, 2014.

(5) Soloviev, A.; Tufeu, R.; Sanchez, C.; Kanaev, A. V. Nucleation Stage in the Ti(OPri)4 Sol-Gel Process. *Journal of Physical Chemistry B* **2001**, *105* (19), 4175–4180. https://doi.org/10.1021/jp0040190.

(6) Claridge, T. D. W. *High-Resolution NMR Techniques in Organic Chemistry*, 3rd ed.; Elsevier Ltd, 2016. https://doi.org/https://doi.org/10.1016/C2015-0-04654-8.

(7) Pagès, G.; Gilard, V.; Martino, R.; Malet-Martino, M. Pulsed-Field Gradient Nuclear Magnetic Resonance Measurements (PFG NMR) for Diffusion Ordered Spectroscopy (DOSY) Mapping. *Analyst* **2017**, *142* (20), 3771–3796. https://doi.org/10.1039/c7an01031a.

(8) Jansen, J. H.; Powell, A. B.; Specht, S. E.; Gerislioglu, S.; Hermans, I. Understanding the Structure and Reactivity of Mixed Titanium(IV) Alkoxide and Tin(II)/(IV) Carboxylates as Esterification Catalysts. *ACS Sustain Chem Eng* **2022**, *10* (7), 2484–2493. https://doi.org/https://doi.org/10.1021/acssuschemeng.1c07633.

Chapter 2. Tin/Titanium Mixed Metal Lewis Acids a Polyester Catalysts

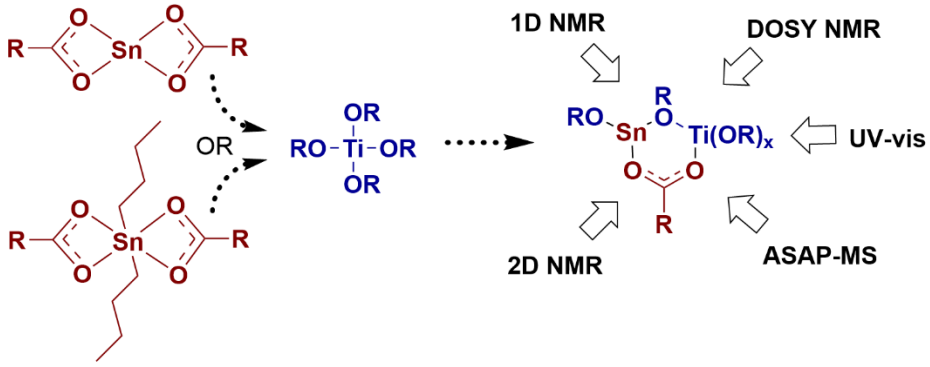

In this chapter, a set of compounds made by mixing titanium(IV) alkoxides with tin(II) dicarboxylates or tin(IV) dialkyl dicarboxylates and are studied as esterification catalysts. These mixed Ti/Sn catalysts outperform titanium alkoxides or tin complexes alone as polyesterification catalysts and have been in industrial use for polyesterification reactions since the 1970s. However, the tin complexes employed are toxic and efforts are underway to remove them from environmental circulation. This study elucidates the structures generated from mixed Ti/Sn complexes and how they lead to improved reactivity. A suite of characterization techniques was utilized in structural elucidation including ^{1}H, ^{13}C{^{1}H}, ^{119}Sn NMR, as well as ^{13}C-^{1}H HSQC, ^{1}H-^{1}H COSY, ^{119}Sn-^{1}H HMQC (heteronuclear multiple quantum coherence), DOSY (diffusion-ordered spectroscopy) NMR, and ASAP-MS (atmospheric solids analysis probe – mass spectrometry). These characterization techniques led to the identification of Sn-Ti heterobimetallic dimers, regardless of the tin source (*viz.* Sn(II) or Sn(IV)). The greater stability of the catalysts to agglomeration was identified *ex situ* by UV-vis spectroscopy by observing colloid formation. Probe reactions of Fischer esterification and transesterification were used to characterize catalyst robustness under reaction conditions and catalyst activity relative to pure Ti or Sn complexes. Using ^{119}Sn NMR of reaction mixtures, it was discovered that catalyst-alcohol reaction to make Sn-alkoxide is facile

and is likely the resting state of the catalyst. Additionally, literature suggests that there is synergy between proximal metal centers in a cluster, but initial rate studies here suggest that is not the case.[1]

[1] The work presented in this chapter is largely adapted from the following publication: Jansen, J. H.; Powell, A. B.; Gerislioglu, S.; Specht, S. E.; Hermans, I. Understanding the Structure and Reactivity of Mixed Titanium(IV) Alkoxide and Tin(II)/(IV) Carboxylates as Esterification, *ACS Sustainable Chem. Eng.* **2022**, 10, 7, 2484-2493. J. H. Jansen wrote the publication and conducted all of the materials synthesis, reaction studies, and characterization present, with the exception of the ASAP-MS measurements which were collected by S. Gerislioglu.

2.1 Introduction

Esterification is a ubiquitous transformation throughout the chemical industry with large-scale uses in plastics production (*viz* polyester synthesis), coatings, and pharmaceutical synthesis, among others.[1] In this work we explore the structure and reactivity of tin/titanium mixtures as an example of an industrially relevant esterification system. Ti/Sn mixed catalysts have been known to be effective polyesterification catalysts ever since BASF first patented their use as PET catalysts.[2,3] They were demonstrated to be less prone to agglomeration when exposed to water (a common deactivation pathway), and the time needed for polyester synthesis was reduced when compared to either titanium alkoxides or tin complexes alone (Figure 2.1). Evidently a new compound was formed as mixing titanium alkoxides with either Sn(II) dicarboxylates or Sn(IV) dialkyl dicarboxylates produced heat and was associated with a change of color: the colorless compounds change to red, yellow, or orange.

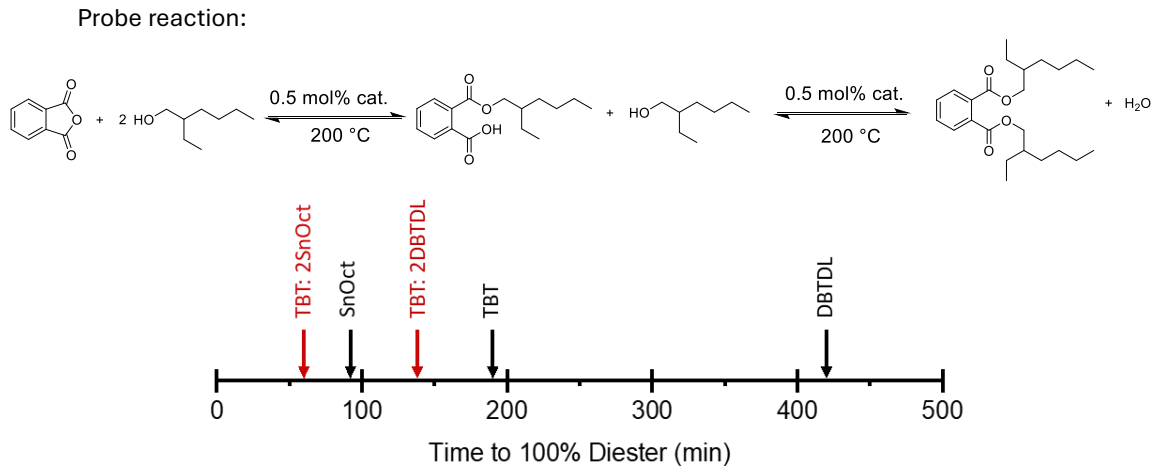

Figure 2.1. Time needed for full conversion to diester as reported in BASF patents.

Where it was known that a new and effective catalyst compound was made, the structures generated in the mixtures were not and have not, to the best of our knowledge, been reported. Elucidation of a catalyst structure is, however, quite important if we want to understand why this mixture of compounds

has superior reactivity. One possible structural change is the exchange of alkoxide and carboxylate ligands between metals to make monomeric complexes which possess more optimal ligand sets for stability towards water, thus suppressing irreversible deactivation. The new compounds may be analogous to distannoxanes where small Sn_2 or Sn_4 clusters serve as stable and active esterification catalyst by forming clusters which may also incorporate titanium.[4] Whatever structure these compounds take on, their reactivity is reported almost exclusively in patents and so thorough reports unravelling the structure-reactivity relationship of these compounds are sparce.

Lewis acidic metals are commonly chosen as esterification and transesterification catalysts for their high activity and the precursor complexes chosen in this study each falls under this category.[4] Titanium alkoxides are among the most employed in industrial applications as evidenced by the many patents claiming them for esterification processes.[5,6] Stannous octoate has been studied as a catalyst for the ring opening polymerization of ε-caprolactone,[7,8] and dibutyltin dilaurate is a common catalyst for polyurethane synthesis.[9] All these compounds act as Lewis acids to catalyze polymerization, but they are also oxophilic and susceptible to hydrolytic agglomeration, leading to deactivation. It is often the case that additional catalyst must be added before a reaction reaches its end point because of catalyst deactivation.[2,3] A more stable catalyst such as a those formed when Sn and Ti complexes are mixed is useful in preventing this while still being composed of inexpensive and highly available compounds.

There are, however, downsides to using these catalysts when viewed through the lens of sustainability. Tin is known to form toxic complexes with various effects, depending on the ligands, including neurotoxicity, hepatotoxicity, renal toxicity, or dermal toxicity. Generally, increasing the number of alkyl ligands as well as decreasing their chain length (methylated tin being highly toxic) leads to worse health effects.[10] One example of harmful tin compounds are tributyltins which were banned from their common use as antifouling agents in maritime coatings due to harming local aquatic life.[11] Dibutyltin complexes

also show toxicity where studies on pregnant rats showed decreased birth weights and a greater number of birth deformities.[12] Stannous octoate is not as toxic but is still labeled as a suspected reproductive toxin, and as a short- and long-term aquatic toxin.[13] It is concerning that tin complexes used in the synthesis of PET plastics, for example, can go on to cause harm to ecosystems. The goal of our study is to address this sustainability issue by gaining an understanding of what structural features are allowed by tin to determine if alternative metals may be substituted.

The mixtures of titanium butoxide (TBT) with stannous octoate (TBT: $Sn(Oct)_2$) or TBT with dibutyltin dilaurate (TBT: DBTDL) were characterized using a suite of spectroscopic techniques including UV-vis, ^{1}H, $^{13}C\{^{1}H\}$, ^{119}Sn, ^{119}Sn-^{1}H Heteronuclear Multiple Quantum Coherence (HMQC) NMR. The molecular weights of the compounds were measured in solution by diffusion order spectroscopy (DOSY) NMR *via* an external calibration curve and supported by atmospheric solids analysis probe – mass spectrometry (ASAP-MS) data. Additionally, the mechanism was investigated though initial rate studies and through ^{119}Sn NMR of reaction mixtures.

2.2 Results

2.2.1 Testing catalyst stability with UV-vis

Catalyst stability for mixed and pure Ti and Sn complexes was investigated by observing changes in the baseline of UV-vis absorbance spectra. Colloidal metal oxides are produced during the agglomeration of these catalysts, and form more readily from less stable compounds yielding cloudy solutions. The cloudiness causes light scattering (Tyndall scattering) during collection of a UV-vis spectrum that can be detected as a baseline increase in the spectrum.[14] Water was added to pure and mixed catalysts diluted in hexane and then a UV-vis spectrum was collected. If no visible change was seen initially, the catalysts were stored in sealed vials for 5 days and then a follow-up spectrum was acquired. Titanium butoxide is well known to agglomerate quickly (Figure A 2.1a), but stannous octoate too shows clouding of the

solution immediately (Figure 2.2a). SnOct is unstable enough to water that changes are observed from DBTDL is significantly more stable than SnOct and shows little change immediately after water is added (Figure A 2.1b). For mixed catalysts, no change in the UV-vis is observed (Figure 2.2b, black and red lines), only the carbonyl-based n → π* transition at *ca.* 300 nm can be seen. After 5 days in the presence of water (Figure 2.2b, blue line), there is only a small shift in the UV-Vis baseline as evidence that agglomeration is slowed significantly relative to pure Sn or Ti complexes.

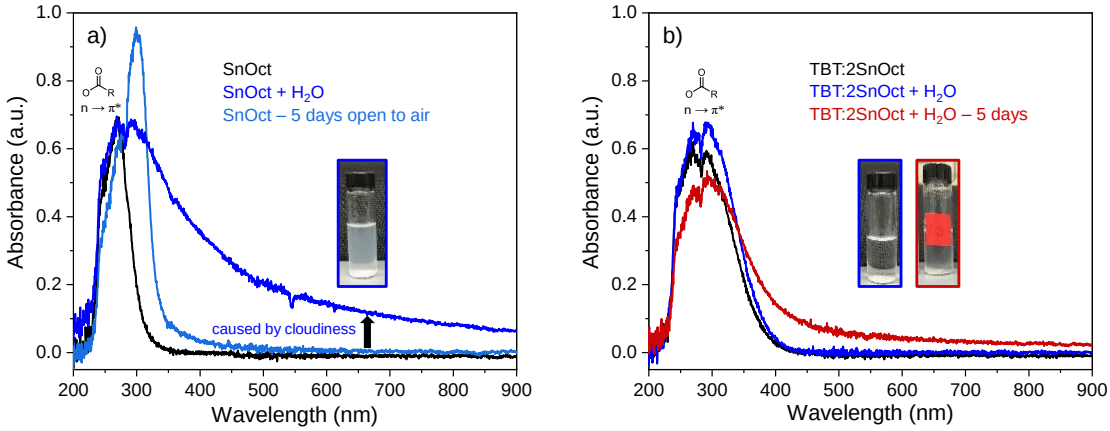

Figure 2.2. Overlaid UV-vis spectra of (a) SnOct or (b) TBT:2SnOct showing baseline shifts caused by Tyndall scattering from clouding by metal oxide colloids in solution. SnOct was allowed to sit open to air for 5 days before collection of a subsequent spectrum. TBT:2SnOct was mixed with water then allowed to sit in a sealed vial for 5 days before collection of a subsequent spectrum. The major absorbance is attributed to the carbonyl-based n → π* transition.

2.2.2 TBT:2SnOct Characterization

We began thoroughly characterizing the mixed catalysts by examining ^{1}H, ^{13}C, ^{119}Sn NMR spectra (results are summarized in Table 2.1). DOSY NMR was also utilized to estimate the molecular weights and nuclearity of the new catalyst compounds. Mixing stannous octoate and titanium tetrabutoxide lead to intriguing spectroscopic observations described and discussed below.

Table 2.1. Tabulated NMR shifts of ^{119}Sn NMR, and diagnostic ligand signals in ^{1}H and ^{13}C NMR spectra.

Catalyst	δ ^{119}Sn (ppm)	δ ^{1}H (ppm)		δ ^{13}C (ppm)	
		Butoxide (α-C*H*$_2$)	Carboxylate	Butoxide	Carboxylate
Ti(O^{n}Bu)$_4$ (TBT)	--	4.16 (t)	--	74.6	--
Stannous octoate (Sn(Oct)$_2$)	-557.8	--	2.23 (m)	--	186.0 (broad), 182.2
TBT: 2 Sn(Oct)$_2$	-736.4, -736.8, -737.0	4.55*(2H, ddt), 4.35 (4H, t), 4.30*(2H, dt)	2.25, 2.16 (m)	75.5, 75.2, 63.9	183.4, 183.2, 182.9, α-*C*H 49.5, 49.4, 49.2, 49.1
Dibutyltin dilaurate (DBTDL)	-149.4	--	2.35 (t)	--	184.4
TBT: 2 DBTDL	-147.5, -198.7	4.57 (2H, dt), 4.46 (4H, 4t), 4.21 (4H, m)	2.35, 2.25, 2.21	76.9, 75.6, 74.3	184.4, 182.6, 179.8

* indicates protons with observed correlation to Sn in SnH HMQC.

Stannous octoate and titanium butoxide are completely consumed as shown by the disappearance of the diagnostic NMR signals for SnOct and TBT in ^{1}H, ^{13}C, and ^{119}Sn NMR spectra (Table 2.1, see appendix for full ^{13}C and ^{119}Sn spectra). The ^{1}H NMR spectrum of TBT:2SnOct, in Figure 2.3a) shows three major α-C*H*$_2$ butoxide signals appear at 4.55, 4.35, and 4.30 ppm which have a 1:2:1 area ratio. Analysis of the ^{119}Sn spectrum shows three sharp signals shifted upfield from -557.8 ppm (SnOct) to -736.4, -736.8, and -737.0 ppm with roughly a 1:2:1 ratio of intensities (Figure 2.3b). 2-D ^{119}Sn-^{1}H HMQC experiments (Figure 2.3c) allow for ^{119}Sn-^{1}H coupling to be observed between these new α-C*H*$_2$ butoxide resonances and ^{119}Sn resonances (no coupling was observed between ^{119}Sn and octoate ligand ^{1}H for mixed catalysts).

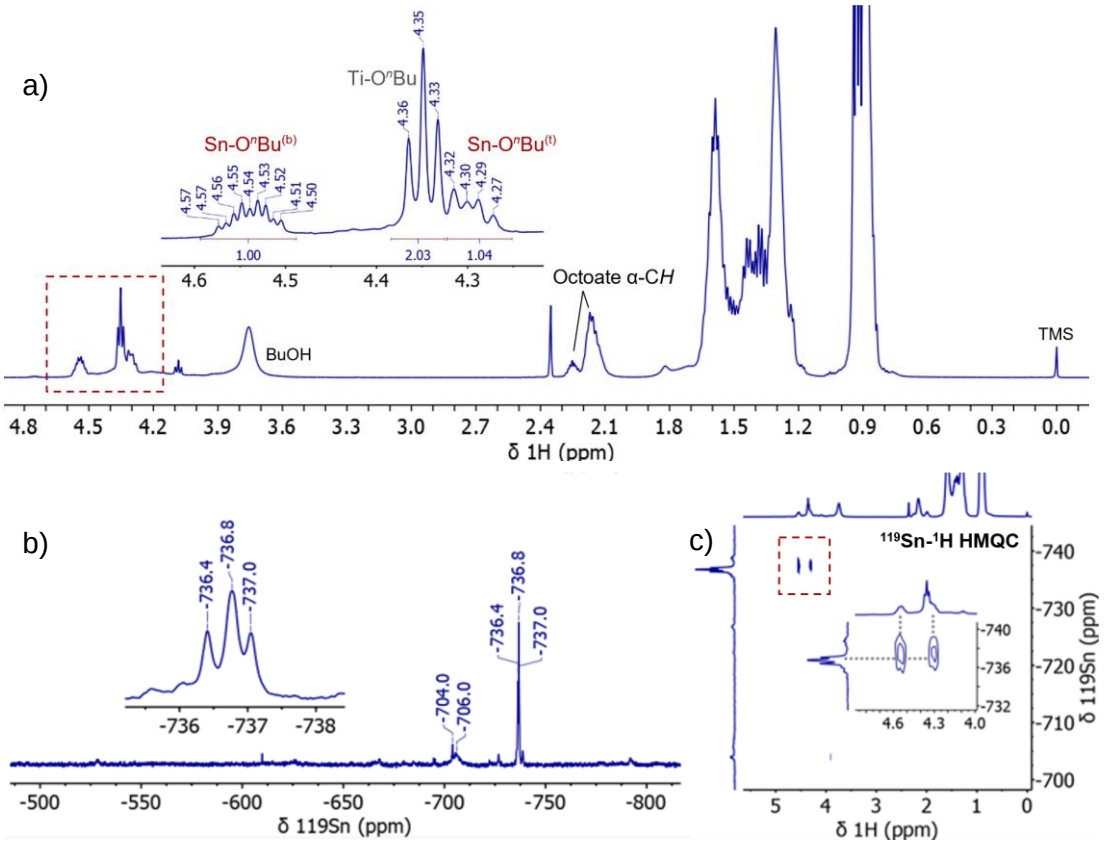

Figure 2.3. NMR spectra of TBT:2SnOct. (a) ^{1}H NMR spectrum showing complex butoxide signal patterns and assignments of bridging$^{(b)}$ and terminal$^{(t)}$ Sn-butoxides and Ti-butoxide., (b) ^{119}Sn spectrum showing three major signals. Signals at 704.0 and 706.0 ppm are attributed to hydrolyzed SnOct.[24] (c) ^{119}Sn-^{1}H HMQC spectrum optimized for 8 Hz coupling constants.

Of the three butoxide signals two of the three signals, those centered at 4.55 and 4.30 ppm, have observable ^{119}Sn-^{1}H correlations. These correlations confirm that butoxide ligands are bonded to a new tin species at -736 ppm and in two main bonding environments. The 4.55 ppm signal is in the shift range of bridging alkoxide ligands, which are deshielded relative to terminal ligands,[15] and many tin(II) dimers with μ^2-bridging alkoxides are known so this is not unlikely.[16] This leads to the assignment of the 4.55 ppm signals to bridging butoxides [Sn-(O^{n}Bu)$^{(b)}$] while the 4.30 ppm signals are preliminarily assigned to terminal butoxide ligands on tin [Sn-(O^{n}Bu)$^{(t)}$], and the remaining signal at 4.35 ppm, without observed

^{119}Sn-^{1}H correlation, is attributed to terminal Ti-(O^{n}Bu)$^{(t)}$. Interestingly, each of the two ^{119}Sn-correlated signals have a more complex pattern of peaks than the expected triplet with ~6 Hz $^{3}J_{HH}$-coupling constant as seen at 4.35 ppm. The 4.55 ppm signal has expected $^{3}J_{HH}$ coupling of ca. 6.7 Hz but unexpectedly, there is a large doublet coupling of 10.5 Hz and a smaller doublet coupling of 3.5 Hz to give a doublet of doublets of triplets (Figure A 2.9). The signal centered around 4.30 ppm also has a doublet coupling around 10 Hz in addition to the expected triplet $^{3}J_{HH}$ coupling. Coupling on the order of 10 Hz matches with geminal coupling of the α-CH_2 and points to a initially surprising magnetic nonequivalence between geminal protons on what is generally an unhindered aliphatic chain. However, this has been observed previously for $Ti_{16}O_x$ clusters capped with μ^2- μ^4 bridging ethoxide groups but little detailed analysis has been reported.[17,18] Since geminal coupling is only observed for bridging alkoxide ligands, according to literature reports, the butoxide ligand with resonance centered around 4.30 ppm which was previously assigned as a terminal butoxide, is now assigned as a bridging butoxide. Another surprising source of ^{1}H-^{1}H spin-spin coupling can be found in the ^{1}H-^{1}H COSY spectrum (Figure 2.4) where the signals at 4.30 and 4.55 ppm show coupling, which normally points to a through-bond coupling of the protons of >3 Hz. This through-bond coupling would be 6-bond coupling and quite unusual. It can be hypothesized that the large number of electrons involved in the metal complex allow for this unusually long-range coupling.

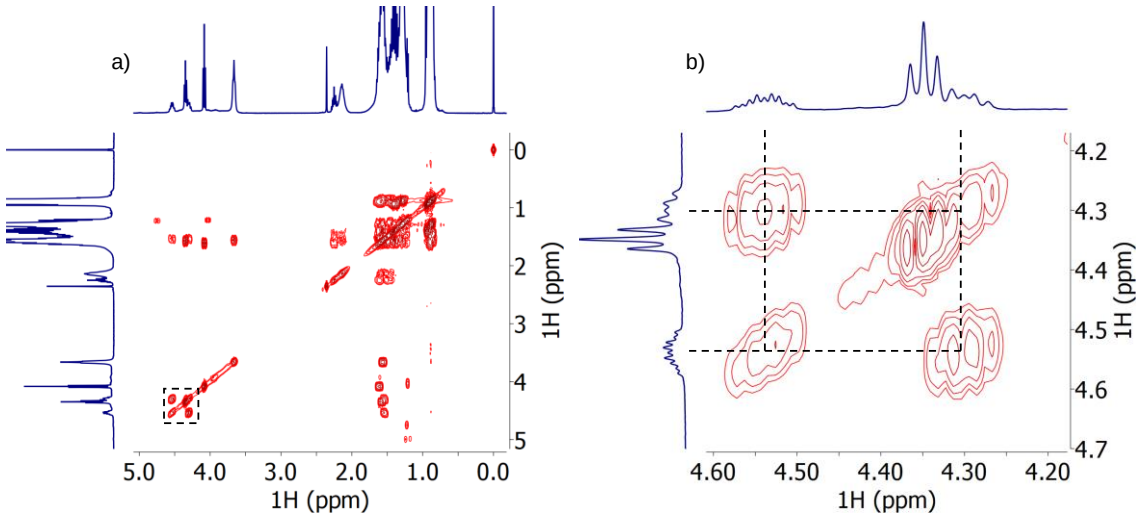

Figure 2.4. (a) ^{1}H-^{1}H COSY NMR spectrum of TBT:2SnOct (b) zoomed in to butoxide region.

DOSY NMR studies provide additional information about the composition and connectivity of the catalyst compound mixtures. Primarily, the set of signals arising from any molecule can be differentiated from other compounds in a mixture by their shared diffusion constant and the diffusion constant can be used to empirically approximate the molecular weight of any compound so long as the signals are not overlapping. If there is signal overlap, a weighted average of the diffusion constants in the overlapping region will be observed. This is the reason, for instance, that there are regions indicating a lower diffusion constant in the 1.6 – 0.8 ppm region of Figure 2.5 as there exist substantial overlapping butanol signals. This technique is often used either to distinguish signals of individual compounds in a mixture or to determine the nuclearity of small clusters.[19] The analysis here powerfully takes advantage of both of these capabilities. Analysis of the DOSY spectrum of TBT:2SnOct shows one new major species is formed as evidenced by the single diffusion constant shared by each diagnostic butoxide resonance (Figure 2.5). The blue line in Figure 2.5 highlighting this shared diffusion constant is also seen to intersect octoate α-C*H* signals near 2.2 ppm indicating some octoate ligation as well. Overlapping signals, however, do not allow for an accurate integration to determine the number of octoate ligands on this compound. To estimate

the molecular weight of the unknown compound, and from this the nuclearity, the diffusion constants for a set of known compounds with similar shapes all at 0.1 M in $CDCl_3$ were found and used to generate a calibration curve. Any differences in solution viscosity of these compounds or the unknown were corrected for using an internal standard of trimethylphenyl silane (TMPS). Using the DOSY determined diffusion constant and this calibration curve the unknown compound is estimated to have a molecular weight of 500 g/mol.

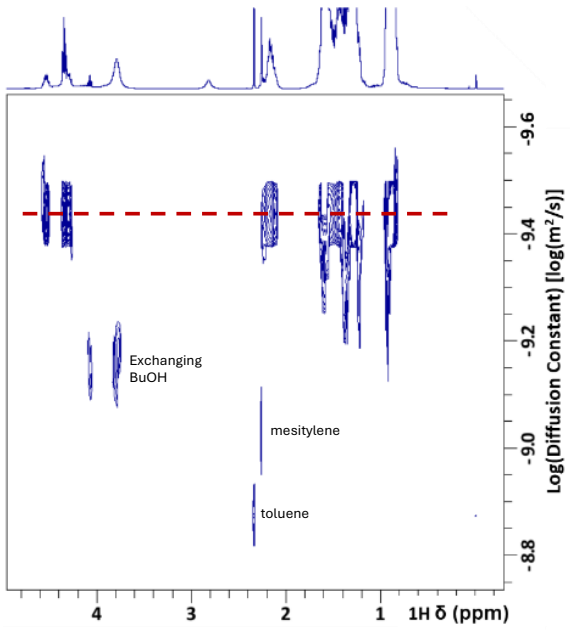

Figure 2.5. DOSY NMR spectrum of TBT:2SnOct. Horizontal lines indicate signals sharing the same diffusion constant. Mass labels indicate the predicted molecular weight based on an external calibration curve.

Attempts to elucidate the catalyst composition using ASAP-mass spectrometry confirmed that nearly all of the tin stays in the +2-oxidation state when mixed with TBT (Figure A 2.11). However, catalyst composition could not accurately be determined from the MS output as in-source clustering of Sn(II) species limited the usefulness of the analysis.

2.2.3 TBT:2DBTDL Characterization

Next, we examined the mixtures with the dibutyltin dilaurate. These mixtures are unique from those with SnOct as the starting tin source is not fully converted into new compounds, and only one new Sn species is formed initially. The TBT:2DBTDL mixtures do share many similar qualities with mixture of SnOct such as higher molecular weight compounds being formed, multiple new downfield shifted butoxide ^{1}H NMR signals, new carboxylate ligand coordination environments being visible in ^{13}C NMR, and a new tin species with resonance shifted upfield.

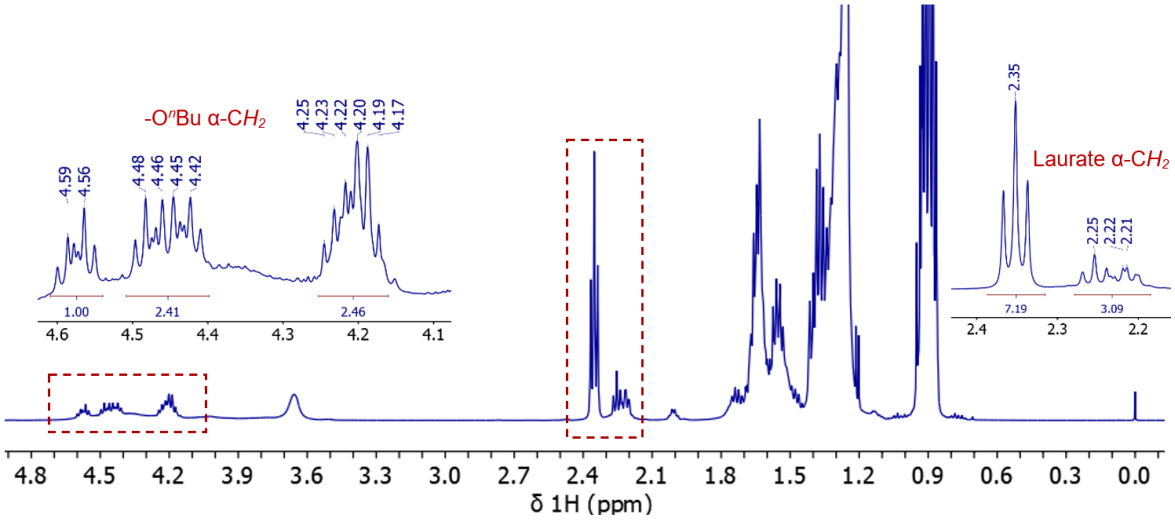

Figure 2.6. ^{1}H NMR spectrum of TBT: 2DBTDL.

Not all of the DBTDL added into the mixture is converted into new compounds when mixed in a 1:2 ratio with TBT. There are residual laurate signals at 2.35 ppm in ^{1}H NMR and at 184.37 ppm in ^{13}C NMR that have no change from pure DBTDL. The ^{1}H signals of butoxide ligands again show *ca.* 10 Hz geminal coupling for signals at 4.57 and 4.47 ppm with a third geminally coupled signal at 4.2 ppm (Figure 2.6, top left blowup). The ^{1}H region around 2.2-2.4 ppm showing laurate signals indicates small amounts of 2 or 3 new laurate species have formed and ^{13}C NMR of the carbonyl region shows two new signals to corroborate this observation. Only one well defined tin species is generated according to ^{119}Sn NMR (Figure 2.7) and is shifted upfield from DBTDL (-147.8 ppm) to -198.7 ppm. The small shift in the baseline around -200 ppm

may be a broadened-out Sn species. It is expected that Sn-OR-Sn connectivity will show visible ^{119}Sn-^{117}Sn coupling in a ^{119}Sn spectrum, even in symmetrical molecules, but this is not observed here. This may point toward a lack of the Sn-O-Sn moiety. Interestingly, upon aging (on the order of months) a new set of signals arise that do show diagnostic ^{119}Sn-^{117}Sn coupling (Figure A 2.4) to indicate a multi-tin cluster similar to reported distannoxanes.[20]

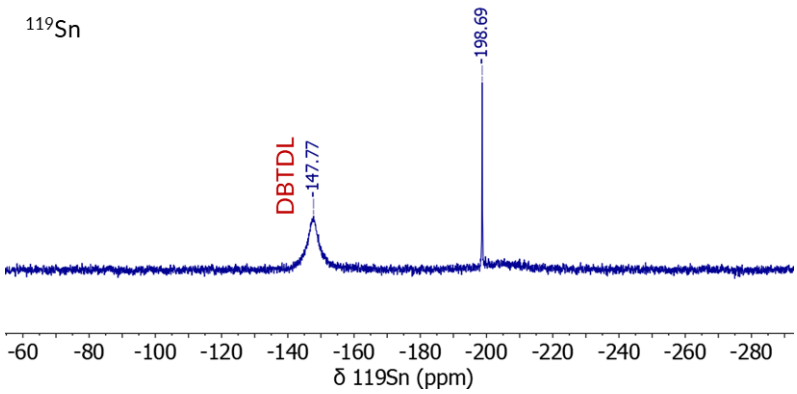

Figure 2.7. ^{119}Sn NMR spectrum of TBT:2DBTDL.

Upon slow hydrolysis during aging, the mixtures indeed show that Sn clusters form as a secondary compound with coupling constants of 111.9 Hz between each Sn (Figure A 2.4). Unfortunately, ^{119}Sn-^{1}H correlations were only butyl correlations were observed (Figure A 2.3) and butoxy signals were not observed in DBTDL mixed catalysts to allow for assignment of Sn- or Ti-bonded ligands.

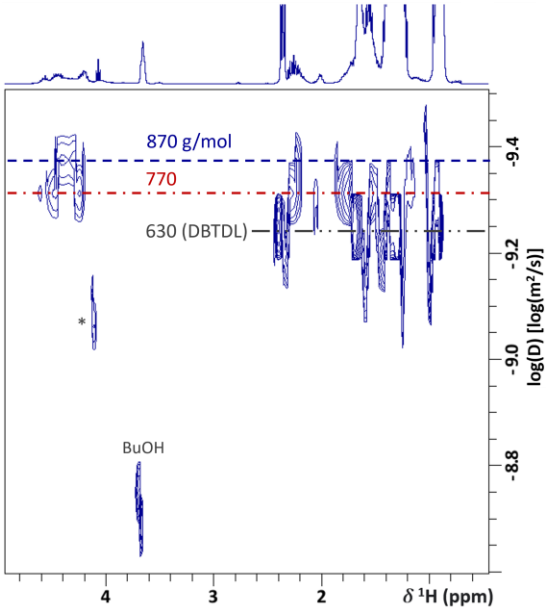

Figure 2.8. DOSY NMR spectrum of TBT: 2 DBTDL. Horizontal lines indicate signals sharing the same diffusion constant. Mass labels indicate the predicted molecular weight based on an external calibration curve. * indicates a titanium complex that increases with catalyst aging but was not analyzed in-depth.

DOSY NMR (Figure 2.8) shows clearly there is unreacted DBTDL at 630 g/mol, and two other higher molecular weight compounds at predicted masses of 770 and 870 g/mol. Of the two new compounds, the one at 770 g/mol is more abundant than the 870 g/mol as judged by intensity of the associated butoxide signals. Both of the new compounds have connectivity with both butoxide and laurate ligands and the ^{119}Sn chemical shift suggests penta- or hexa-coordinate tin.

The presence of titanium cannot be accurately deduced from the NMR spectra collected. However, analysis *via* ASAP-MS, shown in Figure 2.9, indicates Sn-Ti heterobimetallic dimers are major species with parent ions of m/z 647, 773, and 899 which match reasonably well with the DOSY-calculated masses. Note that parent ions are formed by the loss of a ligand during ionization, so the masses detected are likely 73 (butoxide) or 199 g/mol (laurate) less than the neutral compound.

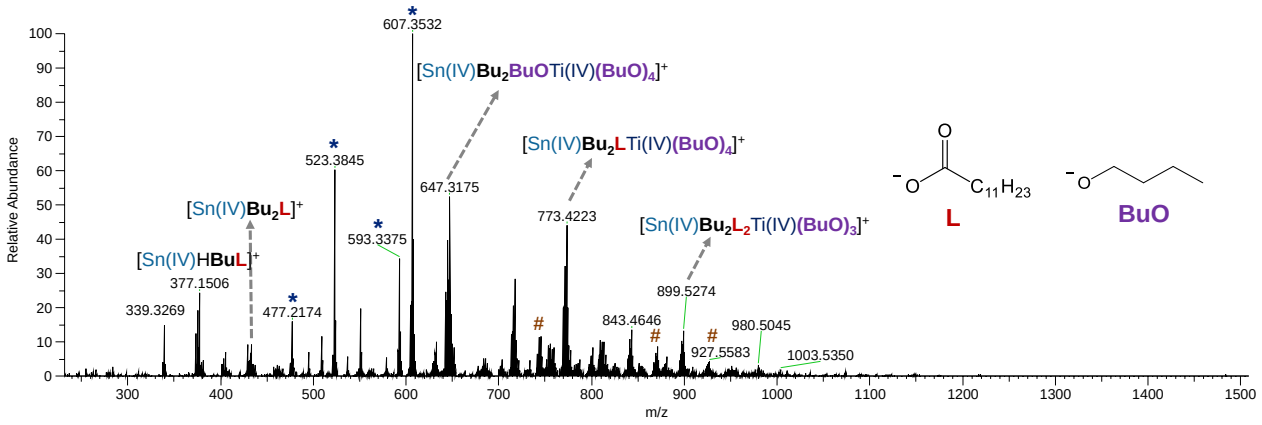

Figure 2.9. ASAP-MS spectrum of TBT: 2DBTDL. Formulas were assigned to peaks based on isotope patterns and by high resolution masses. * indicates Ti-laurate complexes. # labels complexes with laurate impurities of chain length ± C_2H_4.

2.2.4 Optimization of Metal Ratio

With an understanding of the spectroscopic handles of interest for a TBT/SnOct mixed metal catalyst in hand, it was possible to evaluate the optimum synthesis conditions to form the compound of interest. The patent on TBT + SnOct mixtures found a slight benefit in reactivity to a 1:2 ratio and an increase in stability for that ratio as well but there was no explanation provided. [patent ref] The test this a series of metal ratios from 1:4 to 1:0.5 TBT to SnOct were synthesized and quantitative NMR spectra were collected. Figure 2.10 shows a comparison of the ^{1}H and ^{13}C spectra and the diagnostic peaks found in previous sections are highlighted with blue boxes. The butoxy signals of the ^{1}H spectra show cleanly the three diagnostic resonances at mixing ratios of 1:4 or 1:2, these are observable when a 1:1 ratio is employed but are accompanied by other, more prominent signals. The diagnostic signals are not resolved at all once the ratio of titanium to tin is raised to 1:0.5. A 1:4 or 1:2 ratio yields the desired butoxide arrangement, but while a 1:2 ratio also shows no trace of unreacted stannous octoate, a 1:4 ratio evidently has too much stannous octoate to reaction with the available titanium complex and a carbonyl signal at 182.2 ppm indicative of unchanged stannous octoate is seen (red box). It can be concluded that

TBT:2SnOct gives to cleanest yield of the compound of interest, but further analysis was needed to verify this ratio also produces the highest concentration of this compound.

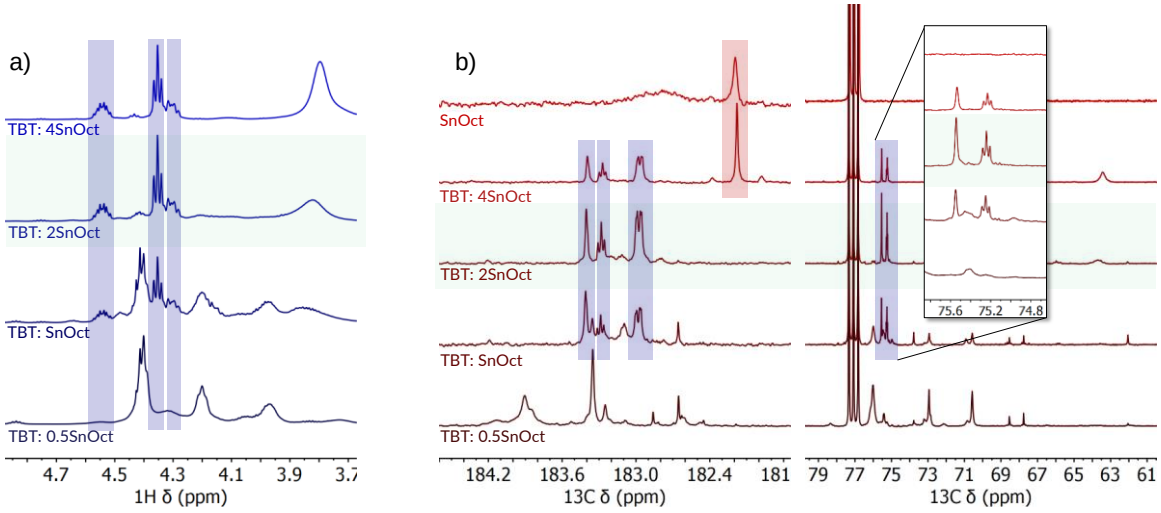

Figure 2.10. (a) ^{1}H NMR and (b) ^{13}C NMR spectra of a range of mixing ratios of tetrabutyl titanate (TBT) and stannous octoate (SnOct) highlighting diagnostic signals with blue-shaded boxes and unchanged SnOct carbonyl signals with a red-shaded box. The optimal mixing ratio of 1-to-2 is highlighted with a green-shaded box.

Equal total metal concentrations of each mixing ratio were analyzed via NMR and a Job plot was produced (Figure 2.11) using the integration of the most well resolved butoxy signal (4.55 ppm) as a spectroscopic handle. Indeed, this analysis makes it clear that a 1:2 ratio of TBT and SnOct produces the highest concentration of the compound of interest. When the ratio of TBT to SnOct is halved to 1:4, the concentration is also roughly halved (ca. 2.9×10^{-5} M to 1.5×10^{-5} M). If it is assumed that all of the available titanium in a 1:4 ratio reacts to generate the compound of interest, then a doubling of the compound's concentration with a doubling in the amount of titanium suggests that nearly all of the titanium also reacts at a 1:2 ratio. At higher ratios it is apparent that other compounds are being generated and these ratios are nonoptimal for synthesizing the compound of interest. With high ratios of TBT and SnOct (1:0.5) the diagnostic signal is at the least poorly resolved.

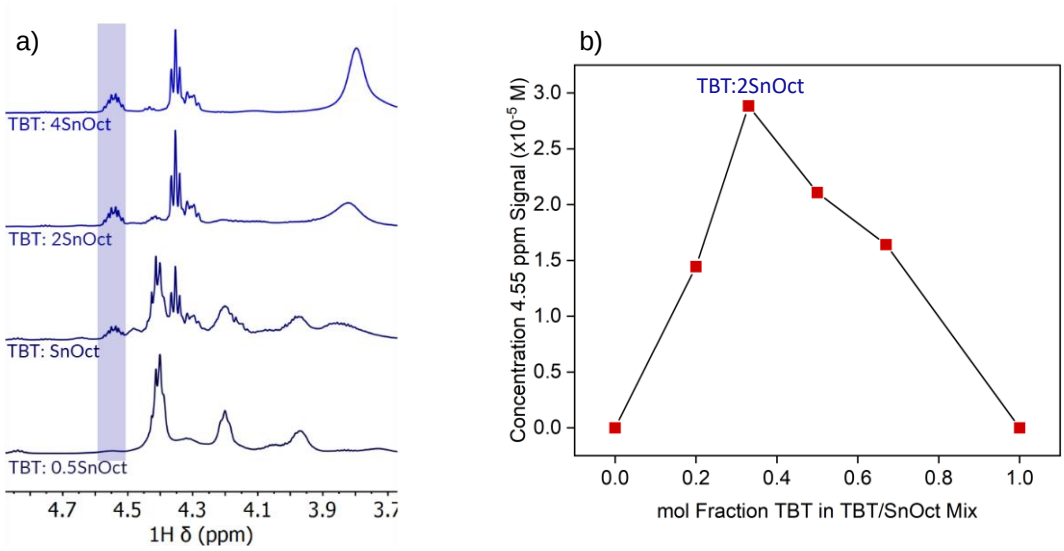

Figure 2.11. (a) Stack of butoxy regions of ^{1}H NMR spectra of TBT/SnOct mixtures at various ratios highlighting the signal used to make a Job plot. (b) Job plot of varied mixing ratios of TBT and SnOct.

Using the same method, mixtures of TBT and DBTDL were analyzed for an optimum mixing ratio. As with the patent for TBT + SnOct mixtures the patent for TBT + DBTDL suggests an optimum at a 1:2 ratio.[2,3] The ^{1}H NMR spectra (Figure 2.12a) shows that the diagnostic doublet of quartets around 4.57 ppm is not very well resolved at a 1:4 ratio but becomes significantly more resolved at higher ratios of Ti to Sn. In the ^{119}Sn NMR shown in Figure 2.12b there is a clear shift from unreacted DBTDL to the new Sn species at -198.7 ppm as more titanium is in the mixture. At a Ti/Sn ratio of 1:0.5, all the DBTDL appears to have been converted into the new species.

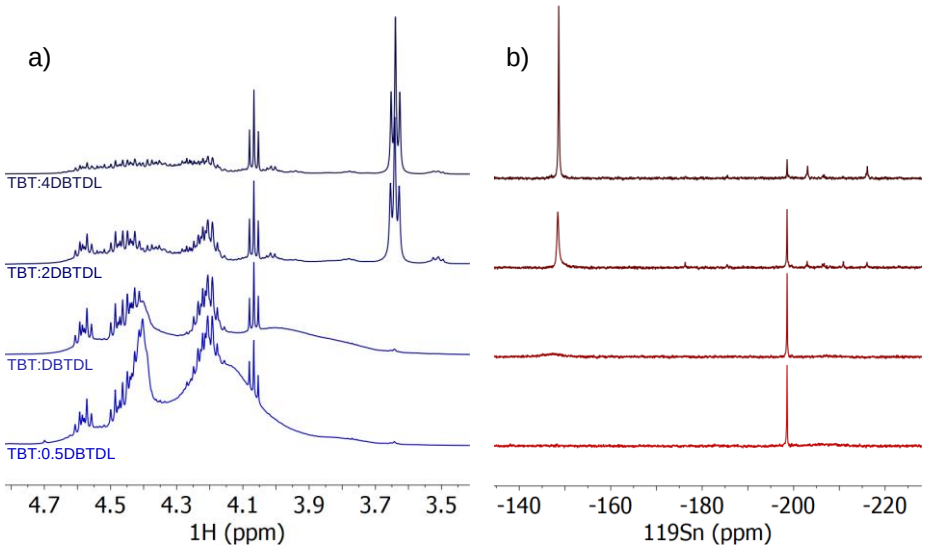

Figure 2.12. (a) ^{1}H NMR and (b) ^{119}Sn NMR spectra of a range of mixing ratios of TBT and DBTDL.

Analysis of the Job plot that results from measuring the concentration of the new compound of interest using the doublet of quartets at 4.57 ppm in the ^{1}H NMR spectra indicates that the optimum mixing ratio is in fact 1:1 instead of the reported 1:2 (Figure 2.13). It may still be advantageous to employ a 1:2 ratio instead of 1:1 as unreacted TBT is more likely to cause polymer discoloration than unreacted DBTDL and a slight excess of DBTDL could ensure all TBT is reacted with tin. This point is speculative but may explain the patent-reported results.

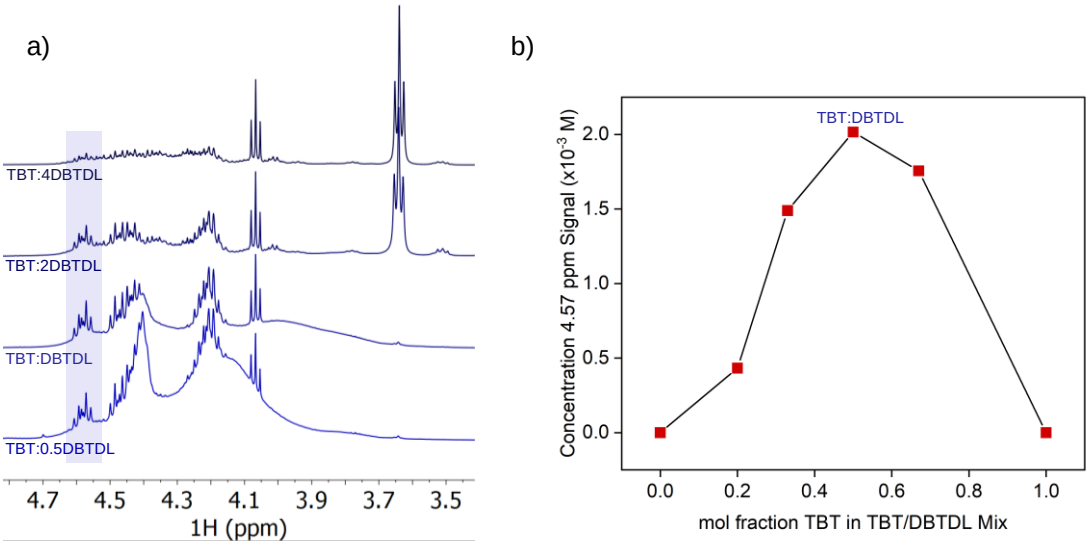

Figure 2.13. (a) Stack of butoxy regions of ^{1}H NMR spectra of TBT/DBTDL mixtures at various ratios

2.2.5 Probe Reactions – Catalyst Activity

Two probe reactions were used to evaluate the reactivity of the mixed Sn/Ti catalysts. The first is an anhydride opening of phthalic anhydride (PA) with 2-ethylhexanol, followed by a Fischer esterification to the diester product with coproduction of water (Figure 2.14) where the ring opening is fast and the Fischer esterification is monitored. On our collaborators advise, a cyclic anhydride and a hindered alcohol were employed to simulate coatings-specific reagents. The second probe is a transesterification of methyl benzoate with 2-ethylhexanol producing methanol as the byproduct. The phthalic anhydride esterification is expected to show differences in catalyst stability more clearly as water leads to faster catalyst agglomeration than methanol.

The phthalic anhydride esterification reaction conditions were set at 205 °C with 0.5 mol% catalyst loading and a 3:1 reactant ratio of alcohol to ester to match the conditions used in the BASF patents.[2,3] The patents reported the time required to reach complete conversion to the diester. These data demonstrated that significantly shorter reaction times are needed for mixed Sn/Ti catalysts as compared to $Ti(OR)_4$, Sn(II) dicarboxylates, or Sn(IV) dialkyl dicarboxylates (Figure 2.1). We, however, were most

interested in the time-course profiles of these catalysts to separate initial activity from catalyst stability at higher conversion. Making distinctions between high activity and high stability is key for determining the reasons why these catalyst compounds are more effective than Ti or Sn alone.

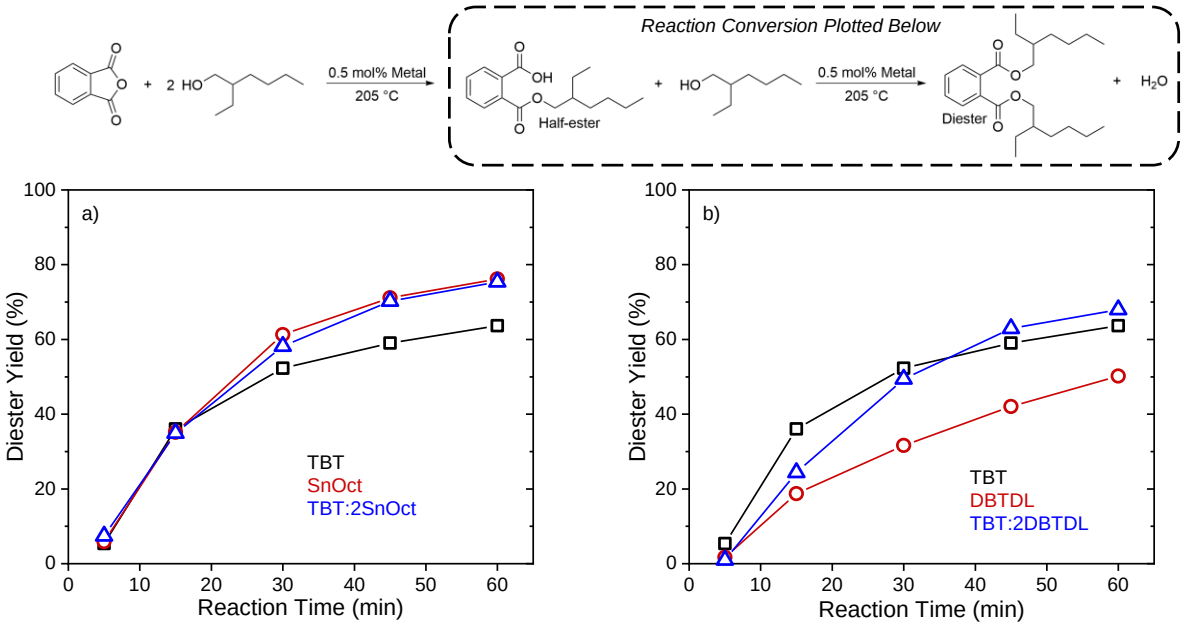

Figure 2.14. Time-course reactivity data for phthalic anhydride with 2-ethylhexanol at 205 °C at 0.5 mol% catalyst loading by total metal. Loading of mixed metal catalysts is same as 0.17 mol% TBT, 0.33 mol% Sn catalyst. (a) Time-course reactivity of TBT:2SnOct compared to TBT and SnOct. (b) Time-course reactivity to TBT:2DBTDL compared to TBT and DBTDL. Time-course data starts at 5 minutes to allow for ring opening to reach completion.

Time-course studies show that deactivation is a vital factor in the productivity of the catalysts over time. TBT starts with a high rate of conversion but the reaction profile begins to flatten more quickly than the other catalysts, and indeed the reaction solution turns visibly cloudy within the first hour to indicate catalyst agglomeration. SnOct also initially shows high activity which is maintained for somewhat longer than TBT. The TBT:2SnOct mixed catalyst, however, shows initial activity similar to the pure compounds

(Figure 2.14a) notable due to lower loadings of either metal being used. DBTDL is a lower activity catalyst than the others tested (Figure 2.14b), but the TBT:2DBTDL mixed catalyst shows improved initial conversion in the first 15 minutes and surpasses the diester yield of even pure TBT by the 45-minute mark.

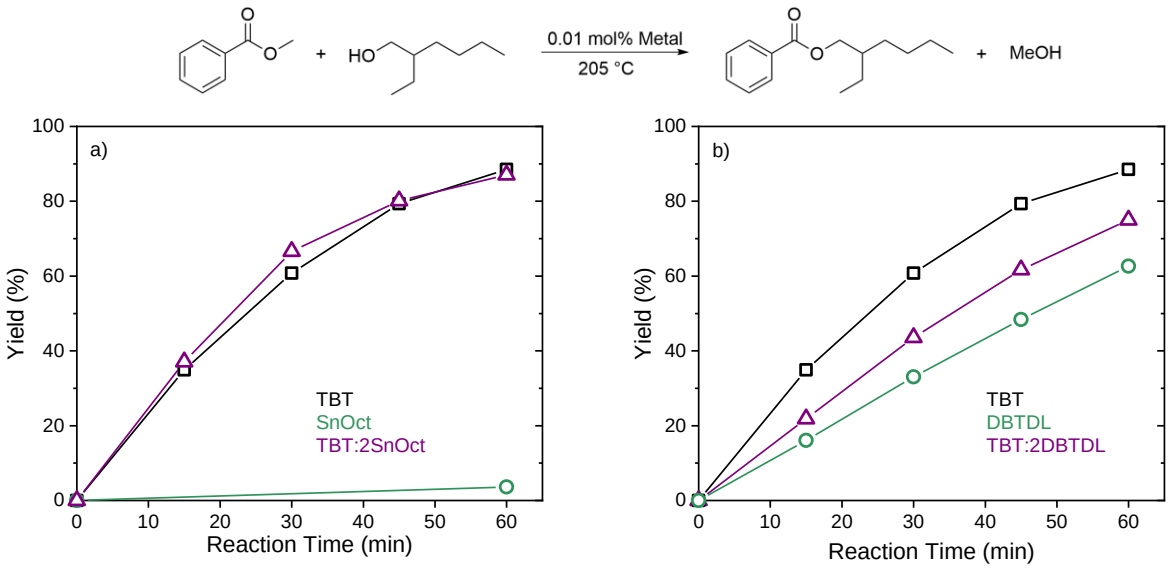

Figure 2.15. Time-course reactivity data for methyl benzoate with 2-ethylhexanol at 205 °C at 0.01 mol% by total metal. (a) Time-course reactivity of TBT:2SnOct compared to TBT and SnOct. (b) Time-course reactivity to TBT:2DBTDL compared to TBT and DBTDL. Loading of mixed catalysts is same as 3.3 mmol% TBT, 6.7 mmol% DBTDL.

The transesterification probe reaction of methyl benzoate and 2-ethylhexanol (Figure 2.15) was generally easier for the catalysts to achieve and could be run with much lower catalyst loading (0.01 mol%). The importance of catalyst stability is less relevant for the transesterification, as methanol is the biproduct and is less reactive than water in forming catalyst agglomerates. The time-course data reflects this as progress does not slow so dramatically as in the phthalic anhydride probe reaction. Interestingly, SnOct proves to be an ineffective catalyst for this reaction, when it showed high activity for the other probe reaction, reaching less than 5% conversion in an hour. The addition of TBT in TBT:2SnOct shows a

remarkable increase in activity to match that of pure TBT (Figure 2.15a) even with only 33% of the Ti loading as pure TBT. The TBT:2DBTDL mixture shows an intermediate activity between the pure compounds, as in the reaction with phthalic anhydride (Figure 2.14b).

2.2.6 Metal-Metal Cooperativity

Previous studies into tin clusters used for esterification, namely distannoxanes, have claimed that the cluster structure of these compounds containing proximal metals can act as an improved template for esterification than a monometallic Lewis acid allowing for faster reactivity than monomeric catalysts.[21] In addition, the hypothesized resting state of the catalyst is with the alcohol reactant associated with the catalyst as a metal-bound alkoxide (Structure 2 in Scheme 2.1)

Scheme 2.1. Proposed mechanism for esterification/transesterification by a tin tetramer/distannoxane. Adapted from Ref. 21.

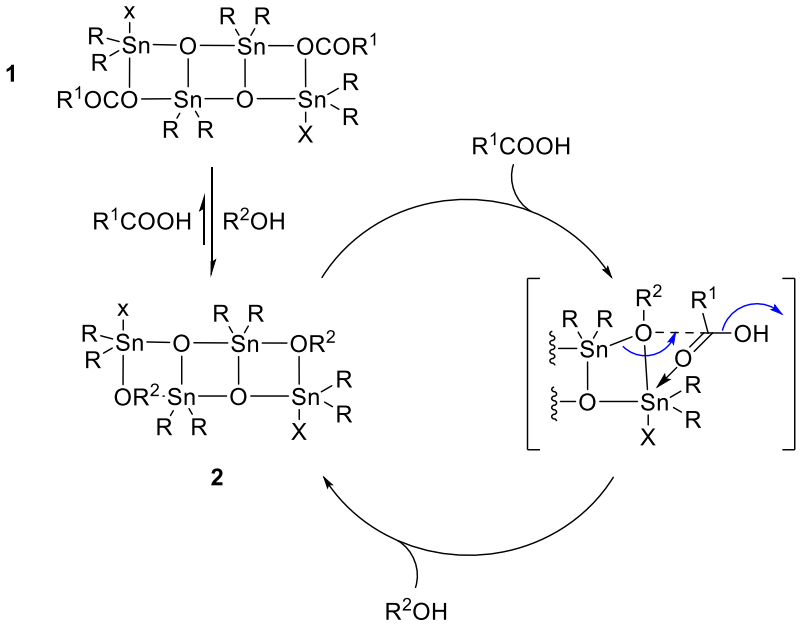

In the work that Otera et. al. did on distannoxanes, they hypothesized that this improved templating of reactants around two proximal tin centers allowed for the improved reactivity they

observed over monomeric tin catalysts.[21] If this was the case, the initial rates of reaction should be improved over monomeric catalysts as well. To test this hypothesis for the mixed metal catalysts of TBT with either SnOct or DBTDL, the initial rates of transesterification of methyl benzoate were measured for unmixed TBT, SnOct, DBTDL, and the mixed metal catalysts (Figure 2.16). The literature on distannoxanes would suggest that clusters would have higher rates of reaction than the linear combination of the component metals. Conversely, the initial rates that were measured for mixed metal catalysts appear to follow a linear trend with the unmixed catalysts to indicate no significant synergy.

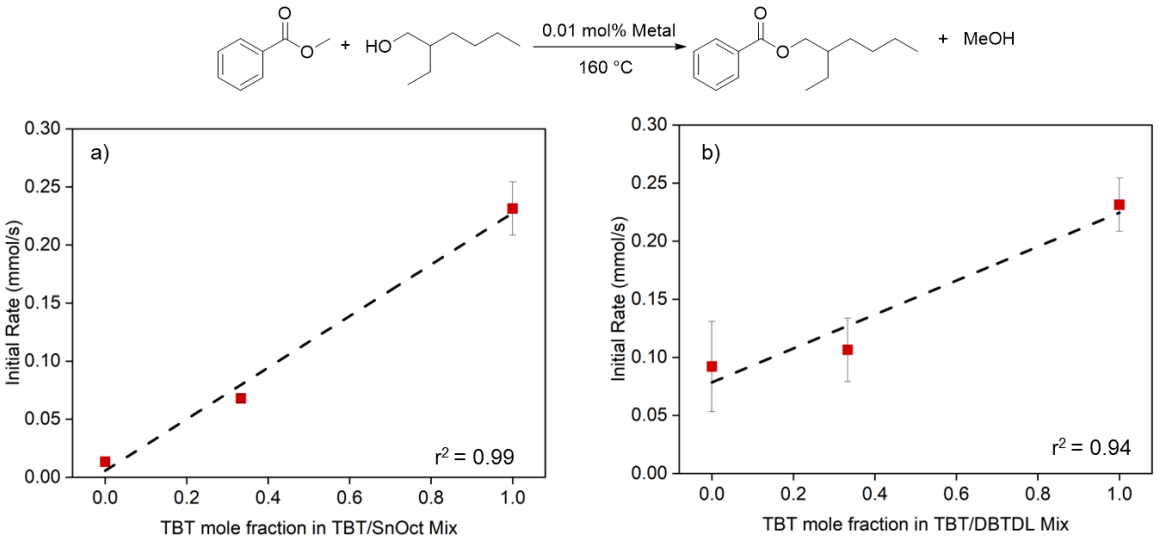

Figure 2.16. Initial rate data of mixed TBT and (a) SnOct or (b) DBTDL at different ratios. Initial rates collected at <10% conversion at a 0.01 mol% catalyst loading by total metal. Error bars represent 2 standard deviations based off independent duplicate runs. Dotted line is a least-squares fit of the experimental data.

2.2.7 Catalyst Characterization Post-Reaction

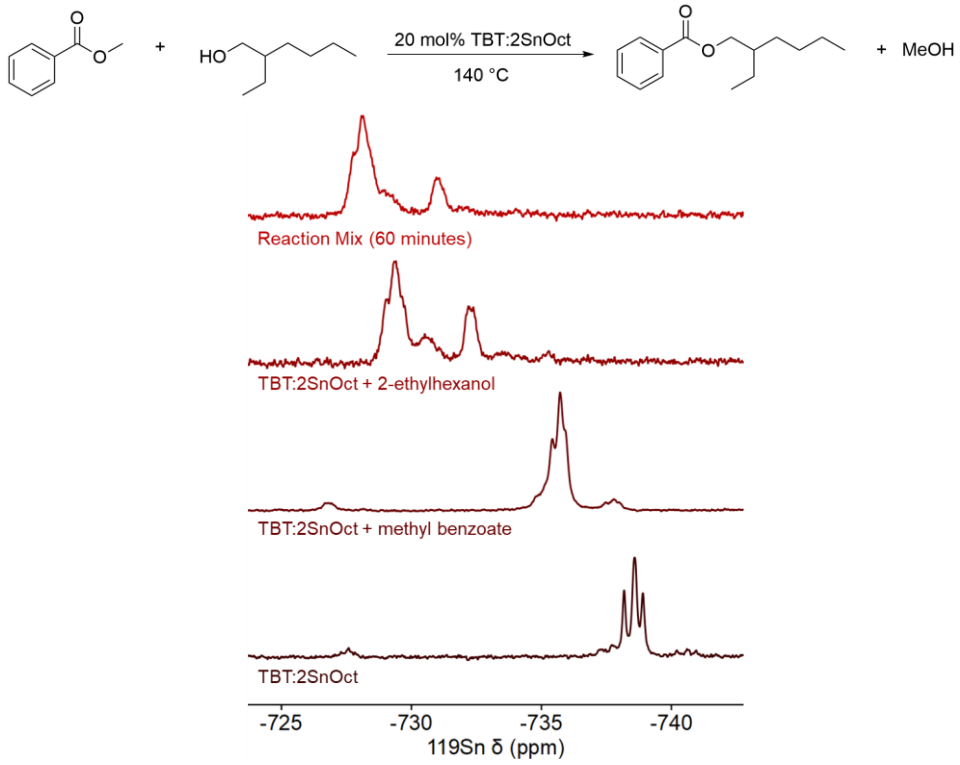

Figure 2.17. ^{119}Sn NMR spectra of TBT:2SnOct after mixing with reactants or after a reaction with both reactants for 60 minutes.

Analysis of the NMR spectra of the pure compound generated by mixing TBT and SnOct in the optimum ratio is useful as a starting point to understanding why the new compound is an effective catalyst when added to an esterification reaction. The next step in answering questions about the reason for effective catalysis is to analyze changes the catalyst undergoes during catalysis. To do this, we realized that analysis of ^{119}Sn NMR could allow for selective analysis of one of the two key metal centers without confusion with signals associated with reactants or other parts of the catalysts that ^{1}H NMR would include. The relatively low receptivity and natural abundance of ^{119}Sn compared to ^{1}H nuclei meant the catalyst concentration needed to be increased for good signal collection, and 20 mol% in a reaction of methyl benzoate with 2-ethylhexanol was found to give sufficient signal. Preliminary steps of the potential analysis using this strategy are shown in Figure 2.17 where the spectrum of the post-reaction solution is

compared to solutions where only one reactant was mixed with the catalyst as well as the pure compound's spectra all at equal tin concentration. The pure compound, again, has three sharp peaks centered around -737 ppm. Mixing methyl benzoate with the catalyst at room temperature yields a small downfield shift (~2 ppm) and still appears as three overlapping signals being the main resonances observed. Mixing 2-ethylhexanol with the catalyst at room temperature, however, presents a larger downfield shift and while the most intense resonance may still be a grouping of three overlapping signals, two smaller signals also appear. Interestingly, when the spectrum of the reaction mixture is analyzed, it matches noticeably with the resonances of the catalyst/alcohol mixture after only room temperature mixing. In fact, the reaction mixture before heating for 60 minutes is very similar to the reaction mixture after only mixing the reactants with the catalyst at room temperature (pre-reaction). An additional level of accuracy and potential usefulness would be to collect ^{119}Sn NMR spectra of the reaction mixture at elevated temperatures to better simulate reaction conditions. A few obstacles that would need to be overcome to collect such data include preventing pressure buildup from methanol formation, enhancing signal as increased temperature decreases NMR signal, and it would be difficult to reach true industrial reaction temperatures of 200 °C,

2.3 Discussion

2.3.1 Discussion of TBT:2SnOct characterization

The butoxide α-CH_2 protons in TBT:2SnOct were observed to form an intriguing pattern of signals at 4.55 and 4.30 ppm which consist of four and two overlapping triplets, respectively, when no significant additional coupling is expected. We postulate that these additional signals are caused by a nonsymmetrical structure with unexchangeable ligands at the NMR timescale, leading to multiple nonequivalent yet similar ligand bonding arrangements and NMR signals. The other possible explanations seem less likely. One possibility stems from these ^{1}H signals exhibiting coupling to each other in the HH COSY spectrum (Figure 2.4). However, this would be 6-bond coupling (H-C-O-Sn-O-C-H) when HH COSY is

normally limited to 4-bond coupling. Even if there was significant coupling between adjacent butoxide ligands, the coupling would be expected to yield triplets of triplets and have small coupling constants if any, so butoxide-butoxide coupling is not likely. Both signals also have correlations with ^{119}Sn, but this coupling would be expected to look like satellites of triplets with ca. 16% of the area of the main signal (from the added abundance of ^{117}Sn and ^{119}Sn) if it were resolved, so does not fit the pattern of four equal triplets or two equal triplets.

The range of information gathered spectroscopically on these compounds allows for some likely catalyst structures to be proposed. From the ^{1}H NMR, three types of butoxides are present, one bridging on tin, one terminal on tin, and two terminal on titanium. DOSY NMR showed that at least one octoate ligand was on the major compound as well, and the molecular weight should be above 500 g/mol. The ^{119}Sn NMR frequency was shifted upfield significantly which, for ^{119}Sn nuclei, is often attributable to an increase in the coordination number of tin.[22,23] Taking these observations into account, a proposed structure is presented in Scheme 2.2 which matches the above observations. This heterobimetallic dimer possesses a single butoxide bridging ligand, a single terminal Sn-bonded butoxide, and two Ti-bonded butoxides. The octoate was placed in a bridging position to maintain a single bridging butoxide and the Sn metal goes from 2-coordinate to 3-coordinate. However, the molecular weight of this suggested compound is 602 g/mol which is ca. 100 g/mol higher than what was calculated from DOSY experiments. This discrepancy may not be unexpected, though. Dimer compounds are known to have underpredicted masses by DOSY when only monomeric calibration standards are used in the calibration curve as was the case in this study.[19] This means that 500 g/mol should be thought of as a lower limit to the true molecular weight. The true mass is most likely higher. This underprediction has previously been attributed to the change in shape of dimers causing changes in diffusion characteristics.

Scheme 2.2. Proposed structure for the major in TBT:2SnOct.

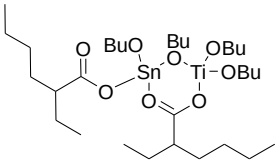

Possible major compound

2.3.2 Discussion of TBT:2DBTDL

From the analysis of the mixed TBT:2DBTDL catalyst by DOSY (Figure 2.8) it was found that two main compounds and a minor compound are present, one of the main compounds being unreacted DBTDL. The other main compound contains only one tin, as shown by a singlet in ^{119}Sn shifted upfield. The shift to -198 from -149 ppm is associated with an increase in coordination number to 5 or 6-coordinate tin(IV).[23] Similarly to TBT:2SnOct, the butoxide α-CH_2 protons on the major new TBT:2DBTDL species exhibit three major groupings where some contain large coupling constants indicative to geminal coupling. DOSY NMR indicates, again, that the butoxide ligands are all on the same compound. This means they can be thought of as μ^2-bridging, terminal Sn-bonded, and terminal Ti-bonded butoxide ligands again. The most downfield resonances at 4.57 ppm fit well into the region where bridging alkoxide ligands have been reported, and DOSY spectra and ASAP-MS show compounds with both butoxide and laurate ligands to confirm ligands are distributed between both tin and titanium.

Considering that the major new compound contains one tin, but also ^{1}H butoxide resonances indicative of bridging, a Sn-Ti dimer is again proposed. A possible structure is shown in Scheme 2.3 that contains the correct ratio of butoxide ligands on Sn, Ti, and bridging and a laurate ligand. The molecular weight of the proposed structure is 789 g/mol, close to the 770 g/mol predicted in DOSY. This structure matches up with the ASAP-MS peak at 673 m/z (Figure 2.9) with an additional butoxide ligand added to form a neutral compound.

Scheme 2.3. Proposed structure of major new compound in TBT:2DBTDL.

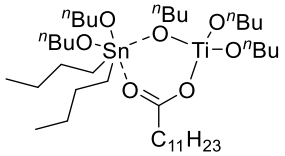

2.3.3 Hypotheses for improved activity

Analysis of the reactivity of each catalyst using a Fischer esterification of phthalic anhydride showed that the catalyst stability, seen *ex situ* by UV-vis, translates into robustness under reaction conditions. Taking the reaction conversion in the first 15 minutes as an approximation of initial activity, the TBT:2SnOct mix has competitive activity with any of the less stable pure complexes, and while the activity of TBT:2DBTDL is not as high as pure TBT, it makes up for the deficiency with better sustained activity. The mixed catalysts are more robust and do not show the usual stability-activity trade-off as comparable activity is maintained relative to the less stable pure compounds.

The stability of Sn-Ti dimers can be explained by analogy to the known improvement in water resistance of Sn_2 dimers (distannoxanes).[4] Higher coordination metal centers in the clusters reduce the accessibility of water to perform hydrolysis reactions. This higher stability can allow for a higher number of catalyst turnovers before deactivation, and in this way give faster times to high yields.

Where the favorable activity of metal clusters may have previously been attributed to the proximity of multiple metals giving higher preorganization of reactants, initial rate studies (Figure 2.16) suggest that this is not the case for these compounds. [21,22] Another possible explanation of high catalyst activity is rooted in the addition of Sn-OBu connectivity upon mixing. SnOct has been utilized as an effective catalyst for ε-caprolactone ring opening polymerization, but it is accepted that SnOct itself is only the precursor to the active catalyst of OctSn-OR or $Sn(OR)_2$.[8] The active catalyst is only formed *in situ* by ligand exchange with coadded alcohol. When the pure stannous alkoxide, $Sn(O^nBu)_2$, is synthesized pre-reaction instead

of *in situ*, faster initial activity is achieved over $Sn(Oct)_2$ demonstrating that the necessary step of alcohol coordination is hindered by the need to remove an octoate ligand. For TBT:2SnOct, the new Sn-butoxide connectivity may be allowing for the more facile association of 2-ethylhexanol or carboxyl reactants onto the metal. The activity of TBT:2DBTDL is a balance between low activity DBTDL and high activity TBT, so are not improved as much as SnOct mixtures by dimer formation.

2.3.4 Prospects

These catalysts have the advantage of having a simple synthesis from highly available starting compounds that results in a relatively complex catalyst structure with improved catalytic characteristics. We imagine that similar structures may be formed by the mixture of titanium alkoxides with oxophilic metals other than environmentally harmful tin complexes. The characterization methods used herein will allow for simple characterization of other compounds by examination of ligand exchange and clustering.

2.4 Conclusion

To summarize, mixtures of titanium *n*-butoxide (TBT) with either stannous octoate (SnOct) or dibutyltin dilaurate (DBTDL) were synthesized and characterized spectroscopically and the reactivity was monitored using two probe reactions designed to simulate industrial polymerization reactions. The stability of the mixtures was demonstrated by a decrease in colloid formation when in an aqueous environment using UV-vis spectroscopy. Structural features were then identified using a suite of techniques including ^{1}H, $^{13}C\{^{1}H\}$, and ^{119}Sn, as well as ^{119}Sn-^{1}H HMQC, ^{1}H-^{1}H COSY, DOSY NMR, and ASAP-MS. A combination of higher observed molecular weights, NMR signals indicative of bridging ligands, and Sn-H correlations led to the identification of likely heterobimetallic dimers. The mixed catalysts showed superior stability during a Fischer esterification and competitive activity in transesterification relative to pure TBT or SnOct. Both ligand exchange onto tin and cluster formation were hypothesized to be contributing factors to the favorable reactivity. Future work should examine whether other oxophilic metals can form stable clusters with titanium complexes as substitutes for regulated tin compounds.

2.5 Experimental

Catalyst Synthesis. A set of mixed catalysts were synthesized from common Ti and Sn sources (*i.e.,* $Ti(O^nBu)_4$ (Sigma-Aldrich, 97%), dibutyltin dilaurate (Sigma-Aldrich, 95%), and stannous octoate (tin(II) 2-ethylhexanoate) (Sigma-Aldrich, 92.5-100%) (Scheme 1). These were generally mixed in a 2:1 mole ratio of Sn to Ti to match the most effective ratio found in the patent literature.[2,3] Syntheses were conducted under a dry N_2 atmosphere although this was found to be unnecessary to form the compounds of interest; synthesis under air indeed showed similar speciation. Storage of the moisture sensitive Ti and Sn precursors was in a dry N_2 glovebox, so synthesis under these conditions was expedient. Each mixture showed a color change from colorless to a shade of yellow to red and a small increase in temperature of 5-15 °C to indicate the exothermic formation of a new compound. Precursor complexes were stirred until the temperature of the mixture had dropped back to room temperature (20-30 minutes) to ensure complete reaction. The resulting viscous oils were stored in amber vials with Teflon caps in a desiccator covered in aluminum foil to prevent excess contact with humidity and possible photoactivity of TiO_2 or SnO_2 which could potentially be formed from catalyst hydrolysis. The catalysts were monitored for decomposition into secondary compounds throughout our study and new catalyst mixtures were regularly synthesized to maintain the primary catalyst species during testing.

Scheme 2.4. Synthesis outline for making TBT:2SnOct and TBT:2DBTDL.

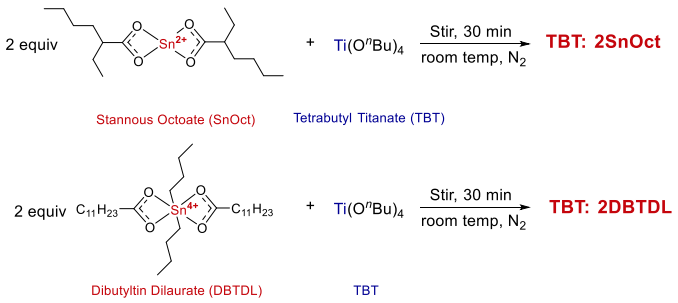

DOSY-NMR. experiments to obtain diffusion data were collected on a Bruker Avance 400MHz instrument equipped with a broadband BBFO probe in 5 mm NMR tubes at 298K, nominally. The pulsed-field gradient pulse sequence used to collect DOSY data follows Jerschow & Muller and uses double stimulated echo pulses and convection compensation to cancel any constant-velocity effects, longitudinal eddy current delay and bipolar gradients to compensate for eddy currents (dstebpgp3s(1d)).[24,25]

Diffusion constants (D) were determined by plotting ln(I/Io) versus $-\gamma^2\delta^2G_Z^2D[\Delta + (4\delta/3 + 3\tau/2)]$. I is the signal intensity, I_0 is the intensity without gradient pulse (at very small gradient values), γ is the gyromagnetic ratio (4.258 x 103 s-1 G-1), δ is the length of the bipolar gradient pulse (p30 x 2, 2000μs), G_Z is the gradient strength (~ 0.60 G cm-1 x gpz1), Δ is the time between pulses (d20, 0.07s), and τ is the gradient ringdown delay (d16 x 2). The diffusion encoding gradient pulse strength was stepped through, while keeping diffusion delay time constant, by changing gpz1 from 98 to 5% over 16 increments with four dummy scans and 8 scans per increment. The diffusion delay time was optimized to allow for intensity (I) to reach 5-10% of I_0 at 95% gradient strength and the gradient duty cycle (p30 / (d1 + aq)) was kept at less than 0.05. Diffusion coefficients were calculated with Dynamics Center software (Bruker, Billerica, U.S.A.) or the T1/T2 module in TopSpin 4.1.

Samples for DOSY NMR data collection were prepared at 0.1 M analyte concentration in $CDCl_3$. An internal reference standard of trimethylphenylsilane (TMPS) was added to each sample at 0.1 M and used to normalize the variation in diffusion constant values caused by differences in viscosity across samples or small temperature differences during acquisition. To apply this correction the diffusion constant of TMPS alone was found (DTMPS(std)) and deviations from the value of log(DTMPS(std)) were corrected by shifting each log(D) in a sample by the difference in log(DTMPS(std)) and the diffusion of TMPS in each specific sample log(DTMPS) (see Equation 2.1). The internal standard showed differences in diffusion constants of up to 11% which is thought to be mostly due to higher sample viscosity when 0.1 M of catalyst

is added since temperature was mostly constant and all runs were performed on the same instrument. Corrections were only due to TMPS diffusing more slowly in catalyst-containing samples.

$$\log(\text{Dcorrected}) = \log(D) - (\log(D_{TMPS(std)}) - \log(D_{TMPS})) \quad (2.1)$$

An external calibration curve was generated from compounds all with a similar shape to approximate the molecular weight of the unknown catalyst species. The importance of molecular shape for comparing diffusion characteristics has been pointed out in previous work. Compounds were chosen for the calibration curve from those suggested by Stalke and coworkers as ellipsoids or diffuse spheres since organometallic compounds diffuse most like diffuse spheres.[26,27] It is possible that the unknown compounds formed in the mixed compounds have different enough shapes to not be ideally fit by the calibration curve of ellipsoids/diffuse spheres as gold dimers were shown to have a different linear relationship between $\log(MW/MW_0)$ and $\log(D/D_0)$ than gold monomers.[19] Molecular weights of unknowns were estimated by averaging all resolved signals at the same diffusion constant and calculating a molecular weight via the calibration curve fit. Calculated molecular weights were rounded to the nearest 10 g/mol to reflect the deviation in diffusion constant between averaged signals.

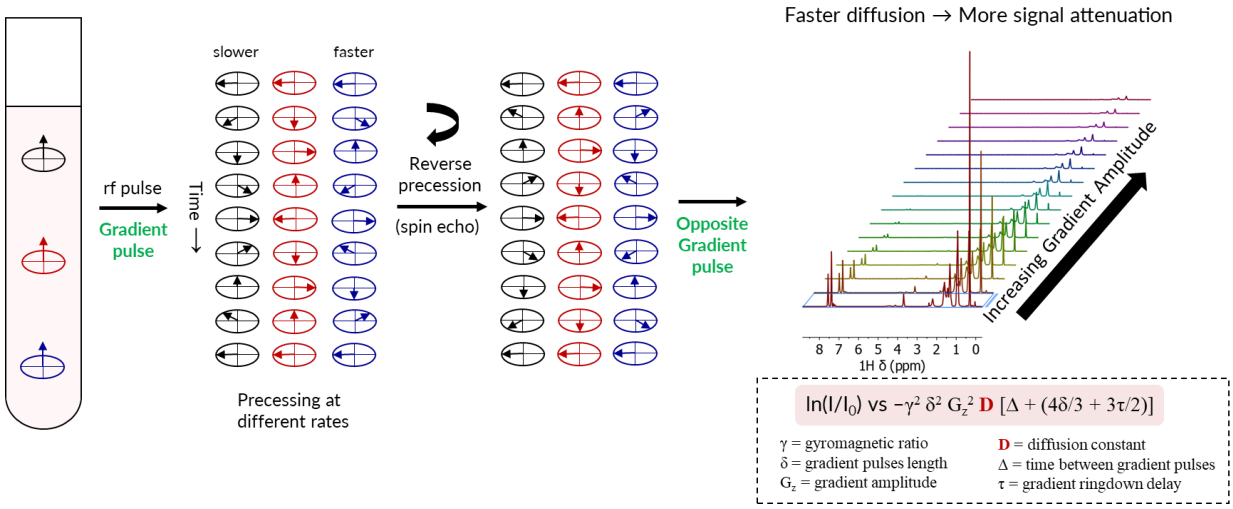

Figure 2.18. Pictorial representation of Diffusion-Ordered Spectroscopy (DOSY) NMR

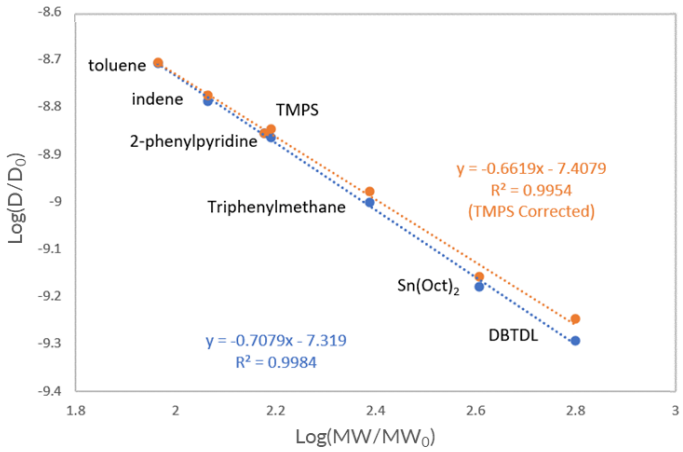

Figure 2.19. External calibration curve for DOSY measurements. The blue line is uncorrected diffusion values and the orange are the corrected values. The orange was used for calculated MW of unknowns.

UV-vis spectroscopic measurements. UV-vis were collected on an Ocean Optics Mayapro spectrometer equipped with a deuterium and halogen lamp. Catalysts were diluted in hexane to ensure the maximum absorbance was less than 1.0. Stability testing was carried out by adding water to a diluted catalyst and shaking to improve catalyst-water contact. Pure TBT or Sn complexes had 100 equivalents of water added. Mixed compounds had 8,700 equivalents of water added to show change over 5 days.

NMR collection. NMR spectra were all collected on a Bruker Avance 400 MHz instrument equipped with a broadband BBFO probe in 5 mm NMR tubes without heating or cooling. All spectra were run in $CDCl_3$ and TMS was used as an internal reference at 0.0 ppm. ^{119}Sn spectra were collected with high analyte concentration of 100-200 µL with 500 µL $CDCl_3$ and a normal spectrum was collected over 2500 scans. TMS in the ^{1}H spectrum was used as an external standard for ^{119}Sn shift to avoid repeated use of toxic Me_4Sn, but the veracity of referencing was double checked once with Me_4Sn as an internal standard set at 0.0 ppm. ^{119}Sn-^{1}H HMQC spectra were collected over a range of optimized coupling constants from 1 Hz to 150 Hz to cover most possible coupling constants. Other two-dimensional spectra were all collected using standard Bruker pulse sequences.

Probe reactions. Probe reactions were run in a 25-mL 2-neck round-bottom flask under a N_2 blanket with a Dean-Stark trap attached to allow for water or methanol removal. Reaction progress was monitored by taking aliquots and measuring the ^{1}H NMR signals of resolved protons with mesitylene as an internal standard.

2.6 References

(1) Otera, J.; Nishikido, J. *Esterification: Methods, Reactions, and Applications, Second Addition*, 2nd ed.; Wiley-VCH Verlag, 2009. https://doi.org/10.1002/9783527627622.

(2) Vogt, H. C.; Parekh, M.; Patton, Jr, J. T. Tin Titanium Complexes as Esterification/Transesterification Catalysts. US4018708A, 1977.

(3) Vogt, H. C.; Parekh, M.; Patton, Jr, J. T. Tin Titanium Complexes as Esterification/Transesterification Catalysts. US4040010A, 1977.

(4) Otera, J. Transesterification. *Chem Rev* **1993**, *93* (4), 1449–1470. https://doi.org/10.1021/cr00020a004.

(5) Donald L. Deardorff. Titanium Compounds. 4788172, 1988.

(6) Bander, J. A.; Lazarus, S. D.; Twilley, I. C. Catalytic Process for Preparation of Polyesters. 4260735, 1981.

(7) Storey, R. F.; Sherman, J. W. Kinetics and Mechanism of the Stannous Octoate-Catalyzed Bulk Polymerization of-Caprolactone. **2002**. https://doi.org/10.1021/ma010986c.

(8) Punyodom, W.; Meepowpan, P.; Molloy, R. Novel Tin (II) Butoxides for Use as Initiators in the Ring-Opening Polymerisation of ε -Caprolactone. *Chiang Mai Journal of Science* **2009**, *36* (2), 136–148.

(9) Houghton, R. P.; Mulvaney, A. W. Mechanism of Tin(IV) -Catalysed Urethane Formation. *J Organomet Chem* **1996**, *518* (1–2), 21–27. https://doi.org/10.1016/0022-328X(96)06223-7.

(10) Pagliarani, A.; Nesci, S.; Ventrella, V. Toxicity of Organotin Compounds: Shared and Unshared Biochemical Targets and Mechanisms in Animal Cells. *Toxicology in Vitro* **2013**, *27* (2), 978–990. https://doi.org/10.1016/j.tiv.2012.12.002.

(11) Jokšas, K.; Stakėnienė, R.; Raudonytė-Svirbutavičienė, E. On the Effectiveness of Tributyltin Ban: Distribution and Changes in Butyltin Concentrations over a 9-Year Period in Klaipėda Port, Lithuania. *Ecotoxicol Environ Saf* **2019**, *183*. https://doi.org/10.1016/j.ecoenv.2019.109515.

(12) Ema, M.; Kurosaka, R.; Amano, H.; Ogawa, Y. Comparative Developmental Toxicity of Butyltin Trichloride, Dibutyltin Dichloride and Tributyltin Chloride in Rats. *Journal of Applied Toxicology* **1995**, *15* (4), 297–302. https://doi.org/10.1002/jat.2550150411.

(13) *Stannous Octoate; CAS RN: 301-10-0; S3252; rev. 6.5; Sigma-Aldrich Inc., St. Louis, MO, June 6, 2023. https://www.sigmaaldrich.com/US/en/sds/aldrich/s3252 (accessed 2023-11-04).*

(14) Mody, B. *Tyndall Effect*. https://chem.libretexts.org/Bookshelves/Physical_and_Theoretical_Chemistry_Textbook_Maps/Supplemental_Modules_(Physical_and_Theoretical_Chemistry)/Physical_Properties_of_Matter/Solutions_and_Mixtures/Colloid/Tyndall_Effect (accessed 2021-11-06).

(15) Lichtenberger, R.; Baumann, S. O.; Bendova, M.; Puchberger, M.; Schubert, U. Modification of Aluminium Alkoxides with Dialkylmalonates. *Monatsh Chem* **2010**, *141* (7), 717–727. https://doi.org/10.1007/s00706-010-0317-1.

(16) Iovkova-Berends, L.; Berends, T.; Zöller, T.; Bradtmöller, G.; Herres-Pawlis, S.; Jurkschat, K. Tin(II) and Tin(IV) Compounds with Scorpion-Shaped Ligands - Intramolecular N→Sn vs. Intermolecular O→Sn Coordination. *Eur J Inorg Chem* **2012**, *2012* (19), 3191–3199. https://doi.org/10.1002/ejic.201200145.

(17) Le Calvé, S.; Alonso, B.; Rozes, L.; Sanchez, C.; Rager, M. N.; Massiot, D. Structure and Surface Reactivity of Transition-Metal–Oxo–Organo Clusters: Contribution of Liquid- and Solid-State NMR to the Characterization of the Cluster Ti16O16(OEt)32. *Comptes Rendus Chimie* **2004**, *7* (3–4), 241–248. https://doi.org/10.1016/J.CRCI.2003.12.010.

(18) Mehrotra, A.; Mehrotra, R. C. Magnetic Nonequivalence of Methyl Protons in Metal Isopropoxides. *J Chem Soc Chem Commun* **1972**, 189–190.

(19) Hamdoun, G.; Bour, C.; Gandon, V.; Dumez, J.-N. Empirical Estimation of the Molecular Weight of Gold Complexes in Solution by Pulsed-Field Gradient NMR. *Organometallics* **2018**, *37* (24), 4692–4698. https://doi.org/10.1021/ACS.ORGANOMET.8B00709.

(20) Nickson,); Kwasnik, A. ; Mathew, H. R. ; Swartz, C. J. ; Wil-Liams, T. D. ; Digiorgo, R. O. ; Yano, T.; Nakashima, K.; Otara, J.; Okawara, R. Tin-119 NMR Spectroscopic Study on Tetraorganodistannoxanes. *Organometallics* **2002**, *4* (9), 1501–1503. https://doi.org/10.1021/OM00128A002.

(21) Otera, J.; Dan-oh, N.; Nozaki, H. Novel Template Effects of Distannoxane Catalysts in Highly Efficient Transesterification and Esterification. *Journal of Organic Chemistry* **1991**, *56* (18), 5307–5311. https://doi.org/10.1021/jo00018a019.

(22) Wang, L.; Kefalidis, C. E.; Roisnel, T.; Sinbandhit, S.; Maron, L.; Carpentier, J. F.; Sarazin, Y. Structure vs 119Sn NMR Chemical Shift in Three-Coordinated Tin(II) Complexes: Experimental Data and Predictive DFT Computations. *Organometallics* **2015**, *34* (11), 2139–2150. https://doi.org/10.1021/om5007566.

(23) Martins, J. C.; Biesemans, M.; Willem, R. Tin NMR Based Methodologies and Their Use in Structural Tin Chemistry. *Prog Nucl Magn Reson Spectrosc* **2000**, No. 36, 271–322.

(24) Jerschow, A.; Müller, N. Convection Compensation in Gradient Enhanced Nuclear Magnetic Resonance Spectroscopy. *Journal of Magnetic Resonance* **1998**, *132* (1), 13–18. https://doi.org/10.1006/JMRE.1998.1400.

(25) Jerschow, A.; Müller, N. Suppression of Convection Artifacts in Stimulated-Echo Diffusion Experiments. Double-Stimulated-Echo Experiments. *Journal of Magnetic Resonance* **1997**, *125* (2), 372–375. https://doi.org/10.1006/JMRE.1997.1123.

(26) Bachmann, S.; Neufeld, R.; Dzemski, M.; Stalke, D. New External Calibration Curves (ECCs) for the Estimation of Molecular Weights in Various Common NMR Solvents. *Chemistry - A European Journal* **2016**, *22* (25), 8462–8465. https://doi.org/10.1002/chem.201601145.

(27) Neufeld, R.; Stalke, D. Accurate Molecular Weight Determination of Small Molecules via DOSY-NMR by Using External Calibration Curves with Normalized Diffusion Coefficients. *Chem Sci* **2015**, *6* (6), 3354–3364. https://doi.org/10.1039/c5sc00670h.

Chapter 3. Non-Tin Metals Mixed with Titanium as Non-toxic Polyester Catalysts

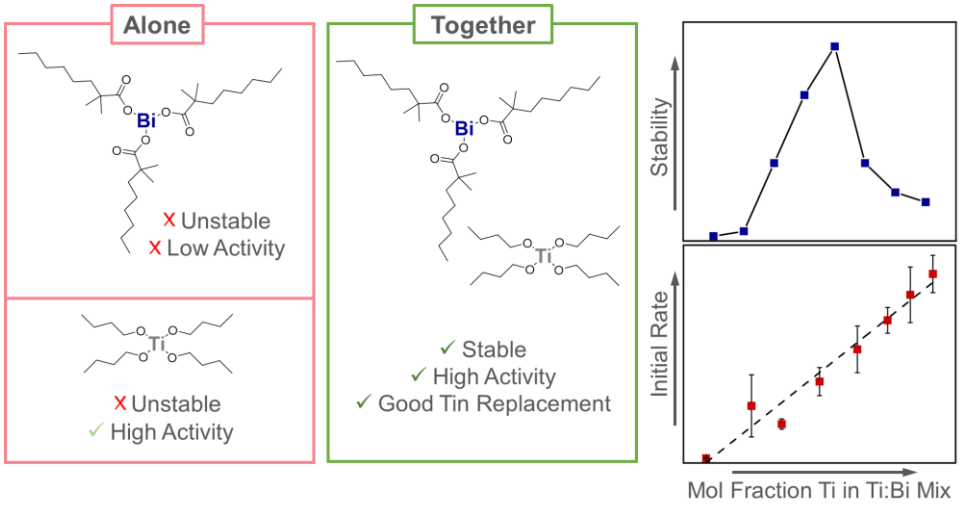

In this chapter, the ideas first investigated in chapter 2 are expanded upon into new directions, namely nontoxic metals instead of tin. Titanate catalysts such as titanium tetrabutoxide (TBT) have long been known to be effective polyesterification catalysts. However, their use on industrial scale has been hindered by their sensitivity to moisture. Previously, this challenge has been addressed by using mixtures of titanate catalysts with tin-based catalysts such as stannous octoate (SnOct), showing both a synergistic effect for hydrolytic stability and polyesterification activity. Unfortunately, due to toxicity concerns around tin catalysts, this efficient catalyst mixture is not a long-term viable solution. Herein we report that mixing TBT with bismuth neodecanoate (BiNeo) leads not only to greater reactivity but also improvements in hydrolytic stability of the catalyst under industrially relevant conditions while being nontoxic. We demonstrate that the 2:1 molar mixing ratio of TBT/BiNeo leads to the best hydrolytic stability. Enhanced

stability of the catalyst led to increased turnovers for the catalyst *vs*. TBT or BiNeo alone, while the inherent activity of the catalyst remained similar to monometallic systems.[2]

[2] The work presented in this chapter is largely adapted from the following publication: Jansen, J. H.; Mathews, D.; Marrione, A.; Román-Matías, J.; Al Abdulghani, A.; Powell, A. B.; Gerislioglu, S.; Keown, W.; Specht, S. E.; Hermans, I. Sustainable and Stable Esterification Catalysts Made from Titanium-Bismuth Clusters. *ACS Sus Chem Eng.* **2024**, 12, 9612-9619. J. H. Jansen wrote the publication and conducted all of the materials synthesis, reaction studies, and characterization present, with the exception of the ASAP-MS measurements which were collected by S. Gerislioglu and DFT calculations performed by A. Al Abdulghani.

3.1 Introduction

Polyesters are one of the highest volume plastic resins produced annually with a wide range of applications.[1] Polyesters are synthesized either *via* transesterification or Fischer esterification from carboxylic acids, and most times a catalyst is added to speed up the time needed to reach a high level of polymerization. These catalysts can be inorganic Brønsted acids, such as sulfuric acid, which can lead to unwanted side products and yellowing of the resulting polymer. Lewis acidic metal catalysts, such as titanium, zirconium, aluminum, or tin, are therefore preferred, especially when processing temperatures exceed 160 °C. Important factors for industrial catalyst selection include high activity, high stability, and low toxicity. The most common class of nontin catalysts are titanates, which are titanium complexes containing primarily oxygen- or nitrogen-based ligation spheres such as titanium tetrabutoxide ($Ti(O^nBu)_4$ or TBT). While these catalysts generally possess high activity and low toxicity, they are also prone to reaction with water to generate less active polyoxometalate clusters. This clustering effect is well-known to correlate with the formation of colloidal TiO_x agglomerates along with clouding and yellowing of resultant polymers.[2,3] A major challenge for the catalysts used for polyesterification is achieving both stability and activity since highly oxophilic metals are both more apt to activate carbonyl-containing reactants, thus promoting esterification *via* oxygen-based coordination, and to accept water as a ligand which can lead to oxide formation and a reduction in Lewis acidity of the metal center. Therefore, to maintain stability and activity, alternatives to simple monometallic complexes have been explored.

We previously reported on the industrially-developed mixed-metal catalyst of TBT and a tin carboxylate, namely stannous octoate (SnOct) or dibutyltin dilaurate (DBTDL).[4,5] In this case there were substantial improvements in catalyst stability, especially in the preferred mixing ratio of 1 mole of TBT for every 2 moles of tin carboxylate (TBT:2SnOct or TBT:2DBTDL). We showed that mixing these metal complexes generated heterobimetallic dimers and we attributed the remarkable stability of the catalysts to this cluster structure. However, these tin compounds are reported as harmful to humans and the

environment, so in an effort to find alternatives to tin, we have set out to expand the understanding of mixed-metal catalysts to nontoxic metal compositions.[6,7]

The rather harsh reactions conditions necessary for polyesterification have in part limited the bimetallic catalysis reported until recently.[4] However, correlations to related transformations with similar mechanisms can be useful for the ideation of potential nontin polyesterification catalysts. For example, in the realm of polyurethanation, Dielmann *et. al*. found that mixtures of lithium carboxylates and bismuth carboxylates spontaneously generated Bi_2Li_4 clusters that improved the reactivity of the bismuth precursor by adding a stronger Lewis acidic metal in lithium.[8] There have also been studies into the complexes generated by mixing different pairs of metals in the realm of metal-oxides for various materials applications.[9–12] These studies often find that mixed-metal complexes form small, heterometallic clusters.

We sought to test tin-free mixed-metal complexes for their efficacy toward polyesterification reactions and identified titanium complexes and bismuth complexes as interesting mixtures for investigation. Examples of bismuth's use as a polyesterification catalyst could not be found, however, widespread literature exists for its use as a tin-free replacement in urethane chemistry.[13,14] This lack of study, especially in combination with other metals, prompted us to explore bismuth as a cocatalyst. In addition to this, bismuth(III) has electronic similarities to tin(II) that has already been shown to have synergistic properties when combined with titanium catalysts. The resulting mixtures of TBT with bismuth neodecanoate (BiNeo) were characterized by their stability to hydrolysis and reaction conversion in a probe esterification reaction. Initial rate studies and characterization *via* diffusion-ordered nuclear magnetic resonance spectroscopy (DOSY NMR) and atmospheric solids analysis probe mass spectrometry (ASAP-MS) along with exchange spectroscopy (EXSY) NMR and DFT calculation on the energetics of likely structures gave understanding of the structure and function of the mixed-metal catalysts.

3.2 Experimental

Catalyst Synthesis. A set of mixed catalysts were synthesized from the following precursors: $Ti(O^nBu)_4$ (Sigma-Aldrich, 97%), bismuth neodecanoate (Sigma-Aldrich), titanium octoate (Thermo Scientific 97%), zirconium octoate (Alfa Aeser 97%). Syntheses were conducted in a dry N_2 glovebox and mixed-metal catalysts were stored in a dark desiccator as previously described.[4] Upon mixing any of the precursors, an increase in temperature of 5-15 °C was observed, indicating an exothermic reaction/complexation. Precursor complexes were stirred until the temperature of the mixture stabilized to room temperature (20-30 minutes) to ensure complete reaction. Mixed compounds denoted using a forward slash (e.g. TBT/BiNeo) refers to mixtures of TBT and BiNeo in general, while mixed compounds denoted using a colon (e.g. TBT:BiNeo or 2TBT:BiNeo) refers to a specific ratio of the precursors.

Probe reactions. Probe reactions were conducted under a constant low flow of nitrogen to prevent catalyst deactivation from atmospheric water. Water or methanol formed during either probe reaction was removed from the reaction via a Dean-Stark trap. Aliquots of 50 µL were taken out of the reaction through a septum and analyzed via 1H NMR using an internal standard of mesitylene. Diagnostic signals in the aromatic region were used for the phthalic anhydride-based probe while the α-CH2 of the esters were used for the methyl benzoate-based probe reaction for quantification. Conversion was calculated by the disappearance of reactant signals. A representative reaction with phthalic anhydride started by mixing 1.89 g (12.8 mmol) of phthalic anhydride (PA) with 6 mL of 2-ethylhexanol (38.3 mmol) to give a 1:3 ratio. To the reactants, 0.5 mol%, relative to phthalic anhydride, of catalyst was added prior to heating. The reaction was then put into an oil bath set to 180 °C and stirred at 300 rpm with a magnetic stirrer bar. The reaction mixture was shown to reach 180 °C roughly 3 minutes after entering the oil bath. Aliquots were taken through the septum starting at 5 minutes to allow for complete ring opening of PA to occur and prevent precipitation of PA upon sampling. The diester product, di-2-ethylhexyl phthalate (DEHP), is a known endocrine disrupter and has reprotoxicity concerns.2 Proper PPE and disposal services should be

used when handling this compound. For transesterification reactions of methyl benzoate with 2-ethylhexanol, 3 mL (19.1 mmol) of methyl benzoate (Sigma-Aldrich, 99%) and 3.72 mL (19.1 mmol) of 2-ethylhexanol were added to a flask for a 1:1 mole ratio. Catalysts were diluted in hexane to help with ease of transferring into the reaction vessel and added at 0.1 mol% loading. The catalyst was added directly prior to heating to 180 °C.

EXSY NMR. EXSY NMR experiments to obtain ligand exchange data were collected on a Bruker Avance 400 MHz instrument equipped with a broadband BBFO probe in 5 mm NMR tubes at 298 K, nominally. Samples were made at 0.1 M in $CDCl_3$ and the mixing time was kept at 0.1 seconds and T1 was 5x the longest of interest to compare between samples.

ASAP-MS Analysis. Mass spectrometry analyses were conducted on a ThermoFisher QExactive quadrupole-orbitrap mass spectrometer equipped with an ASAP as the ionization source. The ASAP source conditions that were used to collect all mass spectra were as follows: discharge voltage at 3.75 kV, discharge current 10.0 µA, capillary temperature at 350 °C, and probe heater temperature at 500 °C. The spectra were collected at *m/z* scan range of 133.4-2000, S-Lens radio frequency level was set to 75.0. The samples were directly applied and adhered onto a glass capillary surface and inserted into the source chamber through the ASAP. The gas-phase ions are generated by desorption of compounds with the heated auxiliary gas (N_2) and corona discharge.

3.3Results

3.3.1 Time-course Reactivity

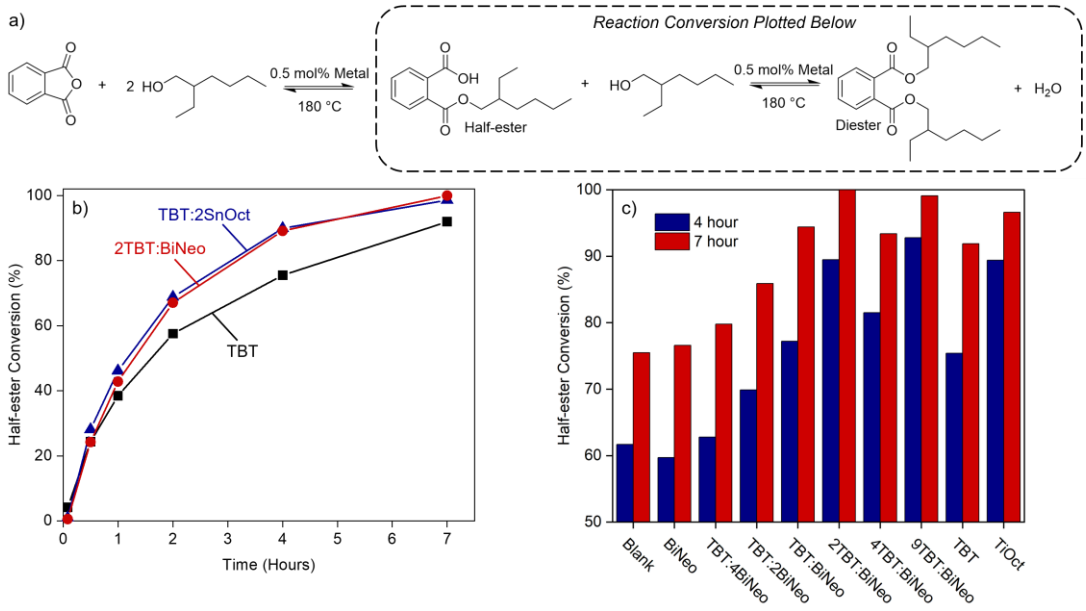

Figure 3.1. a) Probe reaction of phthalic anhydride and 2-ethylhexanol. b) Time-course data for TBT (black squares) and mixed-metal catalysts with stannous octoate (SnOct) (blue triangles) and bismuth neodecanoate (BiNeo) (red circles). c) Reactivity data for different mixing ratios of TBT and BiNeo.

A model probe reaction was selected for the study of these catalysts in consultation with our industrial partner (Figure 3.1a). The reactants were selected due to their structural similarity to monomers used in preparation of industrial polyester-based polymers. For example, the model compound 2-ethylhexanol contains a sterically-hindered primary hydroxyl that serves as a good mimic for the steric profiles of industrially used diols such as 2-methyl-1,3-propanediol and neopentyl glycol. Figure 3.1b contains time course plots for esterification conversion using equimolar amounts of total metal for each of TBT, the previously reported optimal TBT and tin carboxylate mixed catalyst (TBT:2SnOct), and TBT and BiNeo mixed in a 2:1 molar ratio (2TBT:BiNeo) (data on the reactivity and stability of other mixed-metal catalysts can be found in Figure A 3.1 & Table A 3.1). TBT started out with comparable activity to the mixed-catalyst

systems, as judged by the first time-points, but its reactivity slowed down and was accompanied by clouding of the reaction solution (Figure A 3.2a). The time-course for TBT:2SnOct started with a similar level of activity as unmixed TBT but did not slow as quickly and does not show substantial clouding of the reaction mixture. Finally, the time-course for 2TBT:BiNeo matches quite closely with that of TBT:2SnOct and similarly did not result in a cloudy reaction solution.

It has previously been shown that there can be an optimum mixing ratio between TBT and a metal carboxylate such as SnOct.[5] To investigate if there is an optimum ratio for TBT and BiNeo, a set of different ratios were synthesized and tested for the selected probe reaction as shown in Figure 3.1c. Keeping total metal loading constant at 0.5 mol%, the use of bismuth neodecanoate showed reactivity close to the uncatalyzed control reaction. In the TBT/BiNeo mixed catalyst systems as the mole fraction of titanium increased, the total conversion increased with a maximum achieved at 2TBT:BiNeo where 89% conversion was reached in 4 h and 100% conversion after 7 hours. Higher ratios of titanium in the mixtures showed no significant improvement after the 2:1 molar ratio although any higher mole fractions of TBT/BiNeo (*i.e.*, 2:1, 4:1, 9:1) outperformed TBT significantly. To compare the mixed-metal catalysts against a titanium catalyst with bidentate ligands such as carboxylates, titanium octoate (TiOct) was chosen as an industrially-relevant benchmark catalyst and the results were comparable to 2TBT:BiNeo and 9TBT:BiNeo.

3.3.2 Initial Rate Studies

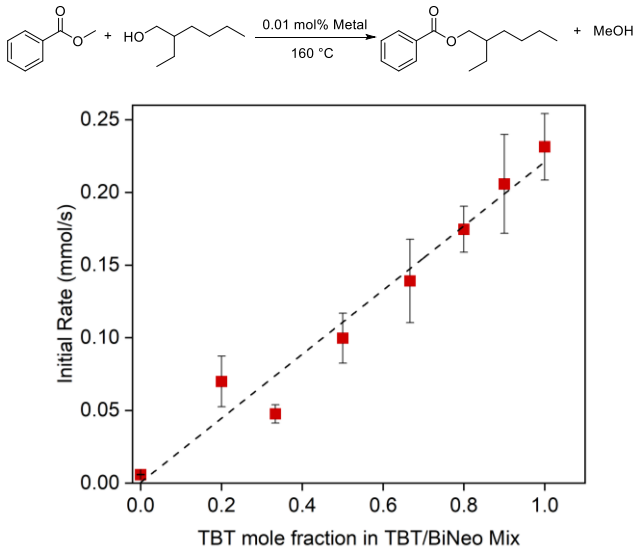

Figure 3.2. Initial rate data of mixed TBT and BiNeo at different ratios. Initial rates collected at <10% conversion at a 0.01 mol% catalyst loading by total metal. Error bars represent 2 standard deviations based off independent duplicate runs. Dotted line is a least-squares fit of the experimental data (R^2 = 0.96).

To explore the synergistic enhancement seen in the mixed catalysts of TBT and BiNeo, the initial rates of a transesterification reaction with mixtures of different TBT/BiNeo ratios were quantified (Figure 3.2). If synergy occurs between the metals, either from greater preorganization of reactants on proximal metals or electronic changes in the Lewis acidity of the metals, a concave down curvature would be expected. However, there is a clear linear trend that correlates the fraction of TBT added to the mix and the initial rate. The next set of experiments were performed to determine the stability of the bimetallic catalysts and their robustness under reaction conditions.

3.3.3 Catalyst Hydrolytic Robustness

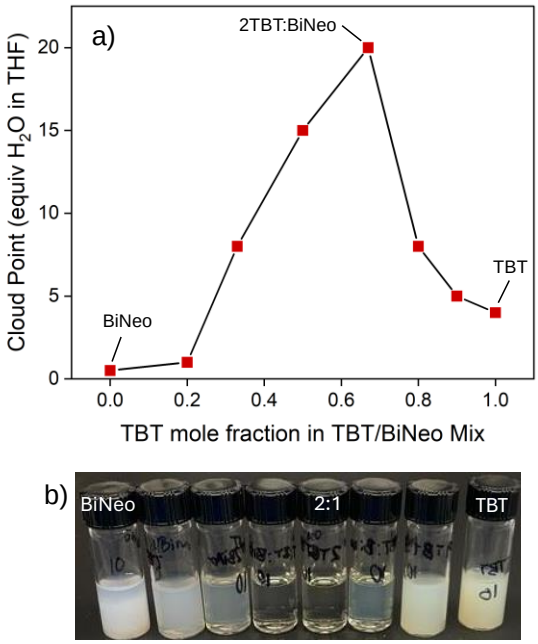

Figure 3.3. Stability of mixed TBT and BiNeo at different ratios. The cloud point is how much water can be mixed into a 0.1 M solution of catalyst (by metal) in THF before visible clouding occurs. a) Cloud points for different ratios of TBT and BiNeo. b) Example image of 10 equivalents of water.

To determine the relative stability of mixtures of TBT and BiNeo, we developed a method to find the minimal amount of water that results in a cloudy appearance when a catalyst is dissolved in a solvent. For this study we found it important to use a solvent like THF that allowed for both water and catalyst to be miscible. **Figure *3.3*** shows the results of this treatment and a volcano plot for stability can be observed where a molar ratio of 2TBT:BiNeo shows the most resistance to becoming cloudy (twenty equivalents of water *vs* catalyst needed to cause a cloudy appearance). However, a wide variety of TBT:BiNeo ratios showed improved resistance to clouding over the unmixed TBT or BiNeo, suggesting the wide breadth of this effect. This ex-situ robustness test in THF allowed for relatively easy catalyst comparisons. It should

be noted however, that polyesterification reactions commonly are performed under either solvent-free conditions or in the presence of hydrocarbon solvents as processing aids. Therefore, it makes sense to explore if the effects observed above apply to relevant catalytic conditions.

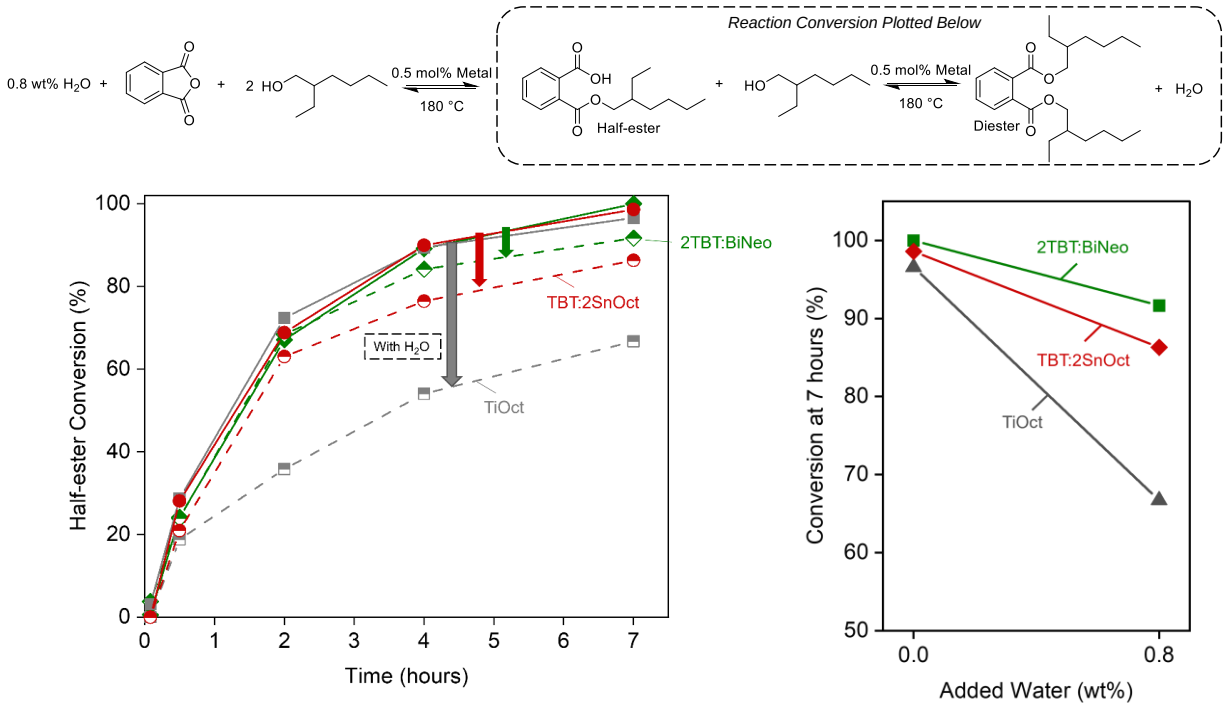

Figure 3.4. Comparison of the ligand-stabilized titanate complex (titanium octoate) with 2TBT:BiNeo and TBT:2SnOct. Water was added at 0.8 wt% H_2O immediately before starting a reaction. Reactions between phthalic anhydride and 2-ethylhexanol with 0.5 mol% metal at 180 °C. Right figure only shows the 7 hour conversion with and without water added.

The most hydrolytically stable mixture of TBT and BiNeo (2TBT:BiNeo) was chosen and compared to the ligand-stabilized titanate (TiOct) as well as the previously studied tin-containing bimetallic catalyst (TBT:2SnOct). A constant amount of water (0.8 wt%) was added at the start of the reactions to simulate the moisture present in industrial assets where polyesterification reactions are typically performed. This comparison sought to determine if ligand- or metal-based stabilization effects were the cause of enhanced robustness to the presence of water under relevant conditions and whether bismuth or tin(II) provided

more robustness. Neodecanoate and octoate ligands are similar ligands being long-chain carboxylates with carbon chains at the α-position. If the hydrolytic stability improvements for 2TBT:BiNeo *vs* TBT alone are solely from ligand exchange from the bismuth complex to the titanium complex it can be expected that titanium octoate would possess similar or better robustness to water *vs* 2TBT:BiNeo. The results of the comparison of 2TBT:BiNeo and TiOct (Figure 3.4) were drastically different. Most noticeably, TiOct had a substantial drop in reactivity when exposed to water, reaching only to 67 % conversion in 7 h, down from 97 % in the absence of intentionally added water. Conversely, 2TBT:BiNeo is much more robust, achieving 92% conversion in the presence of added water, down from 100% conversion for the same reaction time in the absence of intentionally added water. The bimetallic tin-containing catalyst (TBT:2SnOct) also demonstrates enhanced robustness over TiOct, but slightly less than the bismuth-containing catalyst.

3.4 Characterization

Hoping to obtain a structural assignment of the resulting complex(es) generated upon mixing TBT and BiNeo, the growing of crystals suitable for X-ray analysis was attempted. However, the oil evidently has a freezing point below -80 °C [MP(TBT) = -75 °C, MP(BiNeo) = -50 °C] and was practically miscible in common solvents, so no crystal could be obtained for structural analysis. [17,18] Being in the liquid state makes these catalysts especially attractive from an industrial perspective as they can be pumped in through pipes, thus avoiding the need for manual hatch additions. In our previous studies on mixed-metal catalysts of TBT and tin compounds (SnOct or DBTDL), NMR spectroscopy proved to be an invaluable tool in structural assignment.[4]

3.4.1 EXSY NMR spectroscopy

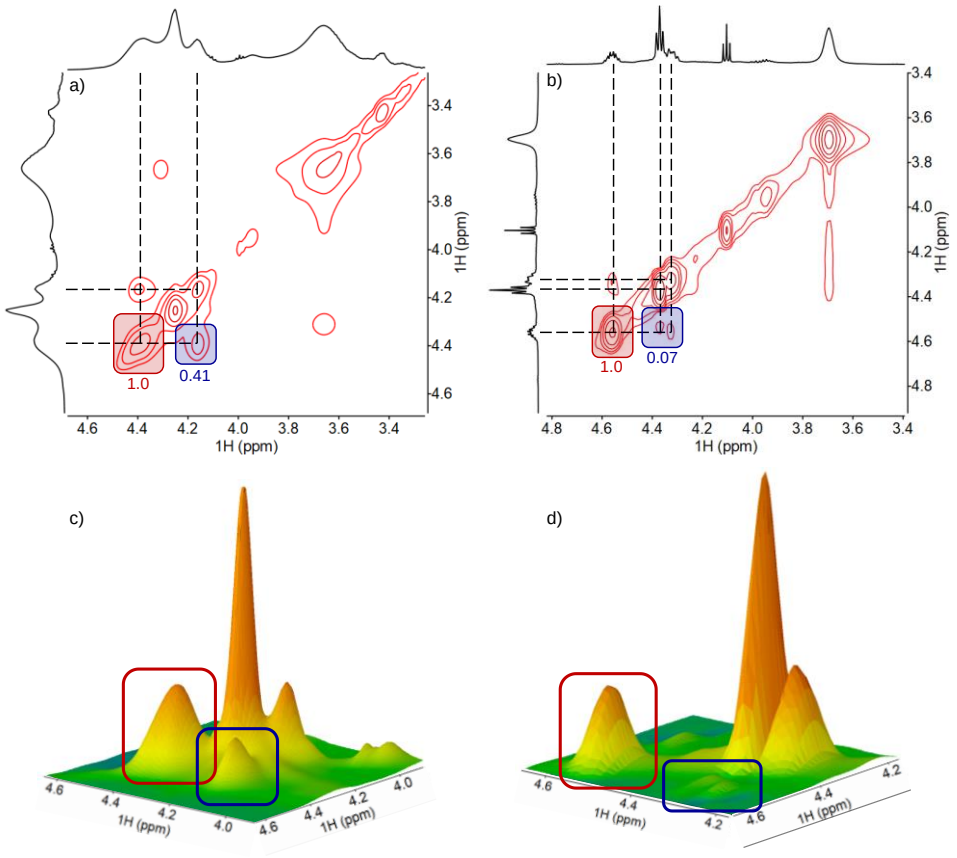

Figure 3.5. 2D EXSY spectra showing ^{1}H NMR signals for α-CH_2 of butoxy ligands (mixing time 0.1 s). Contour plot with dashed lines showing cross-peak correlations to diagonal peaks for (a) TBT:BiNeo and (b) TBT:2SnOct. Red and blue boxed signals show region integrated to quantify cross-peak area (blue box) normalized to red boxed signal. 3D projections of EXSY plot where red and blue boxes match the integrated peaks for in the 2D plots for (c) TBT:BiNeo and (d) TBT:2SnOct.

Surprisingly, the well resolved butoxy signals observed for TBT/SnOct catalyst mixture were not observed for the mixtures of TBT and BiNeo. The ^{1}H NMR spectra for mixtures of TBT and BiNeo show only broad signals (Figure 3.5 1D traces), which suggests fast exchange of butoxy ligands on the NMR time scale between the various possible environments of the resulting complex(es). The much faster exchange of butoxy ligands with the TBT:BiNeo mixtures compared to TBT:SnOct mixtures can be seen clearly using 2D EXSY where the exchange peaks between butoxy signals are much larger (Figure 3.5). The cross peaks in

the 2D contour plots show the exchange of polarization between two different ligands which have switched locations with each other. The larger the cross peak, the more of the ligand from one site has exchanged to the other site. The cross peak integration for butoxide ligand exchange was compared between TBT:BiNeo and TBT:2SnOct normalizing to the most de-shielded resonance. TBT:BiNeo has a much higher exchange peak at 0.41, while a much smaller exchange peak with integration of 0.07 was observed for TBT:2SnOct. This comparison can be seen clearly in a 3D projection of the diagonal and cross peaks of each (Figure 3.5c-d blue boxes). In fact, TBT:BiNeo appears to have the fastest ligand exchange rate out of TBT:ZrOct, TBT:TiOct, and TBT:2SnOct as judged by the broadening of ^{1}H signals in the butoxy region (Figure A 3.4).

A catalyst whose structure possesses excess stability will result in low activity. However, if the catalyst is too active, it can lead to side-products that can be detrimental to catalyst efficacy. Additionally, side-reactions that result in catalyst agglomerates often lead to loss of activity through a lack of available metal sites to interact with reactants and convert them to products.

It was previously shown that TBT mixtures with SnOct or DBTDL tin complexes form dimers.[4] To determine if TBT mixtures with BiNeo form similar clusters, DOSY NMR and ASAP-MS were used as complementary analytical techniques. Pulsed-field gradient experiments were conducted to obtain DOSY plots and diffusion coefficients of the compounds resulting from mixing TBT and BiNeo (Figure A 3.6). The diffusion constant found for TBT:BiNeo is 4.97×10^{-10} m^2/s while BiNeo alone has a significantly faster diffusion constant of 6.09×10^{-10} m^2/s (Figure A 3.7). This reduction of diffusion upon mixing indicates the formation of moderately larger compound such as clusters with a limited number of metals.[4]

3.4.2 ASAP-Mass Spectrometry

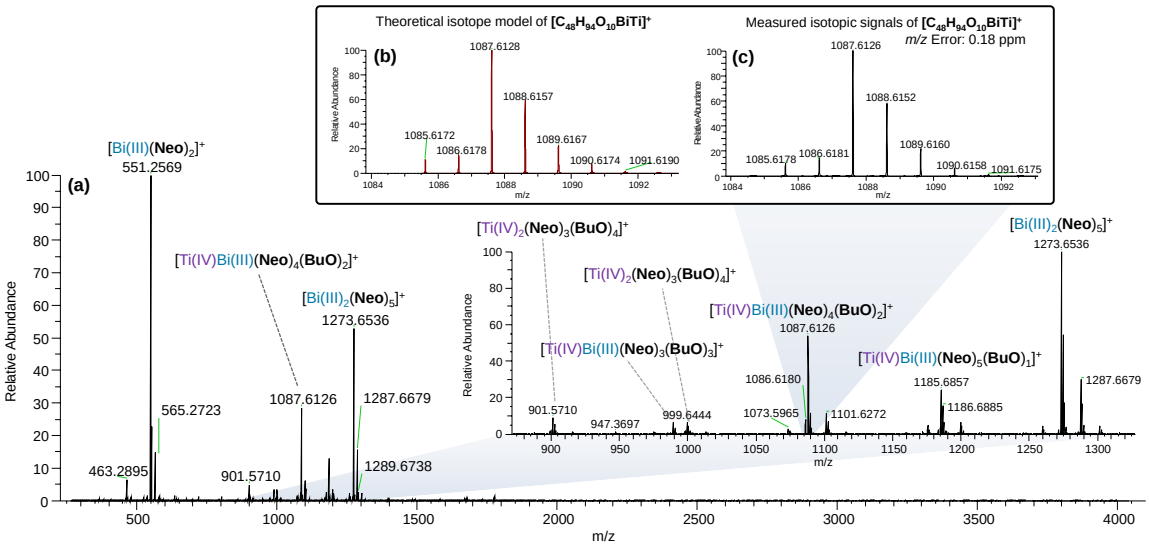

Figure 3.6. ASAP-MS spectrum of TBT:BiNeo sample. The inset shows spectrum expanded over the m/z axis. (b) The theoretical isotope model of the $[Ti(IV)Bi(III)(Neo)_5(BuO)_2]^+$ ($[C_{48}H_{84}O_{10}BiTi]^+$) ion cluster and (c) measured isotopic signal pattern for $[C_{48}H_{84}O_{10}BiTi]^+$.

To support the diffusion data, ASAP-orbitrap-MS was used as a high-resolution mass spectrometry technique with a soft ionization method so that each heterometallic cluster could be identified in intact form. Mass spectrometry is an analytical technique where mass-to-charge (*m/z*) ratio of gas phase ions are measured. Therefore, the heterometallic clusters within the samples needed to be transferred to the gas phase and have a net charge state of at least 1+, allowing them to be detected in positive ion detection mode. This was achieved by desorption/ionization process of ASAP technique under atmospheric pressure, resulting in the loss of a single ligand from each metal complex, while preserving the rest of the cluster as a singly charged cationic complex. Having orbitrap as a high-resolution mass analyzer allowed chemical formula assignment with high confidence through isotope profile matching and high accuracy mass measurement (<1 ppm *m/z* was achieved at *m/z* 1000). ASAP-MS spectrum of TBT:BiNeo showed singly charged ion clusters with monoisotopic signals at *m/z* 999.5444, 1087.6126, and 1185.6857, corresponding to monoisotopic signals of TiBi dimers with different numbers of butoxy and neodecanoate

ligands measured within <1 ppm *m/z* accuracy (Figure 3.6). Mixed catalysts of TBT with TiOct or ZrOct showed higher levels of agglomeration in their mass spectra than TBT:BiNeo (Figure A 3.15 & Figure A 3.16). The agreement between DOSY NMR and ASAP-MS on the presence of dimers supports the assignment of the mixed-metal compounds formed as small clusters.

3.4.3 DFT Structure Energy Calculations

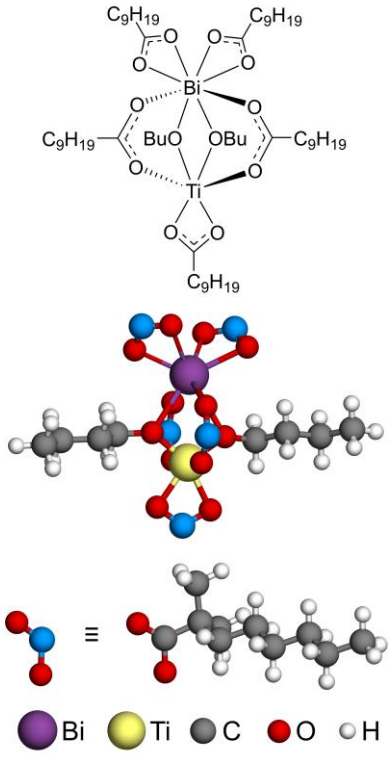

Figure 3.7. Proposed structure for TBT:BiNeo heterobimetallic complex from DFT computation of low energy structures.

DFT calculations were performed using the B3LYP exchange-correlation functional and def2-TZVP basis set, as implemented in Gaussian 16.20 Potential structures were modeled and optimized based on the catalyst composition suggested from the major ASAP-MS ion, $[TiBi(Neo)_4(OBu)_2]^+$. Figure A 3.18 shows a set of different arrangements of $TiBi(Neo)_4(OBu)_3$ and $TiBi(Neo)_5(OBu)_2$, along with their relative DFT energies, referenced to the energies of the isolated alcohol and carboxylic acid. The structure shown in Figure 3.7 was found to have the lowest energy. In this structure, two butoxy and two neodecanoate

ligands tended toward bridging the Ti and Bi atoms. There were two terminal neodecanoate ligands on Bi and one on Ti, all of which were bound to the respective metal as bidentate ligands. Substituting one of the terminal neodecanoate ligands with a butoxy yielded structures that were less stable by 29-31 kJ mol^{-1}. The structure with one terminal neodecanoate ligand on Bi and two on Ti was found to be the least stable by 60 kJ mol^{-1} from the structure shown in Figure 3.7. While Bi exhibited a variable coordination number, Ti always converged as 6-coordinate, making the terminal neodecanoate a monodentate ligand when two terminal ligands were bound to Ti.

3.5 Discussion

Reactivity data (Figure 3.1a) shows that TBT:2SnOct and 2TBT:BiNeo both out-performed TBT alone for esterification. While TBT provides comparable levels of conversion to the mixed-metal catalysts in the beginning stages of reaction, lower total conversion is observed as the reaction proceeds. Comparison of these reaction profiles suggests higher degrees of robustness towards water contamination for the mixed-metal catalysts. Also, noteworthy is that SnOct alone shows activity for esterification (Figure A 3.1c) but BiNeo alone is close to inactive. Thus a lower loading of active metal in the case of 2TBT:BiNeo gives comparable reactivity to TBT:2SnOct.

The reactivity data for different mixing ratios of TBT and BiNeo in the bar chart in Figure 3.1b shows that the highest conversions are reached with ratios of two-to-one or higher where 2TBT:BiNeo gave the highest conversion after 7 hours, marginally more than 9TBT:BiNeo. This optimum ratio is in agreement with the stability data presented in Figure 3.3 showing the 2TBT:BiNeo mixture is the most stable.

It is well known that adding sterically bulky or multi-dentate ligands stabilizes titanium complexes to hydrolysis and thus these ligands often afford improved hydrolytic reactivity *vs* monodentate butoxide ligands.[20] This raises the question of how the mixed-metal catalysts presented here compare with ligand-stabilized titanates. When the 2TBT:BiNeo catalyst was tested against titanium octoate, a ligand-stabilized titanate, superior robustness of the mixed-metal catalyst was observed in the presence of moisture known

to be present under industrially-relevant conditions (Figure 3.4). This demonstrated that the stability of 2TBT:BiNeo is not solely derived from the bulky neodecanoate ligands, but also from a non-ligand-based phenomenon.

Initial rate studies (Figure 3.2) show that stability is the only important synergy that results when TBT and BiNeo are combined. The initial rate scaled linearly with the molar ratio of TBT in the mixture over a range of mixing ratios (9TBT:BiNeo to TBT:4BiNeo). As the reaction is first-order in catalyst, if there was a large reactivity-based synergy between the metals, as has been suggested for previously studied metal clusters, then the initial rate for the intermediate mixing ratios would be expected to possess a concave up curvature which did not occur.[21] The data strongly suggest that the sole active metal in the mixed-metal catalyst is titanium and the secondary component (BiNeo) contributes only toward the stability of the resultant catalyst. A summary of the stability, reactivity, toxicity, and active metal content is provided in Table 3.1 showing the advantages in stability and conversion gained from mixed-metal catalysts, and the improved toxicity profile of 2TBT:BiNeo over TBT:2SnOct.

Table 3.1. Comparison of stability, reactivity, toxicity, and active metal content of catalysts.

Catalyst	TBT	SnOct	BiNeo	TBT:2SnOct	2TBT:BiNeo
Cloud-point[a]	5	5	0.5	10	20
4h Conversion[b]	75.4 %	82.1 %	59.7 %[c]	89.9 %	89.5 %
Toxicity Concern	No	Yes	No	Yes	No
Active metal (mol%)	100%	100%	0%	100%	67%

[a]Equivalents of water needed to cause catalyst clouding at 0.1 M in THF
[b]Half-ester conversion in probe reaction of phthalic anhydride with 2-ethylhexanol at 180 °C and 0.5 mol% metal
[c]An uncatalyzed reaction gave 61.7% conversion

The mixed-metal catalysts were characterized using NMR and ASAP-MS in Figure 3.5 and Figure 3.6. The EXSY NMR spectra shown in Figure 3.5 evidenced the relatively fast ligand exchange of butoxy ligands around TBT:BiNeo vs TBT:2SnOct. This is unexpected as the TBT:BiNeo catalyst is similarly hydrolytically stable. Intuitively, more rapid ligand exchange would indicate that water could also react easily with the

catalyst to lead towards agglomeration and thus deactivation. The observed high exchange rate can be rationalized since bismuth is known to be a weaker Lewis acid than tin or titanium due to being highly polarizable/soft and would be expected to bind the ligands more weakly.[22] Indeed, the converse of this, adding a metal that binds more strongly to oxygen ligands leading to slower ligand exchange, is precedented for Sn_3Ti mixed-metal alkoxide clusters.[23] However, lower oxophilicity of bismuth would also lead to lower reactivity toward water relative to titanium or tin(II). We put forward that this allows for bismuth to act as a spectator metal that does not strongly bind reactants or water but can maintain the overall stability of the proposed cluster. To support the proposed difficulty of bismuth forming BiO_x under reaction conditions, it appears that the preferred deactivation route under reaction conditions is not to the white or yellow oxide but to a black precipitate of Bi^0 (Figure A 3.2).

Based on mass spectrometric analysis and the presence of a slower diffusing compound via DOSY NMR we suggest a dimer with the composition found by mass spectrometry. There are similar core structures between the dimers suggested for TBT:2SnOct and TBT:BiNeo with bridging carboxylate and alkoxide ligands. The analogous core structure is known to form for titanium alkoxides upon mixture with carboxylate ligands or anhydrides.[10,11] We hypothesize that the external butoxide ligands can move freely while bridging ligands and the core structure are maintained. The lack of clouding or blackening of the mixed catalyst when compared to TBT or BiNeo alone, evidence the stability of the newly formed structure.

3.6 Conclusions

In summary, we synthesized bimetallic mixtures of titanium tetrabutoxide (TBT) and metal carboxylates and examined their reactivity towards polyesterification through model reactions. Mixtures of TBT and bismuth neodecanoate (BiNeo) give improved reactivity over TBT or BiNeo and the hydrolytic stability is optimized in a molar ratio of 2:1 (2TBT:BiNeo). The mixture of TBT with BiNeo compares well with a previously studied mixed-metal catalyst of TBT and stannous octoate (SnOct) while requiring less active

metal and being free of tin. This bimetallic catalyst mixture performs especially well relative to industry standard titanium-based Lewis acids when water is present at the beginning of a reaction, simulating industrial polyesterification conditions. The ligand exchange rate is counterintuitively much higher for TBT:BiNeo than TBT:2SnOct while maintaining superior hydrolytic stability. Diffusion-based NMR and ASAP-MS evidence a heterobimetallic cluster structure and DFT calculations of thermodynamic stability inform the ligand arrangement. Overall, the mixed-metal catalyst of 2TBT:BiNeo is more stable than industry standard titanium catalysts, leading to better reactivity and less discoloration without the toxicity concerns around tin-containing alternatives.

3.7 References

(1) Otera, J.; Nishikido, J. *Esterification: Methods, Reactions, and Applications, 2nd ed.;* Wiley-VCH Verlag GmbH & Co. KGaA, 2010. https://doi.org/10.1002/9783527627622.

(2) Yuo, W.-B.; Chen, J.; Chao, Y. Catalytic Compositions for the Preparation for Poly(Ethylene Terephthalate) with Improved Color. US5623047A, 1997.

(3) Rollick, K.; Ferrari, G. Color Control of Polyester-Cobalt Compounds and Polyester-Cobalt Compositions. US11141886B2, 2021.

(4) Jansen, J. H.; Powell, A. B.; Specht, S. E.; Gerislioglu, S.; Hermans, I. Understanding the Structure and Reactivity of Mixed Titanium(IV) Alkoxide and Tin(II)/(IV) Carboxylates as Esterification Catalysts. *ACS Sustain Chem Eng* **2022**, *10* (7), 2484–2493. https://doi.org/https://doi.org/10.1021/acssuschemeng.1c07633.

(5) Vogt, H. C.; Parekh, M.; Patton, Jr, J. T. Tin Titanium Complexes as Esterification/Transesterification Catalysts. US4040010A, 1977.

(6) *Entry 20: Organostannic compounds, Annex XVII to REACH. European Chemical Agency. https://echa.europa.eu/documents/10162/0979d035-4a80-0a4e-ddcc-03d31d5467d6. (accessed 2023-11-05).*

(7) *Stannous Octoate; CAS RN: 301-10-0; S3252; rev. 6.5; Sigma-Aldrich Inc., St. Louis, MO, June 6, 2023. https://www.sigmaaldrich.com/US/en/sds/aldrich/s3252 (accessed 2023-11-04).*

(8) Levent, E.; Sala, O.; Wilm, L. F. B.; Löwe, P.; Dielmann, F. Heterobimetallic Complexes Composed of Bismuth and Lithium Carboxylates as Polyurethane Catalysts – Alternatives to Organotin Compounds. **2021**, *23*, 2747. https://doi.org/10.1039/d1gc00446h.

(9) Artner, C.; Koyun, A.; Czakler, M.; Schubert, U. Mixed-Metal Oxo Clusters Structurally Derived from $Ti_6O_4(OR)_8(OOCR')_8$. *Eur J Inorg Chem* **2014**, *2014* (29), 5008–5014. https://doi.org/10.1002/EJIC.201402499.

(10) Schubert, U. Chemical Modification of Titanium Alkoxides for Sol–Gel Processing. *J Mater Chem* **2005**, *15* (35–36), 3701–3715. https://doi.org/10.1039/B504269K.

(11) Czakler, M.; Artner, C.; Schubert, U. Preparation of Carboxylato-Coordinated Titanium Alkoxides from Carboxylic Anhydrides: Alkoxido Group Transfer from Metal Atom to Carbonyl Group. *Eur J Inorg Chem* **2012**. https://doi.org/10.1002/ejic.201200296.

(12) Parola, S.; Papiernik, R.; Hubert-Pfalzgraf, L. G.; Jagner, S.; Håkansson, M. The Quest for Mixed-Metal Oxide Precursors Based on Bismuth: Synthesis and Molecular Structure of $BiTi_2(\mu_3\text{-}O)(\mu\text{-}OPr^i)_4(OPr^i)_5$ and $[Bi_2(\mu\text{-}OPr^i)_2(OPr^i)_2(acac)_2]$ (acac = acetylacetonate). *J Chem Soc, Dalton Trans* **1997**, 23, 4631–4636. https://doi.org/10.1039/A705365G.

(13) Guhl, D. Alternatives to DBTL Catalysts in Polyurethanes - a Comparative Study. *Polyurethanes for High Performance Coatings, European Coatings Conference,* February 2008, *vol. 5,* pp 119–137. https://doi.org/10.13140/2.1.2416.3209.

(14) Yang, N.; Sun, H. Bismuth: Environmental Pollution and Health Effects. In *Encyclopedia of Environmental Health,* Elsevier, 2011, 414–420. https://doi.org/10.1016/B978-0-444-52272-6.00374-3.

(15) Jerschow, A.; Müller, N. Convection Compensation in Gradient Enhanced Nuclear Magnetic Resonance Spectroscopy. *J Mag Reson* **1998**, *132* (1), 13–18. https://doi.org/10.1006/JMRE.1998.1400.

(16) Jerschow, A.; Müller, N. Suppression of Convection Artifacts in Stimulated-Echo Diffusion Experiments. Double-Stimulated-Echo Experiments. *J Mag Reson* **1997**, *125* (2), 372–375. https://doi.org/10.1006/JMRE.1997.1123.

(17) Titanium(IV) Butoxide, CAS RN: 5593-70-4; 244112; Rev. 6.10; Sigma-Aldrich Inc., St. Louis, MO, June 30, 2021. https://www.sigmaaldrich.com/US/en/sds/aldrich/244112 (Accessed 2023-11-04).

(18) Bismuth Neodecanoate; CAS RN: 34364-26-6; Rev. 6.4; Sigma-Aldrich Inc., St. Louis, MO, March 26, 2023. https://www.sigmaaldrich.com/US/en/sds/aldrich/544132 (accessed 2023-11-04).

(19) Frisch, M. J.; Trucks, G. W.; Schlegel, H. B.; Scuseria, G. E.; Robb, M. A.; Cheeseman, J. R.; Scalmani, G.; Barone, V.; Petersson, G. A.; Nakatsuji, H.; Li, X.; Caricato, M.; Marenich, A. V.; Bloino, J.; Janesko, B. G.; Gomperts, R.; Mennucci, B.; Hratch, D. J. Gaussian 16, Revision C.01. Gaussian, Inc.: Wallingford CT 2016.

(20) Dorf Ketal Tyzor, Organic Titanates and Zirconates. Dorf Ketal. https://www.dorfketal.com/including/PDF Files/K17586_tyzor_gen_brochure_final.pdf.

(21) Davies, A. G. Difunctional Distannoxanes , $XR_2SnOSnR_2X$. *J Chem Res* **2004**, 2, 309–314.

(22) Kepp, K. P. A Quantitative Scale of Oxophilicity and Thiophilicity. *Inorg Chem* **2016**, *55* (18), 9461–9470. https://doi.org/ 10.1021/acs.inorgchem.6b01702

(23) Boyle, T. J.; Segall, J. M.; Alam, T. M.; Rodriguez, M. A.; Santana, J. M. Chemistry of a Novel Family of Tridentate Alkoxy Tin(II) Clusters. *J Am Chem Soc* **2002**, *124* (24), 6904–6913. https://doi.org/10.1021/ja0202309.

Chapter 4. Methods of Lewis Acidity Measurements on Mixed Metal Complexes

In this chapter, a set of methods were tested to find the Lewis acidity of different esterification catalysts, including the different mixed-metal catalysts examined in chapters 2 and 3. Within these previous chapters, methods to measure the stability and initial rate of different esterification catalysts were developed and compared. It would be useful to correlate these bulk robustness and activity measurements with a more fundamental descriptor of the complexes, such as their Lewis acidity. However, the Lewis acidity of a specific complex is not trivial to determine simply based on the metal, especially when multiple metals are involved that are in close proximity. For example, it is possible that metals inductively influence the Lewis acidity of other nearby metals by pulling on their electrons to different extents. The Lewis acidity of a free metal ion will also be different than a metal with ligands and the denticity, hapticity, spatial bulk (sterics) of the ligands, and what atom binds with the metal can be important. When the goal is to correlate reactivity with Lewis acidity, the ability of the Lewis basic carbonyl of an ester, carboxylic acid, or even alcohol reactants to reach the metal and the strength of the bond are the most important variables and so the following experiments have tried to as closely match a measurement of those variables as was possible.

4.1 Introduction

A Lewis acid (LA) is defined as an electron acceptor and conversely a Lewis base (LB) is defined as an electron donor. The catalysts studied within this thesis are Lewis acids which are able to accept electrons from the carbonyl compounds relevant for esterification reactions. This electron accepting interaction activates these starting materials by increasing the partial positive charge on the carbonyl carbon making it a stronger electrophile. The alcohol starting material is also activated by coordinating to the Lewis acid. By increasing the polarity of the RO-H bond to RO-M the alcohol becomes a stronger nucleophile. Effectively, the starting materials are both primed to be more reactive with each other. There are multiple methods that have been published to determine the Lewis acidity of a metal complex, either as a calculated binding energy of a Lewis acid and a Lewis base (global Lewis acidity), a measurable physical/spectroscopic change in a coordinated Lewis base (effective Lewis acidity), or an intrinsic characteristic of the Lewis acid (e.g., LUMO energy, electrophilicity index, electron affinity) (intrinsic Lewis acidity) (See Figure 4.1).[1] In this study, effective Lewis acidity was chosen over global or intrinsic as it was believed to potentially model the catalyst-reactant interaction more realistically since Lewis bases that either were the actual starting materials (for the probe reaction being compared against), or similarly structured Lewis bases could be studied directly. In general, effective Lewis acidity is measured via coordination of the Lewis acid to a Lewis base and measuring a spectroscopic characteristic of the Lewis base that changes with binding strength. Many Lewis bases have been shown to give measurable and consistent spectroscopic changes upon coordination with strong Lewis acids (e.g., boron, aluminum, etc.).[1] That said, to potentially be useful for quantitative comparisons, the equilibrium between unbound Lewis base, and LB-LA adduct must lie far toward the adduct. This fact makes the goal of this study more challenging as the Lewis acids employed as catalysts for industrially practiced polyesterification are only mildly acidic, by design, to avoid significant side reactivity. As will be seen below, to make up for a weaker Lewis acid, choosing a stronger Lewis base could at times drive the adduct formation to a greater extent.

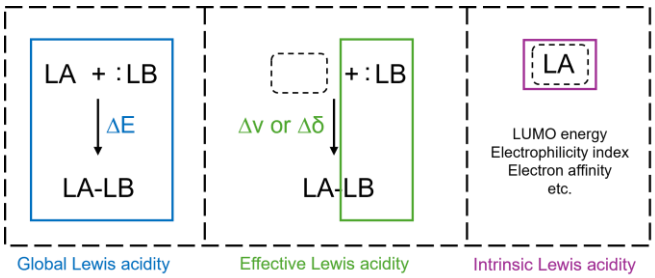

Figure 4.1. Classes of Lewis acidity scaling methods. "LA" is a Lewis acid, "LB" is a Lewis base. Adapted from Ref. 1.

4.2 Results

4.2.1 Alcohol Coordination

The interaction between stannous octoate (SnOct) and different alcohols has previously been explored by looking at the ^{1}H NMR shift of the -O<u>H</u> and -C<u>H$_2$</u>OH.[2] This measurement works through alcohol coordination to the metal complex upon which the -OH proton is effectively transferred to a carboxy ligand which leaves the complex as a free acid and the -OR becomes a metal-alkoxy species (Scheme 4.1a). The free carboxylic acid has a proton shift much further downfield than RO<u>H</u> and the α-C<u>H$_2$</u> of the metal-alkoxy species is measurably more downfield than the α-CH$_2$ of the free alcohol. These ligand movements are all fast on the usual NMR time scale and so each signal pair appears as a single ^{1}H signal at an intermediate shift resulting from the weighted average of the two signals depending on where the equilibrium lies between the free alcohol/metal carboxyl pair vs. the metal alkoxy/free acid pair. Being able to measure the equilibrium of the alcohol coordination reaction would likely be a useful approximation of relative effective Lewis acidity toward alcohol reactants and so the first step was to reproduce a literature precedent. Storey et. al. were able to mix stannous octoate (SnOct) with n-butanol and observe an easily measurable change in the NMR shifts for the alcohol -OH and the α-CH$_2$ signals.[2] When the conditions were repeated, interestingly, a large -OH signal shift was found but there was close to no shift in the α-CH$_2$

signal (Table 4.1). A similar effect was observed when using the alcohol employed for the majority of catalytic reaction testing (2-ethylhexanol).

Table 4.1. ^{1}H NMR shifts of alcohol + SnOct mixtures. Alcohol concentration is 0.1 M in $CDCl_3$ for each mixture.

Literature Precedent (Ref. 2)		
[n-BuOH]:[SnOct] Ratio	δ of BuOH –OH (ppm)	δ of BuOH α-CH_2 (ppm)
1:0	1.41	3.55
1:4	6.89	3.82
This Work		
[n-BuOH]:[SnOct] Ratio	δ of BuOH –OH (ppm)	δ of BuOH α-CH_2 (ppm)
1:0	1.48	3.67
1:4	8.15	3.65
[2-ethylhexanol]:[SnOct] Ratio	δ of 2EH –OH (ppm)	δ of 2EH α-CH_2 (ppm)
1:0	1.67	3.55
1:4	8.50	3.57

While it is unclear why the α-CH_2 signals did not show an appreciable change when the literature conditions were repeated, the -OH shift is clear and seems to be a usable measure for catalyst comparisons. Bismuth neodecanoate (BiNeo), tetrabutyl titanate (TBT), and TBT:BiNeo were compared using 2-ethylhexanol as the alcohol of choice and the results are shown in Figure 4.2. As can be seen, BiNeo demonstrated a sizable shift from 1.63 ppm to 5.74 ppm for the -OH signal, while TBT showed a much smaller shift to 2.09, and the mixture with TBT:BiNeo resulted in an intermediate shift to 3.41 ppm. The stronger and harder Lewis acid, TBT, should be expected to more strongly coordinate an alcohol and a downfield shift greater than that found for BiNeo was initially the expected result. To understand why this was not the case it was realized that the identity of the ligand being exchanged with was important. Scheme 4.1b shows this difference in the reactivity that occurs based on the LA ligand and the shift to 2.09 ppm matches well with an equilibrium between 2-ethylhexanol and n-butanol whereas the shift with BiNeo to 5.74 ppm matches with an equilibrium between 2-ethylhexanol and neodecanoic acid.

Unfortunately, the equilibrium between 2-ethylhexanol and n-butanol does not hold much information about the Lewis acidity of the catalyst.

Observing the α-CH_2 signals, BiNeo gave little shift. The mixture of TBT and 2-ethylhexanol did give a measurable shift, but broadened the signals to an extent that distinguishing the doublet vs triplet of the α-CH_2 of 2-ethylhexanol vs butanol, respectively, could only be accomplished by lowering the temperature during spectrum collection to -20 °C (Figure A 4.1). The spectrum of TBT:BiNeo is interesting because it clearly shows both a sharp triplet for a -OBu species and a sharp doublet for an -Oethylhexyl species even though titanium alone yields very broad signals. At first glance this appears to indicate that TBT:BiNeo inhibits the coordination of 2-ethylhexanol as there is no substantial shift in the signal relative to free 2-ethylhexanol even with titanium present. Contradicting this, the -OBu signal is at 3.63 ppm, indicative of free butanol, to suggest that the butoxy ligands are also displaced from the Ti/Bi complex to a large extent as would be expected if 2-ethylhexanol did undergo the reaction as in Scheme 4.1a. To rectify these seemingly contradictory observations of little α-CH_2 signal change but also seemingly displaced -OBu ligand, it may be possible that a reaction is still occurring with the catalyst but the α-CH_2 shift is too small to be seen. Perhaps a more sensitive measurement could pick up the expected signal shift.

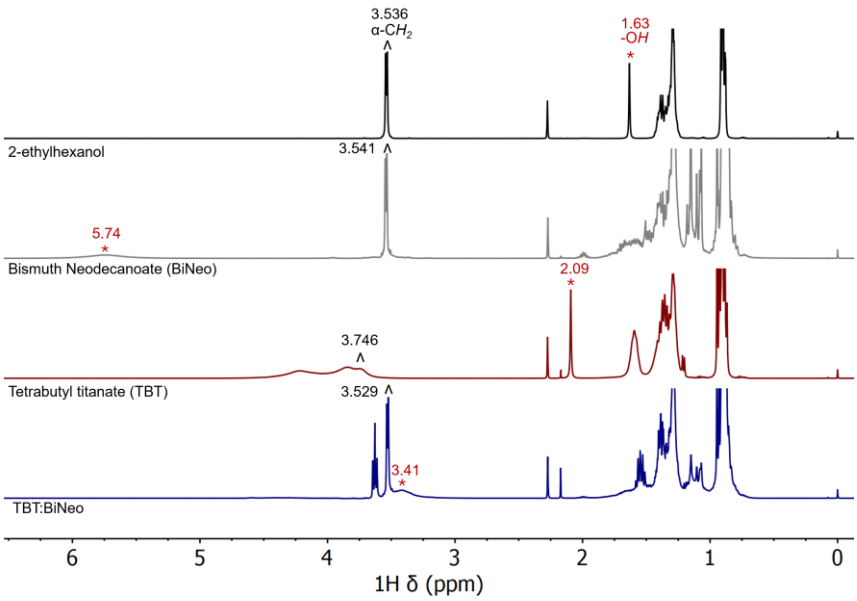

Figure 4.2. ^{1}H NMR spectra of 2-ethylhexanol mixed with catalyst compounds. 2-ethylhexanol:Catalyst ratio is 1:1. Add a scheme above

Scheme 4.1. Difference between -OH NMR shift when 2-ethylhexanol is added to (a) BiNeo vs (b) TBT.

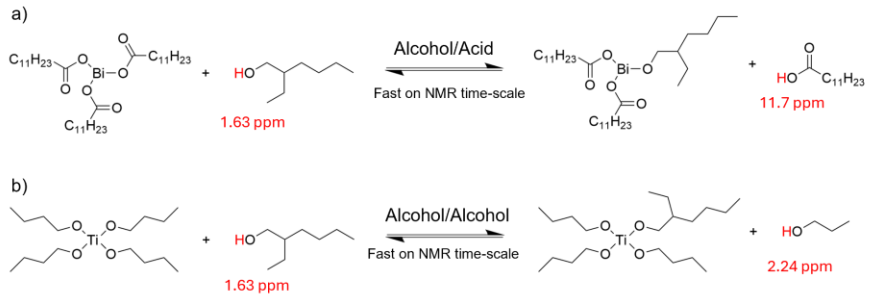

^{13}C NMR has a broader chemical shift range than ^{1}H NMR which can also provide better frequency resolution and potentially provide higher sensitivity to shifting due to coordination. To further improve the potential to see measurable shifts in the NMR spectra, samples were measured at -30 °C to increase resolution and sensitively. A series of the catalysts of interest were tested again using 2-ethylhexanol as the Lewis base (Table 4.2). If 2-ethylhexanol does coordinate to the Lewis acid, it would be expected to cause a downfield shift (positive Δδ (ppm)). A downfield shift is indeed observed for TBT, TiOct, and ZrOct, however, unexpectedly, a small upfield shift is observed for TBT/BiNeo mixtures, and TBT/SnOct or

TBT/DBTDL mixtures. The conclusion from the lack of downfield shift would at first glance be that there was little coordination at all since coordination should be expected to cause a downfield shift. Even if there is additional steric bulk around the carbon atoms of interest due to being in a mixed metal complex a downfield shift should be expected. Contradicting these results are the ^{119}Sn NMR spectra presented in Chapter 2 (Figure 2.17) clearly showing that mixing TBT:2SnOct with 2-ethylhexanol, at room temperature, leads to a change in the coordination sphere around Sn, matching with literature precedent of facile alkoxide formation.[3] Due to the difficulty in interpreting these results, it was decided to try other likely probe Lewis bases.

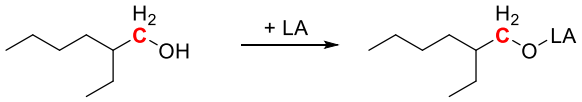

Table 4.2. ^{13}C NMR shifts of α-CH_2 carbons on 2-ethylhexanol in mixtures with Lewis acids. Spectra collected at -30 °C.

Catalyst	**α-CH_2 (^{13}C NMR) (ppm) 1:1 (Cat:ROH)**	**Δδ (ppm)**	**α-CH_2 (^{13}C NMR) (ppm) 5:1 (Cat:ROH)**	**Δδ (ppm)**
None	64.66	0.00	64.90	0.00
TBT	71.40	6.74		
TiOct	67.38	2.72	64.51	-0.39
TBT:2SnOct	64.50	-0.16	64.63	-0.27
TBT:2DBTDL	64.46	-0.20		
4TBT:BiNeo	64.53	-0.13		
TBT:BiNeo	64.63	-0.03	64.69	-0.21
TBT:4BiNeo	64.53	-0.13		
ZrOct	65.89	1.23		
DBTDL	64.45	-0.21		
BiNeo	--	--	64.64	-0.26

4.2.2 Carbonyl Coordination

In addition to the alcohol reactant, an ester was employed to test coordination of the other reactant to the Lewis acids. Methyl benzoate was chosen as a relevant carbonyl compound and TiOct was selected as one of the Lewis acids that had shown significant NMR shift with 2-ethylhexanol to suggest it

was capable of coordinating to a more significant degree. If significant carbonyl coordination were to occur, a downfield shift in at least the -ortho and -para positions of the aromatic ring would be expected. As can be seen in Table 4.3, there was little change in the observed shifts and what change that did occur was slightly upfield. As TiOct has been shown to coordinate to Lewis bases like 2-ethylhexanol, it was concluded that methyl benzoate was not a strong enough Lewis base to generate significant LA-LB adduct under room temperature conditions, at least. Stronger Lewis basic carbonyls have been used for Lewis acidity measurements in literature, so it was decided to test some of the literature standard methods using strongly Lewis basic carbonyl probes.

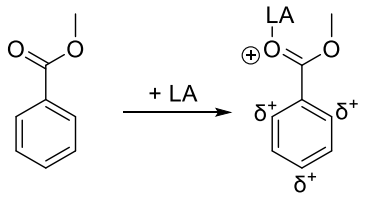

Table 4.3. ^{13}C NMR shift of 1.0 M methyl benzoate and 1.0 M titanium octoate (TiOct) in $CDCl_3$. Spectra collected at -30 °C.

Position	Methyl Benzoate (MB) [ppm]	TiOct + MB (1:1) [ppm]	Difference [ppm]
ipso-	129.87	129.82	-0.05
ortho-	129.66	129.60	-0.06
meta-	128.56	128.45	-0.11
para-	133.23	133.15	-0.08
carbonyl-	167.38	167.22	-0.16

4.2.3 Gutmann-Beckett Method

The most used method of Lewis acidity measurement in the literature is the Gutmann-Beckett method.[4-6] This method uses triethylphosphine oxide (TEPO) as the Lewis base and takes advantage of the significantly less complicated ^{31}P NMR spectrum to measure the strength of coordination to a Lewis acid. TEPO is a stronger Lewis base than an ester, or even an amide, due to the strongly polarized P-O bond. It is also a hard Lewis base due to binding through oxygen. Rigorously dry conditions are necessary to

perform these experiments because any available water will be coordinated to TEPO and convolute the NMR shift. It is standard to use a 1:1 molar ratio between TEPO and the Lewis acid of choice, and these data for a set of catalysts can be seen in Figure 4.3.

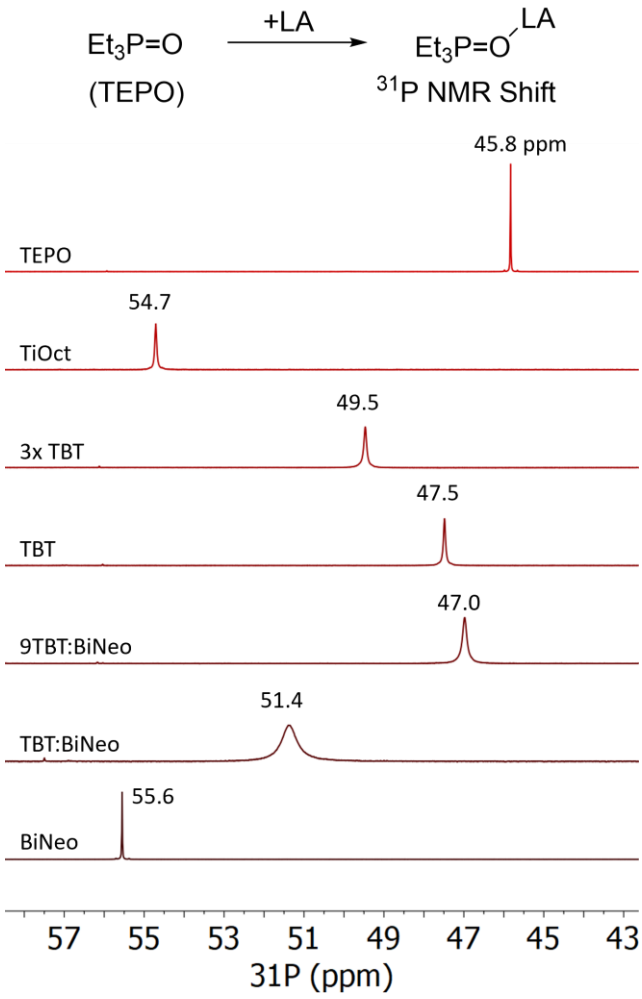

Figure 4.3. Gutmann-Beckett method results of various catalysts mixed with triethylphosphine oxide (TEPO) in a 1:1 molar ratio unless otherwise stated in C_6D_6 showing ^{31}P NMR shifts. NMR solutions prepared from dry C_6D_6 at approximately 1.4 M in a dry N_2 atmosphere and sealed in a J-Young tube before removal, then heated at 50 °C for 10 minutes before cooling to room temperature and spectral collection.

TEPO alone has a ^{31}P NMR shift of 45.8 ppm. TBT has an unexpectedly small downfield shift of just 1.7 ppm being much less than the supposedly weaker LA of BiNeo that shifted 9.8 ppm downfield.[7] A 1:1 ratio of TEPO to LA assumes that each TEPO molecule coordinates to one and only one LA, that is not necessarily the case.[8] To test if perhaps there was insufficient TBT for TEPO to coordinate to due to structuring/clustering of TBT in solution making Ti coordination sites less available, a 3x excess of TBT was also tested but still gave a small shift. Intriguingly, a titanium complex with only a different ligand set (TiOct) showed a much larger shift than TBT. When a mixed-metal catalyst was tested (TBT:BiNeo) the NMR shift was close to an average of the pure compounds although the signal was noticeably broadened to perhaps indicate TEPO exchanges between coordination on either metal. As there is apparently a poor correlation between the ^{31}P NMR shift of TEPO coordinated to TBT and BiNeo and the initial rate kinetics of these catalysts (Figure 3.2), our attention moved toward other methods.

4.2.4 Child's Method

It is intriguing that changing the ligand around Ti from -OBu to -O(O)ethylhexyl had such a significant influence on the apparent ability or strength of TEPO coordination using Gutmann-Beckett parameters. Another common probe molecule to measure Lewis acidity using a carbonyl is named Child's method.[9] The probe molecule is trans-crotonaldehyde and the standard reported value is the shift in the distal vinyl proton (labelled as H3 above Table 4.4) as it is less effected by the local sterics around the coordinated Lewis acid and so may be more agnostic to ligands than TEPO. It is also standard to collect the spectrum under low temperature conditions (-20 °C in the original report) to promote higher levels of coordination. Literature reports show downfield shifts of around 1.0 ppm for titanium(IV) chloride and tin(IV) chloride and while chlorides are stronger Lewis acids than alkoxide or carboxylate ligated complexes, it is still a surprise that no discernable change in the shift of H^3 was noticed with TBT or dibutyltin dilaurate (DBTDL) (Table 4.4).

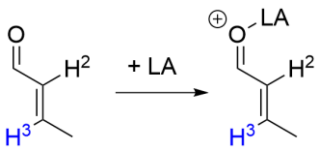

Table 4.4. ^{1}H chemical shift differences (Δδ) of trans-crotonaldehyde on complexation with various Lewis acids.[a] Literature values from Ref. 9.

Lewis Acid	H^3 / Δδ (ppm)
BCl_3 (lit)	1.35
$AlCl_3$ (lit)	1.23
$TiCl_4$ (lit)	1.03
$SnCl_4$ (lit)	0.87
TBT *(this work)*	0.00
DBTDL *(this work)*	0.00

[a]in ppm (± 0.01). Chemical shift of uncomplexed trans-crotonaldehyde: 6.93 (m, 1H, H^3). Δδ is positive for a downfield shift. 0.3 M solution in dichloromethane for literature values and $CDCl_3$ for "this work" at -20 °C.

4.2.5 ATR-FTIR using N,N'-dimethylbenzamide as a probe molecule

Another classic method of effective Lewis acidity measurement using a carbonyl Lewis base takes advantage of the infrared spectrum of the carbonyl stretch. The interaction between a Lewis acid and Lewis basic carbonyl is well-known to lower the energy of the C=O stretch and the magnitude of the change can indicate the strength of the interaction.[10] In addition to the magnitude, IR has a far faster time-scale for signal collection than NMR, so that the confusion of apparent signal averaging seen in TBT:BiNeo can be resolved in IR and different coordination environments are able to be distinguished. To start this study, the IR spectrum of different aromatic carbonyl compounds mixed with TBT or BiNeo were collected in hexane using ATR-FTIR. It was discovered that only the strongest Lewis basic carbonyl, N,N'-dimethylbenzamide (NNDMB), exhibited a red-shift and only with TBT out of the two. However, upon heating the carbonyl-LA mixture to 50 °C for 10 minutes, BiNeo also exhibited a red-shift with NNDMB. The carbonyl signal was strong with a NNDMB concentration of 1.0 M and heating up to 80 °C gave close to the same result as heating to 50 °C (Figure A 4.3). The IR spectra of a selection of the Lewis acids tested for reactivity mixed with NNDMB can be seen Figure A 4.4.

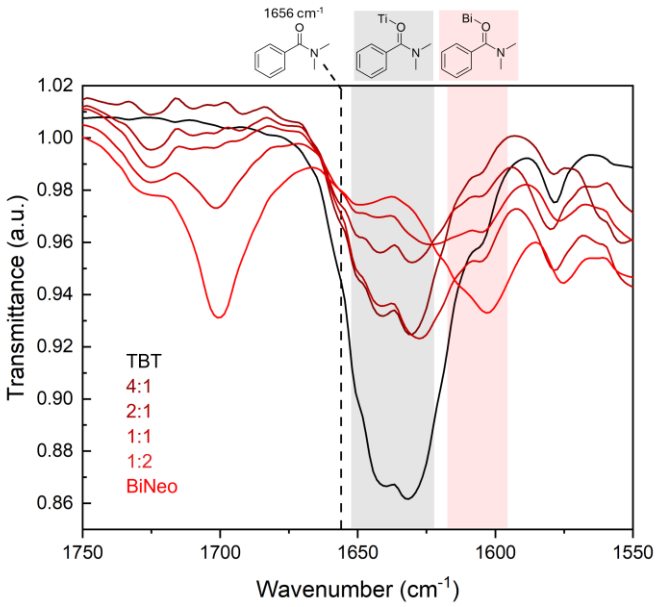

Figure 4.4. ATR-FTIR spectra of 1.0 M TBT/BiNeo catalysts (by metal) with 1.0 M N,N'-dimethylbenzamide dissolved in hexanes. Dotted line indicates peak wavelength of only NNDMB *v*(C=O). Shaded boxes indicate titanium or bismuth-bound NNDMB *v*(C=O). Mixture premixed for 10 minutes at 50 °C.

Now having a method that can identify the redshift associated with both TBT and BiNeo coordination to an aromatic carbonyl in hand, the IR spectra of different mixtures of the two were examined (Figure 4.4). TBT alone has multiple apparent binding environments yielding multiple C=O stretches red shifted 15 or 24 cm^{-1} for the most intense but smaller shoulders can also be observed. BiNeo alone has a broad set of C=O stretches with the most intense centered at 1601 cm^{-1} and a redshift of 55 cm^{-1}. Counterintuitively, BiNeo yields a larger redshift than TBT although it is a far less active catalyst for carbonyl addition reactions. As there are structural differences between TBT, BiNeo, and their mixtures, it is reasonable to expect that the IR spectra of NNDMB and the mixed metal catalysts, such as TBT:BiNeo, would have alternative coordination sites to either TBT or BiNeo alone (e.g., by bridging between Ti and Bi). However, when the spectra for different mixing ratios of the mixed metal catalysts are overlaid with

those for TBT and BiNeo, each coordinated to NNDMB, it becomes clear that the visible C=O stretches closely resemble either the same stretches as seen with only TBT or only BiNeo. More TBT in the mixture gives more TBT-similar stretches and more BiNeo gives more BiNeo-similar stretches (highlighted in the gray or red box of Figure 4.4, respectively). This observation suggests that NNDMB either coordinates to Ti or Bi and in a similar way as it would without the other metal present. This would also suggest that the activity of a mixed metal catalyst will be the linear combination of the activities of the complexes added to the mixture, which matches with the initial rate data presented in Chapter 2 and Chapter 3.

4.2.6 EXSY NMR

There are several experimental observations and literature observations that were synthesized to come up with the experiments in the following section. In Chapter 3, 2D EXSY NMR was employed to determine the relative exchange rate of the butoxy ligands of TBT:BiNeo vs. TBT:2SnOct (Figure 3.5). Also, during the search for carbonyls that may show an NMR shift upon coordination for Section 4.2.2, it was found in literature that N,N'-dimethylformamide (DMF) exhibits a shift in the methyl groups upon coordination to a Ag-based Lewis acid.[11] Additionally, the exchange rate of C-N bond rotation of DMF is a textbook example to explain how EXSY NMR works.[12] What's more, there are examples of Lewis acids that did not significantly coordinate to trans-crotonaldehyde in Child's method, as seen with the esterification catalysts of interest to this study, but could be coordinated to N,N'-diisopropylbenzamide (NNDIB).[13] Upon coordination of NNDIB the singlet attributable to the methine protons of the isopropyl groups turned into two distinct signals to evidence the slowing of the exchange relative to the NMR time-scale of the isopropyl groups from cis- to trans- position that would be expected upon LA coordination to the carbonyl. In summary, a single coalesced peak for the benzamide isopropyl groups could be resolved to two distinct isopropyl signals when a LA was coordinated to the carbonyl oxygen. This technique appeared promising but when the NMR spectrum of NNDIB was collected on a 400 MHz instrument, there was not the reported singlet of the isopropyl groups, but already two broad and partially overlapping signals indicating the

exchange was already slow on the NMR time-scale. It would likely be possible to coalesce these signals to a singlet that then may be converted back to a doublet upon LA coordination by either speeding the exchange rate by heating during the NMR spectrum collection or using a lower field magnet to decrease the spectrum resolution. Either of these options presented significant challenges as the temperatures reported to coalesce the signals is close to as high as the NMR spectrometers in the Paul Bender Instrumentation Center can reach and so would not be able to control the temperature precisely. For using a low-field instrument, reference spectra for NNDIB collected at 60 MHz indeed show a singlet, and a training instrument of 60 MHz was tracked down within the physical chemistry teaching labs, but the need to do significant rebuilding and scheduling issues precluded an easy experiment. Even with the ability to do peak coalescence experiments, the procedure is to measure either the peak width or, more ideally, the point of coalescence, and from this measurement determine an exchange rate. This gives an exchange rate based off one low precision measurement. Given the limitations, a new method of measuring the exchange rate of N,N'-disubstituted amides coordinated to Lewis acids using EXSY NMR was developed.

The first attempt of this experiment was to do a 2D EXSY experiment using NNDIB and a strong Lewis acid. As previously noted, the isopropyl groups are broad and overlapping, which gave poorly distinguished EXSY signals. To help solve this, NNDMB was switched to and has sharp and largely resolved signals for the N-substituents. The 2D EXSY experiment is relatively time consuming (~1 h). EXSY NMR works on the same pulse sequence as NOESY NMR used for through-space proximity determinations where nuclei are pulsed into the transverse plane as in a normal 1D collection sequence but then a certain "mixing time" is allowed for nuclei to transfer their polarization between either nearby nuclei through the nuclear Overhouser effect or through chemical exchange before signal acquisition. If a particular signal is selectively excited with a selective gradient pulse, this same sequence can be accomplished but only for the selected signal and the exchange events that are directly related to that signal. In the case of N,N'-substituted amides, the chemical exchange between the cis- and trans- geometric isomers can be

observed. The 1D selective spectrum can be collected in a couple of minutes and so it became practical to collect a large series of spectra where the mixing time is varied to obtain a build-up curve of the exchange and calculate an exchange rate with much greater precision (Figure 4.5).[14] This method proved to supply higher quality exchange rate data in less time.

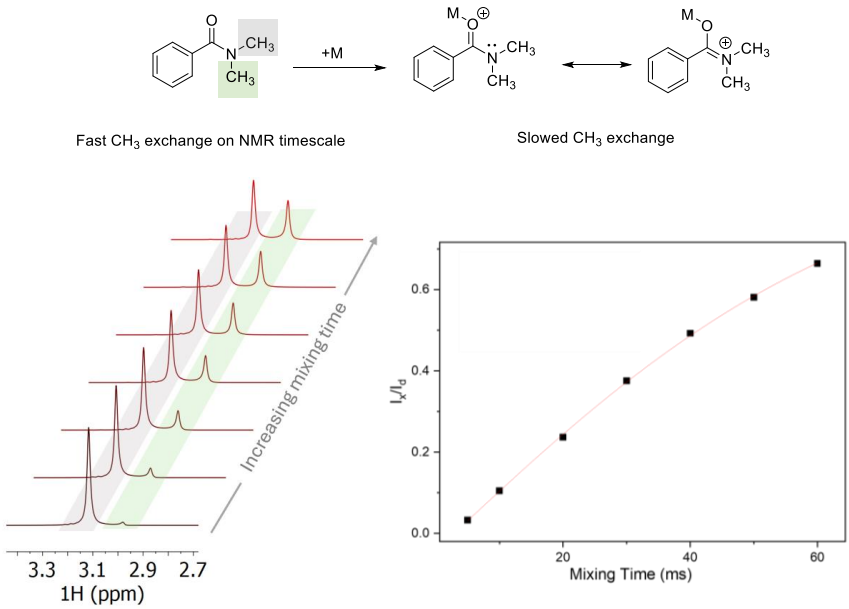

Figure 4.5. 1D-EXSY exchange rate measurement explanation for N,N'-dimethylbenzamide coordinated to a Lewis acid. Mixing time refers to the time between selective excitation of the leftmost resonance and FID collection.

When a set of Lewis acids were tested in this protocol, well-fit data was obtained that showed measurable differences in exchange rate (Table 4.5). Stronger Lewis acids should coordinate more strongly, induce more double-bond character in the C-N bond and slow the exchange rate of the benzamide methyl groups. This exchange rate can be calculated by fitting Equation *(4.1*.

$$\frac{\boldsymbol{I_x}}{\boldsymbol{I_d}} = \left[\mathbf{1} - \boldsymbol{e}^{(-\boldsymbol{k_{exch}} * \boldsymbol{T_{mix}})}\right] / \left[\mathbf{1} + \boldsymbol{e}^{(-\boldsymbol{k_{exch}} * \boldsymbol{T_{mix}})}\right] \tag{4.1}$$

Where I_x is the signal intensity of the signal growing in, I_d is the signal intensity of the excited signal, k_{exch} is the exchange rate constant, and T_{mix} is the mixing time.[15] Interestingly, the fastest exchange rate was

associated with TBT and this was different than the other titanium complex, TiOct, indicating a ligand dependence to the exchange rate. A ligand dependence was expected as greater steric bulk around the carbonyl likely would hinder methyl group exchange, and the longer and bulkier octoate ligands did appear to slow exchange. Another interesting point is that BiNeo, supposedly a weak Lewis acid by reactivity, slowed the exchange rate even more than titanium or zirconium with a similar ligand set, albeit with possibly fewer ligands than these due to its 3+ oxidation state.

Table 4.5. Exchange rates for N,N'-dimethylbenzamide coordinated to some unmixed Lewis acidic compounds as measured by 1D selective EXSY NMR. Exchange rates calculated from 10 mixing times ranging from 10 – 100 ms. Selective gradient pulse application at 3.18 ppm.

Catalyst	k_{exch} (ms^{-1})
TBT	0.0353 ± 0.0005
BiNeo	0.0235 ± 0.0008
TiOct	0.0292 ± 0.0004
ZrOct	0.0313 ± 0.0005

Next, different ratios of TBT/BiNeo mixed metal catalysts were tested (Figure 4.6 and Table 4.6). It is intriguing but unexplained that TBT shows no different exchange rate than no catalyst at all as if there is little or no coordination. As more BiNeo is added to the mix, the exchange rate is slowed although not in a linear fashion which possibly suggests a synergetic effect. A study simply on how BiNeo concentration effects exchange rate is necessary to determine if this nonlinearity is attributable to the bimetallic mixture or not. A preliminary concentration study using 0.4 M TBT:BiNeo instead of 0.2 M, to make the sample 0.2 M in titanium and 0.2 M in bismuth gave the same exchange rate as simply 0.2 M is BiNeo alone. This indicates that even in a mixed metal compound, titanium likely is not affecting the exchange rate.

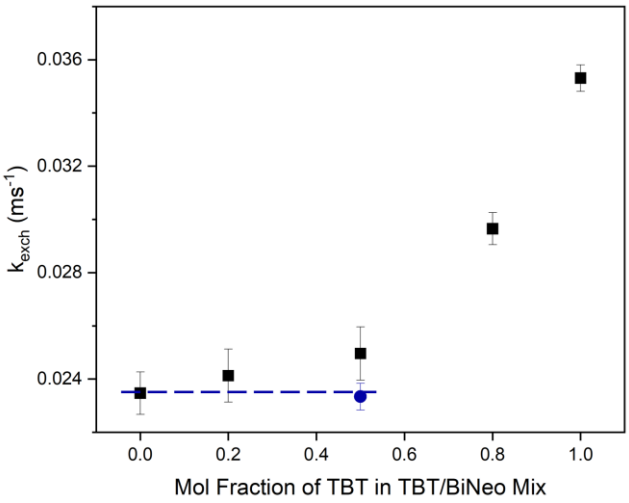

Figure 4.6. Exchange rates of N,N'-dimethylbenzamide mixed with TBT/BiNeo catalysts. 0.2 M in NN'-DMB, black squares are 0.2 M in catalyst by metal, blue circle is 0.4 M in catalyst by metal (0.2 M in Ti, and 0.2 M in Bi). Error bars are standard error in fitting function.

Table 4.6. Exchange rates for N,N'-dimethylbenzamide coordinated to mixed TBT/BiNeo Lewis acidic compounds as measured by 1D selective EXSY NMR. Exchange rates calculated from 10 mixing times ranging from 10 – 100 ms. Selective gradient pulse application at 3.18 ppm.

Catalyst	**Catalyst Conc (M)**	**k_{exch} (ms^{-1})**
No Catalyst	0.0 (0.2 M DMB)	0.0356 ± 0.0005
TBT	0.2	0.0353 ± 0.0005
4TBT:BiNeo	0.2	0.0297 ± 0.0006
TBT:BiNeo	0.2	0.0250 ± 0.001
TBT:BiNeo	0.4	0.0233 ± 0.0005
TBT:4BiNeo	0.2	0.0240 ± 0.001
BiNeo	0.2	0.0235 ± 0.0008

It is noted that switching solvents from $CDCl_3$ to C_6D_6 increased the exchange rate by roughly and order of magnitude. This evidences that the local solvation environment has a large effect on the exchange rate and may be a variable to investigate in the future.

4.2.7 Fluorescence

Reports of the red-shifting of fluorescence upon LA coordination of carbonyl fluorophores have been shown to be a quantitative measure of LA strength.[16,17] Compounds such as aromatic esters, which are not fluorophores themselves, when coordinated to complexes such as organic tin(IV) compounds, exhibited fluorescence upon irradiation of the absorption band by allowing for more efficient intersystem crossing and stronger Lewis acid coordination yields lower energy fluorescence. A variety of fluorophores, concentrations, LA strength, solvents, and excitation wavelengths were tested. Fluorophores tested included methyl benzoate, benzoic acid, benzaldehyde, N,N'-dimethlybenzamide, and 2-naphthaldehyde. Lewis acids tested included TiOct, TBT, DBTDL, SnOct, and aluminum trichloride. Excitation wavelength/the absorption band was found by collecting UV-vis spectra of the fluorophore and catalyst mixtures. The samples were heated to 50 °C before measurement to give better coordination as in IR measurements using NNDMB. Samples were also sparged with N_2 to remove dissolved oxygen which has been reported to quench fluorescence. Even with a systematic exploration of variables and following literature precedent, no aromatic carbonyl fluorescence was observed in any case.

4.3 Discussion

A summary of the methods and results can be found in Table 4.7, but a discussion of the mixed results of the presented attempts to measure Lewis acidity is in order. In section 4.2.1, the coordination of an alcohol was monitored using the downfield shift of NMR signals. Of the -OH and α-CH_2 signals that are potentially effected by coordination only the α-CH_2 signals could give reliable results regardless of the catalyst ligand set. There was substantial reason to believe a shift would be observed based on literature, and previous ^{119}Sn NMR studies of TBT:2SnOct mixed with 2-ethylhexanol. Where titanium and zirconium complexes gave measurable shifts, the other compounds did not, even mixtures with titanium compounds (i.e., TBT:BiNeo). Section 4.2.2 discusses carbonyl coordination being monitored by NMR shift and no useful data was obtained as no significant shift was observed upon mixing with any Lewis acid of interest.

The Gutmann-Beckett method in Section 4.2.3 using the ^{31}P NMR shift of triethylphosphine oxide (TEPO) yielded difficult to interpret results, suggesting that TBT vs TiOct were substantially different, even though they possess similar initial rate activity (Figure A 3.3). In addition to this, BiNeo appears to be more strongly coordinated than TBT even though BiNeo is actually a far inferior catalyst. Child's method in Section 4.2.4 using an aldehyde probe molecule gave no discernable shift in the diagnostic signals. Fluorescence spectroscopy of coordinated fluorophores (Section 4.2.7) also gave no fluorescence, contradicting literature reports measured under similar conditions. Some interpretable results could be pulled from using the red shift of carbonyl stretching of an aromatic amide in IR spectroscopy (Section 4.2.5). An amide proved to be necessary for significant red shifting, and presumably Lewis acid coordination. Heating the LA/amide mixture before measurement to hypothetically overcome any activation barrier to coordination also was necessary for many of the catalysts. Mixed metal catalysts of TBT and BiNeo showed that the coordination environments available to a mixed metal catalyst are very similar to those available to either one catalyst alone, suggesting the metals act separately. Additionally, BiNeo gave a larger red shift than TBT, which, counter to reactivity, suggests stronger LA-amide bonding. A new method was developed in Section 4.2.6 using 1D selective EXSY NMR experiments and this also gave difficult to interpret results. TBT alone gave no measurable change in the N,N'-dimethylbenzamide exchange rate suggesting it does not coordinate, and BiNeo gave the greatest slowing of exchange rate suggesting it coordinates strongly.

The expectation for any of these methods was that the catalysts with the fastest initial rates (i.e., Ti) would have spectroscopic indicators of stronger bonding to either an alcohol or a carbonyl and poor catalysts (i.e., Bi) would either have no indication of binding or very weak indications of binding. The goal was to correlate these relatively easy Lewis acidity measurements with reactivity as an explanation for the catalyst's activity to add insight into the working principles of mixed metal catalysts. Literature studies on Lewis acids have admitted that some of these techniques were inadequate for Lewis acidity measurements due to low levels of coordination etc.[10] However, in the case of this set of studies, even stronger Lewis

bases than are relevant for esterification (i.e., TEPO) gave results that contradicted kinetic experiments. After trying a range of Lewis base probe molecules measured using multiple spectroscopic techniques, none of the methods matched well with the kinetic data for these catalysts.

One set of ideas that may be pulled out of these experiments are that TBT easily underwent ligand exchange with an alcohol while BiNeo did not seem to nearly as easily (as seen in Section 4.2.1). For carbonyls, BiNeo appears to coordinate more strongly than TBT (as seen in Sections 4.2.3, 4.2.5, and 4.2.6). An attractive hypothesis from these observations is that a bimetallic catalyst of the two may allow for easy alcohol coordination through titanium and strong carbonyl coordination through bismuth and so a synergistic activity. This hypothesis is not supported by the kinetic study of the mixtures, though, as no kinetic synergy is observed. What does seem apparent and is agreed upon between most of the methods tested is that Ti and Bi behave separately. The main takeaway is to be cautious when trying to employ even well-precedented methods for effective Lewis acidity measurement and multiple complementary methods have a better potential to give useful information.

Table 4.7. Summary of Lewis acidity measurement techniques and summarized results of experimentation.

Method	*Description*	*Summarized Results*
Alcohol Coordination in NMR 4.2.1	Coordination of 2-ethylhexanol (or other ROH) *Measured:* -O<u>H</u> and/or α-CH_2 in ^{1}H or ^{13}C	▪ -OH shift is clear but only when the metal complex has carboxylate ligands ▪ α-C<u>H_2</u> (^{1}H) show measurable deshielding for Ti complexes, but unmeasurable shift for Zr or Bi complexes ▪ α-<u>C</u>H_2 (^{13}C) show measurable deshielding for Ti and Zr complex, but small opposite shift for mixed-metal or Bi complexes
Carbonyl Coordination in NMR 4.2.2	Coordination of methyl benzoate (or other O=CR) *Measured:* ^{13}C NMR shift	▪ Small shielding or not measurable shift in carbonyl ^{13}C shift
Gutmann-Beckett Method 4.2.3	Coordination of triethyl phosphine oxide (TEPO) *Measured:* ^{31}P NMR shift	▪ TBT has little shift while BiNeo has a large shift while TiOct also has a large shift ▪ TBT:BiNeo roughly has a weighted average shift of the pure complexes
Child's Method 4.2.4	Coordination of trans-crotonaldehyde *Measured:* ^{1}H NMR shift of distal vinyl proton (collected at -20 °C)	▪ No measurable shift
ν*(C=O) Red-shift via IR 4.2.5*	Coordination of a carbonyl *Measured:* red-shift magnitude	▪ Red-shift observed in most catalysts after heating at 50 °C ▪ BiNeo has larger red-shift than TBT ▪ TBT/BiNeo mixed catalysts have a combination of stretches that look either like pure TBT or pure BiNeo coordination
1D-EXSY Amide Bond Rotation 4.2.6	Coordination of N,N'-dimethylbenzamide *Measured:* rate of conversion between cis to trans methyl	▪ Influence of ligand sterics may be observed ▪ TBT shows no influence on exchange rate even when adduct formation is likely occurring ▪ Non-linear correlation between BiNeo concentration and exchange rate
Carbonyl Fluorescence 4.2.7	Coordination of a carbonyl fluorophore *Measured:* shift in fluorescence wavelength	▪ No carbonyl-based fluorescence observed/unable to reproduce literature

4.4 Experimental

Alcohol coordination. Stannous octoate (Sigma-Aldrich 92.5-100%), bismuth neodecanoate (Sigma-Aldrich), and tetrabutyl titanate (Sigma-Aldrich 97%) were stored under dry, inert conditions and used as received. 2-ethylhexanol (Sigma-Aldrich 96%) was also used as received. Mixtures were made in NMR tubes where the concentration of 2-ethylhexanol was kept constant at 0.1 M in a total volume of 0.6 mL in $CDCl_3$ and the concentration of catalyst was varied as described in Table 4.1 and Figure 4.2. NMR spectra were collected using standard ^{1}H and ^{13}C sequences and processed in MestreNova v.12.0.4 software. ^{13}C NMR spectra were collected at -20 °C using a chiller attached to the NMR spectrometer and allowed to equilibrate at the lower temperature for 5 minutes before spectral acquisition.

Carbonyl coordination. The procedure for carbonyl coordination was the same as for alcohol coordination, but the temperature was lowered to -30 °C.

Gutmann-Beckett Method. Triethylphosphine oxide (Sigma-Aldrich 97%) was opened and stored under a dry, inert glovebox. Dry C_6D_6 was obtained from an ampule and opened within a glovebox. Any glassware employed or brought into the glovebox was first oven dried at 110 °C overnight to remove moisture. Any mixed metal catalysts used were synthesized fresh in oven dried glassware in the glovebox. A J-Young tube was used to transport and acquire NMR spectra under N_2. Prior to acquisition, the J-Young tube and contents were heated in a water bath at 50 °C for 10 minutes then cooled back to room temperature. The catalysts were mixed with triethylphosphine oxide (TEPO) in a 1:1 molar ratio (1.4 M in each) unless otherwise stated in C_6D_6 and standard ^{31}P NMR sequencing was used to collect the NMR spectra using TMS as an external reference. Only one ^{31}P signal was observed in any spectrum.

Child's Method. Literature precedent was followed to collect Child's method data other than the NMR solvent which was switched from d_2-dichloromethane to $CDCl_3$. Trans-crotonaldehyde (Sigma-Aldrich >99%) was stored in a 4 °C fridge to prevent decomposition but used as received. Trans-

crotonaldehyde/catalyst mixtures were made at 0.3 M in aldehyde and 0.3 M in catalyst and spectra were collected at -20 °C.

***v*(C=O) Red-shift via IR.** N,N'-dimethylbenzamide (NNDMB) (Sigma-Aldrich 99%) was used as received and dissolved readily in hexanes. A single-reflection hammer-and-anvil style ATR-IR apparatus was used to collect spectra. Spectral resolution was 0.2 cm^{-1}. NNDMB/catalyst mixtures were made at 1.0 M in each in hexane. The mixtures were heated in vials in a water bath at 50 °C for 10 minutes then cooled back to room temperature.

1D-EXSY Amide Bond Rotation. To collect 1D-EXSY NMR data a solution that was 0.2 M in catalyst and 0.2 M in NNDMB were mixed in $CDCl_3$. The NNDMB as received did not fully dissolve in $CDCl_3$ and lowering the solute to solvent ratio still did not give full dissolution. It was thought that there may be an impurity that did not dissolve so 10 mL of $CDCl_3$ was used to dissolve a set amount of NNDMB then pushed through a Kimwipe plug to remove solids. An internal standard of mesitylene was used to find the concentration of NNDMB in the solution and proper dilutions were used to reach the desired concentration. The selective gradient pulse used to excite just one of the methyl resonances was chosen so there was no excitation of the other methyl signal at 3.18 ppm and checked by measuring a spectrum with 0 ms mixing time. To have practically zero excitation of the undesired signal, a 500 MHz instrument was used instead of a 400 MHZ instrument to decrease signal width. The mixing time (D8 parameter for Bruker) was iterated from 0 ms to 100 ms using 11 different mixing times and the 10 points from 10 to 100 ms were plotted and fit due to difficulty phasing the 0 ms spectrum. Experiments run in C_6D_6 were carried out in the same manner as those in $CDCl_3$.

Carbonyl Fluorescence. A stock solution was made of either 100 mg 2-naphthaldehyde (Sigma-Aldrich 98%) or methyl benzoate in 10 mL of hexane, MeCN, or THF to make a ~ 0.065 M solution in carbonyl-containing compound. A solution of 1.3 g or 0.60 g TiOct and 200 or 400 uL of carbonyl stock solution were

mixed then the solvent of choice was added up to ~3 mL of total volume. Each sample was heated to 50 °C then cooled and sparged with N_2 for 15 minutes before being measured. A 4-sided quartz cuvette was used to collect the spectra using a Hitachi F-4500 fluorimeter. The excitation wavelength was started at 230 or 280 nm for methyl benzoate and 280 nm for 2-naphthaldehyde then spectra using excitation wavelengths ±50 nm were explored.

4.5 References

(1) Erdmann, P.; Greb, L. What Distinguishes the Strength and the Effect of a Lewis Acid: Analysis of the Gutmann–Beckett Method. *Angewandte Chemie - International Edition* **2022**, *61* (4). https://doi.org/10.1002/ANIE.202114550.

(2) Storey, R. F.; Sherman, J. W. Kinetics and Mechanism of the Stannous Octoate-Catalyzed Bulk Polymerization of-Caprolactone. *Macromolecules* **2002**, *35*, 1504–1512. https://doi.org/10.1021/ma010986c.

(3) Otera, J.; Nishikido, J. *Esterification: Methods, Reactions, and Applications, Second Addition*, 2nd ed.; Wiley-VCH Verlag, 2009. https://doi.org/10.1002/9783527627622.

(4) Mayer, U.; Gutmann, V.; Gerger, W. The Acceptor Number - A Quantitative Empirical Parameter for the Electrophilic Properties of Solvents. *Monatsh Chem* **1975**, *106* (6), 1235–1257. https://doi.org/10.1007/BF00913599.

(5) Seno, C.; Pokratath, R.; Unniram Parambil, A. R.; Van den Eynden, D.; Dhaene, E.; Prescimone, A.; De Roo, J. Complexation and Disproportionation of Group 4 Metal (Alkoxy) Halides with Phosphine Oxides. *Dalton Transactions* **2024**. https://doi.org/10.1039/d4dt01299b.

(6) Beckett, M. A.; Strickland, G. C.; Holland, J. R.; Varma, K. S. A Convenient n.m.r. Method for the Measurement of Lewis Acidity at Boron Centres: Correlation of Reaction Rates of Lewis Acid Initiated Epoxide Polymerizations with Lewis Acidity. *Polymer (Guildf)* **1996**, *37* (20), 4629–4631. https://doi.org/10.1016/0032-3861(96)00323-0.

(7) Kepp, K. P. A Quantitative Scale of Oxophilicity and Thiophilicity. *Inorg Chem* **2016**, *55* (18), 9461–9470. https://doi.org/10.1021/acs.inorgchem.6b01702.

(8) Pires, E.; Fraile, J. M. Study of Interactions between Brønsted Acids and Triethylphosphine Oxide in Solution by 31P NMR: Evidence for 2 : 1 Species. *Physical Chemistry Chemical Physics* **2020**, *22* (42), 24351–24358. https://doi.org/10.1039/D0CP03812A.

(9) Childs, R. F.; Mulholland, D. L.; Nixon, A. The Lewis Acid Complexes of α,β-Unsaturated Carbonyl and Nitrile Compounds. A Nuclear Magnetic Resonance Study. *Can J Chem* **1982**, *60* (6), 801–808. https://doi.org/10.1139/v82-117.

(10) Velasquez, J.; Pillai, E. D.; Carnegie, P. D.; Duncan, M. A. IR Spectroscopy of M +(Acetone) Complexes (M = Mg, Al, Ca): Cation-Carbonyl Binding Interactions. *Journal of Physical Chemistry A* **2006**, *110* (7), 2325–2330. https://doi.org/10.1021/jp0574899.

(11) Kuhn, J.; Mcintyre, J. S. Nuclear Magnetic Resonance Investigation of Adducts of N-Methylformamide with HCl and HBr and N,N-Dimethylformamide with Protonating Acids and Silver Salts. *Can J Chem* **1965**, *43* (5), 995–998.

(12) Claridge, T. D. W. *High-Resolution NMR Techniques in Organic Chemistry*, 3rd ed.; Elsevier Ltd, 2016. https://doi.org/https://doi.org/10.1016/C2015-0-04654-8.

(13) Liberman-martin, A. L.; Bergman, R. G.; Tilley, T. D. Lewis Acidity of Bis(per Fl Uorocatecholato)Silane: Aldehyde Hydrosilylation Catalyzed by a Neutral Silicon Compound. *J Am Chem Soc* **2015**, *137*, 5328–5331. https://doi.org/10.1021/jacs.5b02807.

(14) Perrin, C. L.; Engler, R. E. Accurate Rate Constants for Chemical Exchange from Improved Weighted Linear-Least-Squares Analysis of Multiple 1D-EXSY Data. *J Magn Reson A* **1996**, *123* (2), 188–195. https://doi.org/10.1006/jmra.1996.0234.

(15) *2D & 1D-selective EXCHSY (exchange spectroscopy)*. https://www.colorado.edu/lab/nmr/sites/default/files/attached-files/exchsy_0.pdf (accessed 2024-07-04).

(16) Ohkubo, K.; Menon, S. C.; Orita, A.; Otera, J.; Fukuzumi, S. Quantitative Evaluation of Lewis Acidity of Metal Ions with Different Ligands and Counterions in Relation to the Promoting Effects of Lewis Acids on Electron Transfer Reduction of Oxygen. *Journal of Organic Chemistry* **2003**, *68* (12), 4720–4726. https://doi.org/10.1021/jo034258u.

(17) Fukuzumi, S.; Ohkubo, K. Fluorescence Maxima of 10-Methylacridone-Metal Ion Salt Complexes: A Convenient and Quantitative Measure of Lewis Acidity of Metal Ion Salts. *J Am Chem Soc* **2002**, *124* (35), 10270–10271. https://doi.org/10.1021/ja026613o.

Chapter 5. Mixed Metal Catalyzed Glycolysis of Polyethylene Terephthalate Waste Plastic

In this chapter, the catalyst development of mixed metal compounds in the previous chapters is reapplied to another pressing area of study that esterification reactions are relevant to, polyester recycling. Plastic recycling is a field of growing importance and interest where depolymerization of polyethylene terephthalate (PET) is a challenge actively being researched by many in the catalysis community. Having developed a highly effective and non-toxic catalyst capable of polyesterification reactivity, studying the reverse reaction of depolymerization was an area we were interested in testing the new catalyst for. We found that the mixed metal catalyst still outperformed either of the precursor compounds. Under most conditions, the industrially most popular catalyst, zinc acetate, is a better catalyst, although some preliminary results suggest this is not the whole story as adding or removing water do not have the expected results.[3]

[3] This chapter consists of unpublished work. Alex Marrione, Oscar Li, Arianna Alirez, and Yamil Adorno were instrumental in collecting reactivity and characterization data presented here.

5.1 Introduction

Polyethylene terephthalate (PET) is a highly useful and widely used polyester with uses including food packaging, fibers for textiles, etc. Because of this usefulness, PET has been produced at huge volumes for the past decades.[1] With only partial recycling in much of the world (the US recycling rate was only 18% in 2023) there is buildup of waste both in landfills and in the environment.[2] The inertness of PET is a property that has allowed its use in so many areas, but also causes it to degrade on very long timescales where it is known to accumulate in the environment.[1] PET is by-in-large synthesized from fossil resources, generally terephthalic acid (PTA), dimethyl terephthalate (DMT), or bis(2-hydroxyethyl) terephthalate (BHET) and ethylene glycol (EG). Meaning its production contributes to the volume of crude oil being extracted and the production will follow a linear economy from extraction to production, use, and then disposal. Ideally, this linear economy would be transitioned to a circular economy where disposal can be largely removed in favor of recycling. Out of all the types of plastics used in the US, PET is recycled at the highest rate, but this recycling is almost entirely through mechanical recycling methods.[3] Mechanical recycling means the plastic is ground up, melted, and reformed into a new polyester material. In the waste collection process and in the mechanical recycling steps, impurities are introduced, and reactivity of the polymer chains occurs under the temperatures employed. This makes it unlikely the recycled PET (rPET) will meet high quality standards used for food contact uses (e.g., water bottles). Unfortunately, a large portion of PET that is used in the US is in food packaging so rPET from mechanical recycling cannot currently replace most virgin polymer.[4] An alternative solution must be implemented to achieve a circular PET economy. One possibility is fully depolymerizing the waste PET back to the monomers, doing a simpler purification of the monomers, then repolymerizing to PET. This chemical recycling pathway can give food-grade PET and successfully replace virgin PET, potentially removing some of the need for additional fossil resource extraction.[4] To do chemical recycling, one must choose which monomer to try to break the PET polymer down into. As stated above, the most common are PTA, DMT, and BHET (Scheme 5.1).[5] Terephthalic acid

is generated by depolymerizing PET with water and generally requires strongly acidic or basic reaction conditions. Dimethyl terephthalate production using methanol (methanolysis) as the depolymerization agent, which at the temperatures needed for economical reaction rates requires a more expensive high pressure reaction vessel and a difficult to separate azeotrope is made. Bis(2-hydroxyethyl) terephthalate production using ethylene glycol (glycolysis) as the depolymerization agent has the advantages of being able to react at ambient pressures and this has led to multiple companies commercializing the technology.[6] However, even close to the boiling point of ethylene glycol (190 °C) the uncatalyzed reaction is quite slow and necessitates a catalyst to increase the reaction rate. Previously the most used catalyst has been zinc acetate [$Zn(OAc)_2$], but titanium catalysts, other metallic salts, dinuclear cluster compounds, ionic liquids, and heterogeneous catalysts have been explored to search for a more effective option.[3,4,7–13] With our discovery of bimetallic catalysts capable of esterification highlighted in Chapter 3, we wondered if these new catalysts would be competitive with the known catalysts for the depolymerization of PET and chose glycolysis, as the most attractive depolymerization reaction, to test the hypothesis.

Scheme 5.1. Different PET depolymerization pathways and product monomers.

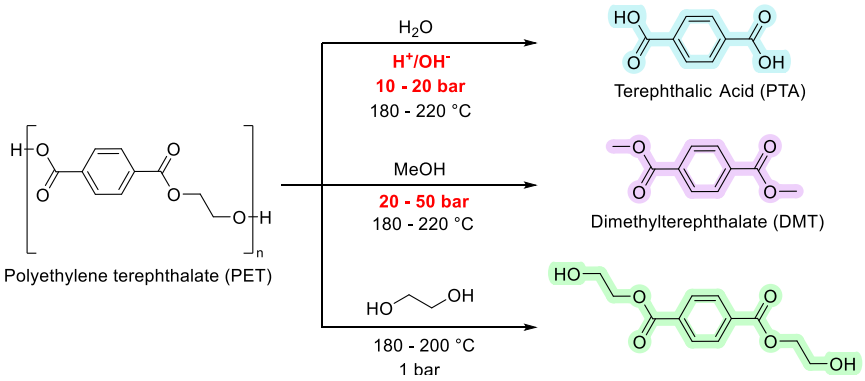

5.2 Results

5.2.1 Catalyst Solubility

In early testing, TBT was used as the primary catalyst used in optimizing the reaction parameters. TBT was added to the reaction in a solution with ethylene glycol to help with fluidity and help wash the

catalyst into the vessel quantitatively. When the mixed metal catalysts were attempted to be used in the same manner it became evident that the catalyst, and in fact any of the compounds containing long carboxylate ligands, were insoluble in ethylene glycol even at reaction temperatures. This would likely severely affect the ability of the complex to contact PET and EG to catalyze the reaction. We found that if a relatively small amount of monomer (3 wt%) was added as a cosolvent to a heated EG mixture, 2TBT:BiNeo could then be dissolved. The condition of having BHET in solution clearly occurs after the reaction has proceeded to a substantial extent and so the catalyst may become more active over the reaction progress if not agglomerated irreversibly by the insolubility in reaction solvent. However, if these reactions were run industrially in a continuously stirred reactor (CSTR) where reactant is slowly added and product is slowly removed constantly, then a base level of BHET would constantly be present and the mixed metal catalysts would maintain solubility throughout. To simulate these conditions, reactions after this observation were run with 3 wt% of BHET added before reaction.

5.2.2 Reaction Sampling Method and Reproducibility

After generating a calibration curve using known amounts of monomer (BHET) dissolved in methanol, a test reaction using 1 mol% TBT at 190 °C with excess ethylene glycol was allowed to react for 180 minutes. At later time points during this reaction, the calculated monomer yield leveled off at around 145%. The HPLC workup procedure was validated for all steps after sampling from the reactor, so the method of sampling was tested. To the reactor, 4.0 g of BHET was added along with the normal amount of ethylene glycol used in a reaction, pressurized to 20 bar to enable sampling through the dip tube, heated to 190 °C, then 5 samples were taken in close succession. After HPLC workup these samples gave a predicted value of 5.92 ± 0.34 g of BHET, a significant overprediction of ca. 150%. We then tested if the pressurization of the reactor was having an effect on the sampling, hypothesizing that the rapid depressurization during removal of the reaction solution via the dip tube may be leading to flash distillation of a significant amount of ethylene glycol and the concentration of the remaining BHET. When

a septum was fashioned onto the reactor and the same conditions were tested as before (4.0 g BHET, 70 g EG, 190 °C) but at atmospheric pressure, the following HPLC workup calculated 4.20 ± 0.20 g of BHET was in the reactor, much closer to accurate, although still slightly overpredicting the true amount. After repeating the experiment and seeing that the slight overprediction was reproducible and likely systematic, we noticed that the first of the series of samples taken would lead to a calculated BHET mass significantly greater than the following samples. During sampling through a septum, the stirring is turned off to prevent the needle hitting into the stirring propeller and a sample was being taken immediately after turning the stirring off. We found that if some delay was added between turning off the stirring to the reactor and when a sample was taken, the variation between the first and second samples was reduced from 12.6% to 2.2%. This may be due to settling of unreacted PET that could have been interfering with sampling through a needle.

With this sampling method seemingly reproducible, accurate, and precise, a new calibration curve was generated. This calibration was done in a similar manner to the testing described above, where a known amount of BHET was added to the reaction in EG, heated to reaction temperature, then sampled in triplicate. Making the calibration in this manner should account for some of the variation in sampling from the reactor. The calibration gave a linear fit with R^2 of 0.994 and can be found in Figure 5.1a.

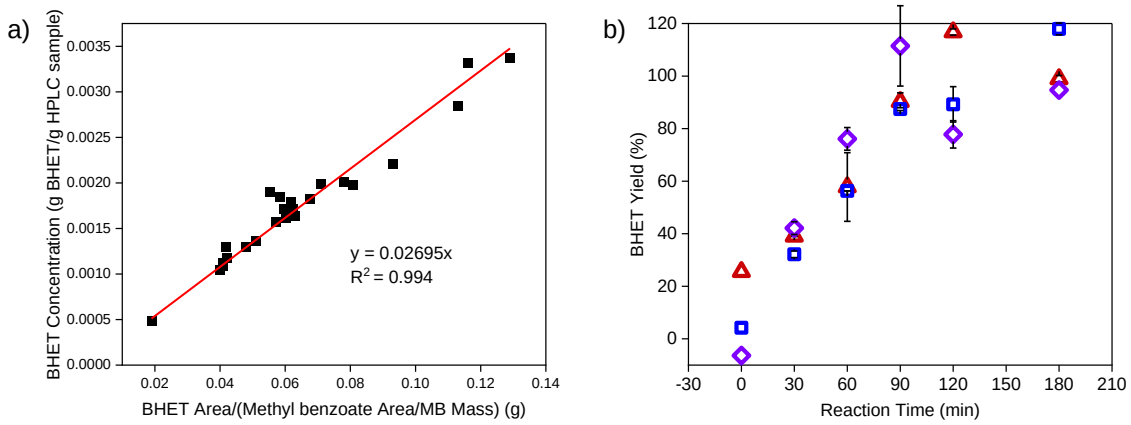

Figure 5.1. a) Calibration curve of HPLC-derived BHET concentration in reactor. b) Time-course plots of triplicate reactions with conditions of 2 g PET, 2 g of BHET, 70 g ethylene glycol, 1 mol% 2TBT:BiNeo, 190 °C sampled in duplicate and error bars representing 1 standard deviation.

The reaction-to-reaction reproducibility was tested by running three reactions using 1 mol% 2TBT:BiNeo at 190 °C and sampling in duplicate at each time point for 180 minutes (Figure 5.1b). The variation between each duplicated sample within a run is relatively low (4.1%), but the variation at a given time point between runs is higher (12.5%). The source of variation between the runs has not fully been understood to this point although two different reactors with different temperature controllers were being employed and may cause variation.

5.2.3 Catalyst Comparisons

The first set of comparisons that were made between catalysts was examining the relative reactivity of the mixed metal catalyst, 2TBT:BiNeo, and the unmixed precursors, TBT and BiNeo. As can be seen in Figure 5.2a and Figure 5.2b, reactions should be run at least at 190 °C to get close to full PET conversion in 3 hours. It should be noted that there have been abnormal time-course reactivity profiles reported for PET glycolysis due to multiple factors including the breakdown of PET. When the mixed catalyst is compared to TBT or BiNeo alone in Figure 5.2c, the mixed catalyst clearly outperforms either

precursor reaching 100% BHET yield in around 90 minutes while TBT takes 180 minutes and BiNeo only reached around 70% monomer yield in 180 minutes. It is interesting that in the probe esterification reactions that were used in Chapters 2 and 3, BiNeo gave no reaction over background, but it can achieve some catalysis for the depolymerization reaction where the background reaction gave less than 15% BHET yield under the same conditions.

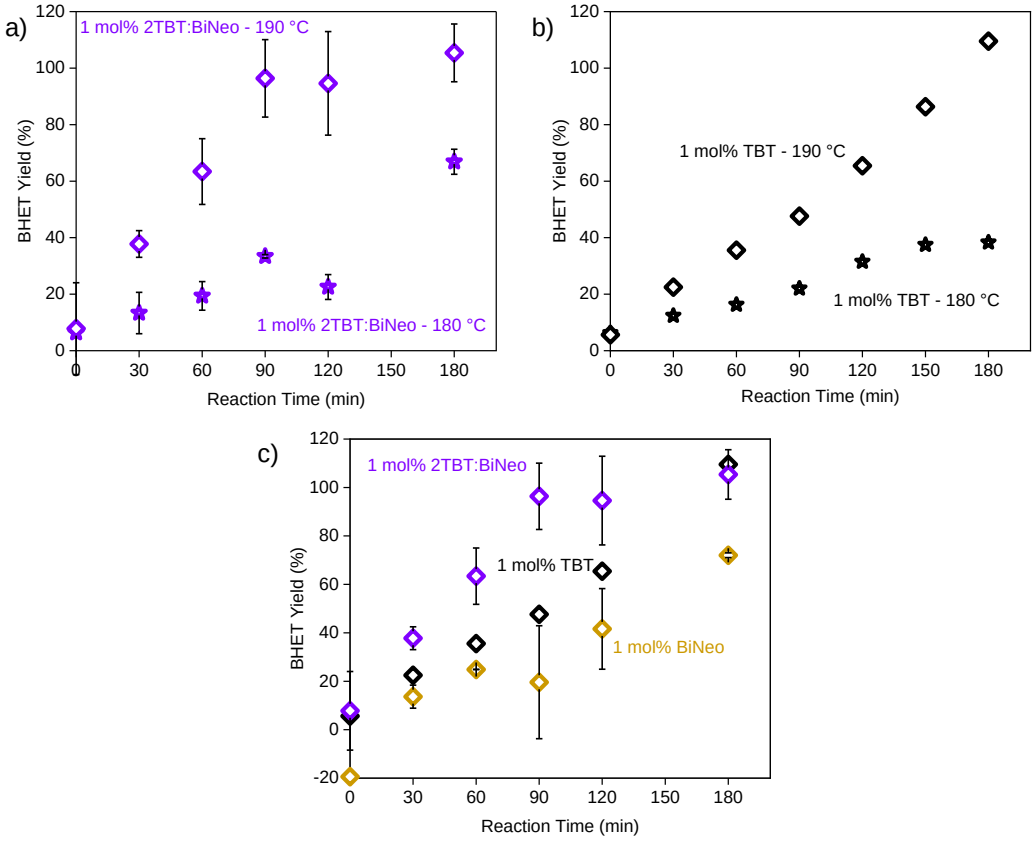

Figure 5.2. Time-course plots of PET depolymerization reactions with conditions of 2 g PET, 2 g of BHET, 70 g ethylene glycol. a) Comparison of 2TBT:BiNeo at 1 mol% loading at 180 and 190 °C. b) Comparison of TBT at 1 mol% loading at 180 and 190 °C. c) Comparison of 2TBT:BiNeo to TBT and BiNeo each at 1 mol% loading.

Understanding now that 2TBT:BiNeo did catalyze the PET depolymerization reaction more efficiently than the precursors the most common industrially used catalysts, zinc acetate ($Zn(OAc)_2$) was compared against 2TBT:BiNeo. Figure 5.3a demonstrates this comparison using the most standard reaction conditions utilizing bottle flakes as the plastic source and showed that $Zn(OAc)_2$ even outperformed 2TBT:BiNeo. It was hypothesized that the difference in catalyst's abilities to interact with the PET polymer could influence reactivity and that longer chain ligands would allow for better interaction between the solid PET even if the catalysis of the transesterification was slower. To test this, the reaction with bottle flakes was compared to the reaction with lower surface area PET pellets. The results of this test can be seen in Figure 5.3b and show that the pellets do react more slowly and the end results are perhaps not as different (40% difference vs 20% difference after 60 minutes for flakes and pellets, respectively), the zinc catalyst still clearly outperforms the mixed metal catalyst.

As studied in previous chapters of this thesis, one of the highlights of 2TBT:BiNeo was the robustness towards water it possesses. Zinc acetate has been reported to undergo conversion to zinc hydroxide or agglomerate with water present, so we tested the amount of water present within the reaction.[14] To estimate the amount of water that would be present on a waste water bottle entering a recycling facility without intentional drying, bottles were washed with water, and the amount of water that stuck to the bottle was weighed at about 20% of the mass of plastic. This ends up being about 0.6 wt% of the total reaction mixture being employed or about 0.4 mL. On the other hand, an extra dry reaction was also set up by drying the ethylene glycol being used with 3Å mol sieves. These reactions can be seen in Figure 5.3c and Figure 5.3d, respectively, and summarized in Figure 5.3e and Figure 5.3f. With added water, $Zn(OAc)_2$ is relatively unaffected and outperforms 2TBT:BiNeo, but under dry conditions $Zn(OAc)_2$ has depressed reactivity while 2TBT:BiNeo is unaffected. Under dry conditions, 2TBT:BiNeo in fact outperforms $Zn(OAc)_2$.

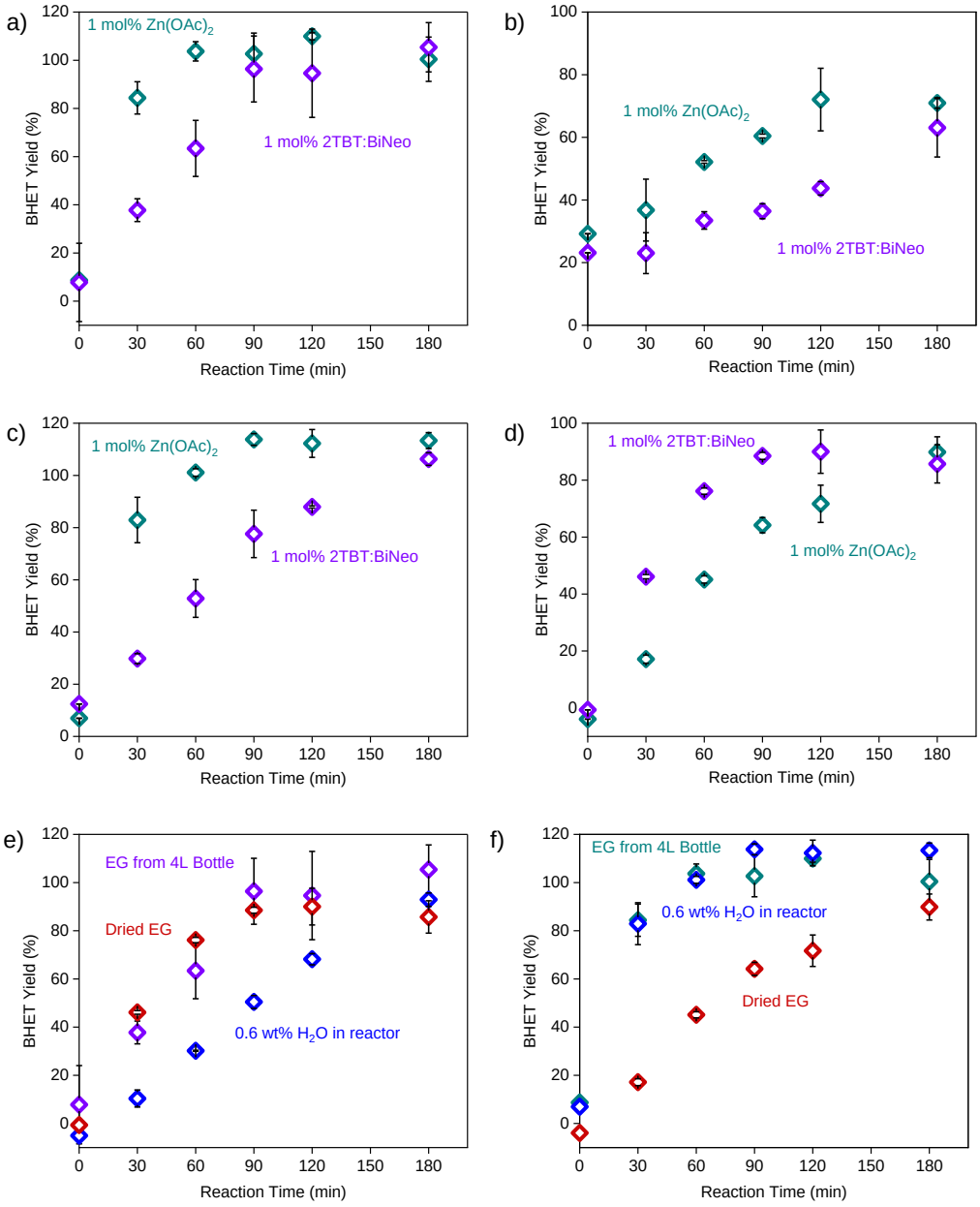

Figure 5.3. Time-course plots of PET depolymerization reactions comparing 2TBT:BiNeo with $Zn(OAc)_2$ with conditions of 2 g PET, 2 g of BHET, 70 g ethylene glycol, and 190 °C. a) Using bottle flakes, b) using cryo-ground and sieved PET pellets (425-850 μm), c) with 0.6 wt% water added using bottle flakes, d) with dried ethylene glycol using bottle flakes. e) 2TBT:BiNeo with different moisture levels and f) $Zn(OAc)_2$ with different moisture levels. Conditions of 2 g PET flakes, 2 g of BHET, 70 g ethylene glycol, at 190 °C. EG from 4L Bottle refers to glycol taken from the bottle without additional treatment.

5.2.4 Plastic Characterization

Additional characterization of the two plastic sources used in reactivity testing was done using thermogravimetric analysis and differential scanning calorimetry (TGA-DSC). DSC data can show differences in glass transition temperature (expected between 67 °C (amorphous PET) and 81 °C (crystalline PET)), the melting point of 245-260 °C, and the crystallinity by quantifying the crystallization that happens between the glass transition and melting. When each plastic source was heated from 25 °C to 600 °C, only the melting points and decomposition around 350-450 °C are observed. The expected positive heat flow for crystallization is not visible, which may suggest both sources are very crystalline. PET is generally semi-crystalline and the more crystalline, the lower permittivity to things like water. It would make sense for a plastic bottle to have a relatively high crystallinity, but it is still expected that some of the material would be amorphous.

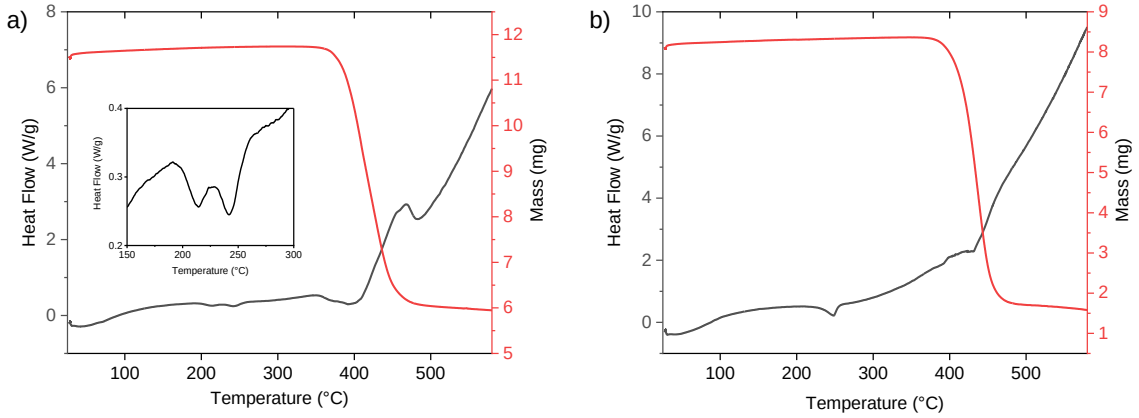

Figure 5.4. TGA-DSC plots for a) cryo-ground PET pellets, and b) water bottle flakes.

5.2.5 Future Directions

We have developed a system to analyze PET decomposition. We hope this will be useful in the future for studies on other reaction parameters or catalysts for the reaction or related reactions. The

challenges associated with sampling from a significantly heterogeneous mixture were largely solved. As it stands, the industrial catalyst outperforms 2TBT:BiNeo as a mixed metal catalyst comparison under most conditions. The intriguing result that dried ethylene glycol led to lower reactivity from zinc acetate but not for 2TBT:BiNeo should be further explored. We hypothesize that a certain amount of water could activate the zinc which is unnecessary for 2TBT:BiNeo. More rigorous studies into the amount of water in each reaction condition are underway. The effect of higher temperatures may also be examined as zinc acetate is known to be inactive past 245 °C.[15] Additionally, to test at even more industrially relevant conditions, the effect of different contaminants including pigments, should be examined.

5.3 Experimental

Materials. Transparent poly(ethylene terephthalate) (PET) water bottles (Great Value) with a measured thickness of 110 μm were washed with EtOH, dried in an oven at 60 °C overnight, the thicker plastic around the top and bottom of the bottle as well as the label and label adhesive was removed then the remaining plastic was cut into 1x1 cm flakes. PET pellets (Sigma-Aldrich) were cryo-ground using a coffee grinder with added dry ice and sieved to 425-850 μm. Bis(2-hydroxyethyl) terephthalate (BHET, Sigma-Aldrich 96%), ethylene glycol (EG, Fisher Chemical 99.7%), methyl benzoate (MB, Sigma-Aldrich 99%), methanol (MeOH, Fisher Chemical, HPLC Grade) were all used as received unless otherwise stated.

Reaction Procedure. To a 100-mL stainless-steel autoclave vessel (Parr pressure reactor, Moline, IL) equipped with pressure gauge, thermocouple, and propeller stirrer driven by a magnetically coupled overhead stirrer, 2 g of PET flakes, 2 g of BHET (ca. 2.7 wt% of reaction mixture), and 70 g of ethylene glycol were added. (Note: BHET was added to the reactor pre-reaction to improve catalyst solubility.) After sealing the reaction vessel, the stirring was set to 600 RPM and the temperature to 190 °C using an autotuned PID temperature controller (Parr 4836 Controller). Reaction temperature was measured through a thermocouple (J-type) submerged in the reaction medium, and a secondary temperature control box was employed as a safety measure and set at a maximum of 300 °C to monitor and control the

heating well the vessel sits within. Care was taken that the heating ring within the heating well was snug around the vessel for best heating. The autoclave and heating well were covered in aluminum foil to prevent excess heat loss and typical heating from room temperature to 190 °C would take 30-40 minutes. After reaching the desired reaction temperature, catalyst was added through a septum via syringe which was then washed in with ethylene glycol and this marked time = 0 for a reaction. Sampling from the reactor was done via syringe through a septum and stirring was stopped for 60 seconds before a sample was taken to improve sampling consistency.

In the case of adding water, the amount of water was determined by filling three water bottles roughly 1/3 full, shaking with the cap on, dumping out the water, weighing how much water remained on the bottle, then averaging the value between the three trials.

Sample preparation and HPLC analysis. Samples of 0.2-0.4 g were taken from the reactor into a weighed vial. This was dissolved in 5 g of MeOH/methyl benzoate (ca. 0.04 g MB/g MeOH). Methyl benzoate was obtained from Sigma-Aldrich as used without purification. In a new weighed vial, 1 g of the previous mixture was added and diluted a second time with 4 g of MeOH. This diluted mixture was then pushed through a 0.22 μm nylon syringe filter (Thermo-Fischer, 13 mm diameter) into an HPLC vial. HPLC samples were analyzed using a C18 reverse-phase column and 75/25 v/v MeOH/H_2O mobile phase flowing at 0.2 mL/min. A DAD (UV-vis) detector (Agilent 1200 Series) equipped with halogen and deuterium lamps was set to collect signal at 254 nm. The peaks of interest were integrated using autointegration within the Chemstation software and the areas relative to the methyl benzoate peak/mass of methyl benzoate were calculated. A sample chromatogram can be seen below where the peaks are BHET (7.728 min), dimer (10.010 min), and methyl benzoate (12.602 min).

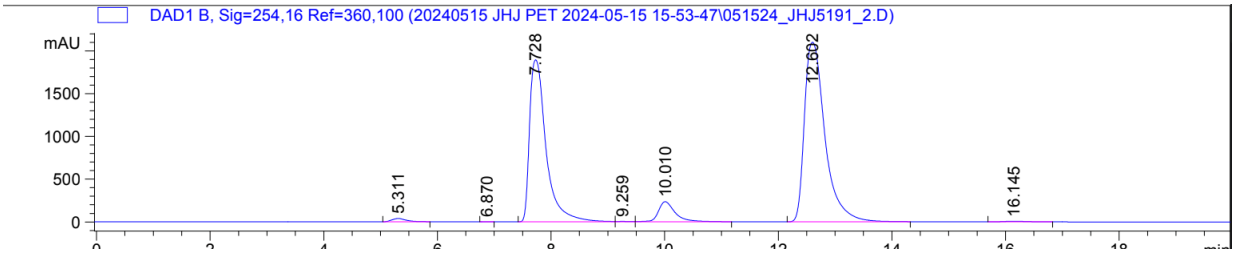

Figure 5.5. Sample chromatogram of reaction mixture with added methyl benzoate.

Thermogravimetric analysis-differential scanning calorimetry. (TGA-DSC). Dry 10 mg of PET was added to an aluminum crucible. Temperature programming was as follows: under a 50 mL/min flow of N_2 heating started from 25 °C, ramped to 600 °C at 10 °C, held for 60 minutes.

5.4 References

(1) Geyer, R.; Jambeck, J. R.; Law, K. L. Production , Use , and Fate of All Plastics Ever Made. *Sci Adv* **2017**, No. 3, 25–29.

(2) Diakhaby, M.; Feber, D.; Mirza, Y.; Nordigarden, D.; Shields, B.; Wallach, J. *Filling the Gap: Boosting Supply of Recycled Materials for Packaging*; 2023.

(3) Xin, J.; Zhang, Q.; Huang, J.; Huang, R.; Jaffery, Q. Z.; Yan, D.; Zhou, Q.; Xu, J.; Lu, X. Progress in the Catalytic Glycolysis of Polyethylene Terephthalate. *J Environ Manage* **2021**, *296* (February 2021), 113267. https://doi.org/10.1016/j.jenvman.2021.113267.

(4) Carta, D.; Cao, G.; Angeli, C. D.; Interuniversitario, C.; La, N. Chemical Recycling of Poly (Ethylene Terephthalate) (PET) by Hydrolysis and Glycolysis. *Environmental Science & Pollution Research* **2003**, *10* (6), 390–394.

(5) Benyathiar, P.; Kumar, P.; Carpenter, G.; Brace, J.; Mishra, D. Polyethylene Terephthalate (PET) Bottle-to-Bottle Recycling for the Beverage Industry: A Review Patnarin. *Polymers (Basel)* **2022**, *14* (12), 1–29.

(6) Lu, S.; Jing, Y.; Feng, B.; Guo, Y.; Liu, X.; Wang, Y. H2-Free Plastic Conversion: Converting PET Back to BTX by Unlocking Hidden Hydrogen. *ChemSusChem* **2021**, *14* (19), 4242–4250. https://doi.org/10.1002/CSSC.202100196.

(7) Mohammadi, S.; Bouldo, M. G.; Enayati, M. Controlled Glycolysis of Poly(Ethylene Terephthalate) to Oligomers under Microwave Irradiation Using Antimony(III) Oxide. *ACS Appl Polym Mater* **2023**, *5* (8), 6574–6584. https://doi.org/10.1021/acsapm.3c01071.

(8) Saadet, O.; Orbay, M. Simultaneous Glycolysis and Hydrolysis of Polyethylene Terephthalate and Characterization of Products by Differential Scanning Calorimetry. *Polymer (Guildf)* **2003**, *44*, 7609–7616. https://doi.org/10.1016/j.polymer.2003.09.062.

(9) Pardal, F.; Tersac, G. Comparative Reactivity of Glycols in PET Glycolysis. *Polym Degrad Stab* **2006**, *91* (11), 2567–2578. https://doi.org/10.1016/j.polymdegradstab.2006.05.016.

(10) Cot, S.; Leu, M. K.; Kalamiotis, A.; Dimitrakis, G.; Sans, V.; de Pedro, I.; Cano, I. An Oxalate-Bridged Binuclear Iron(III) Ionic Liquid for the Highly Efficient Glycolysis of Polyethylene Terephthalate under Microwave Irradiation. *Chempluschem* **2019**, *84* (7), 786–793. https://doi.org/10.1002/cplu.201900075.

(11) Zhang, S.; Hu, Q.; Zhang, Y.-X.; Guo, H.; Wu, Y.; Sun, M.; Zhu, X.; Shang, J.; Gong, S.; Liu, P.; Niu, Z. Depolymerization of Polyesters by a Binuclear Catalyst for Plastic Recycling. *Nat Sustain* **2023**, No. 6, 965–973. https://doi.org/https://doi.org/10.1038/s41893-023-01118-4.

(12) Troev, K.; Grancharov, G.; Tsevi, R.; Gitsov, I. A Novel Catalyst for the Glycolysis of Poly (Ethylene Terephthalate). *J Appl Polym Sci* **2003**, *90*, 1148–1152.

(13) Bartolome, L.; Imran, M.; Gyoo Cho, B.; Al-Masry, W. A.; Hyun Kim, D. Recent Developments in the CHemical Recycling of PET. In *Material Recycling: Trends and Perspectives*; 2012; pp 65–84. https://doi.org/10.5772/33800.

(14) Al-sabagh, A. M.; Yehia, F. Z.; Eshaq, G.; Rabie, A. M.; Elmetwally, A. E. Greener Routes for Recycling of Polyethylene Terephthalate. *Egyptian Journal of Petroleum* **2016**, *25* (1), 53–64. https://doi.org/10.1016/j.ejpe.2015.03.001.

(15) Campanelli, J. R.; Kamal, M. R.; Cooper, D. G. Kinetics of Glycolysis of Poly(Ethylene Terephthalate) Melts. *J Appl Polym Sci* **1994**, *54*, 1731–1740.

A2. Chapter 2 Appendix

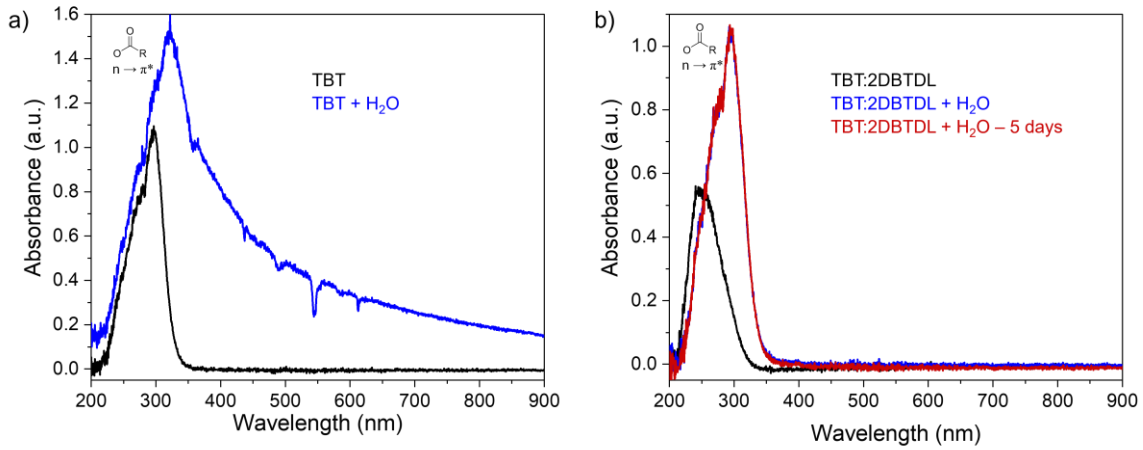

Figure A 2.1. Overlaid UV-vis spectra of (a) TBT or (b) TBT:2DBTDL showing baseline shifts caused by Tyndall scattering from clouding by metal oxide colloids in solution. TBT:2DBTDL was mixed with water then allowed to sit in a sealed vial for 5 days before collection of a subsequent spectrum. The major absorbance is attributed to the carbonyl-based n → π* transition.

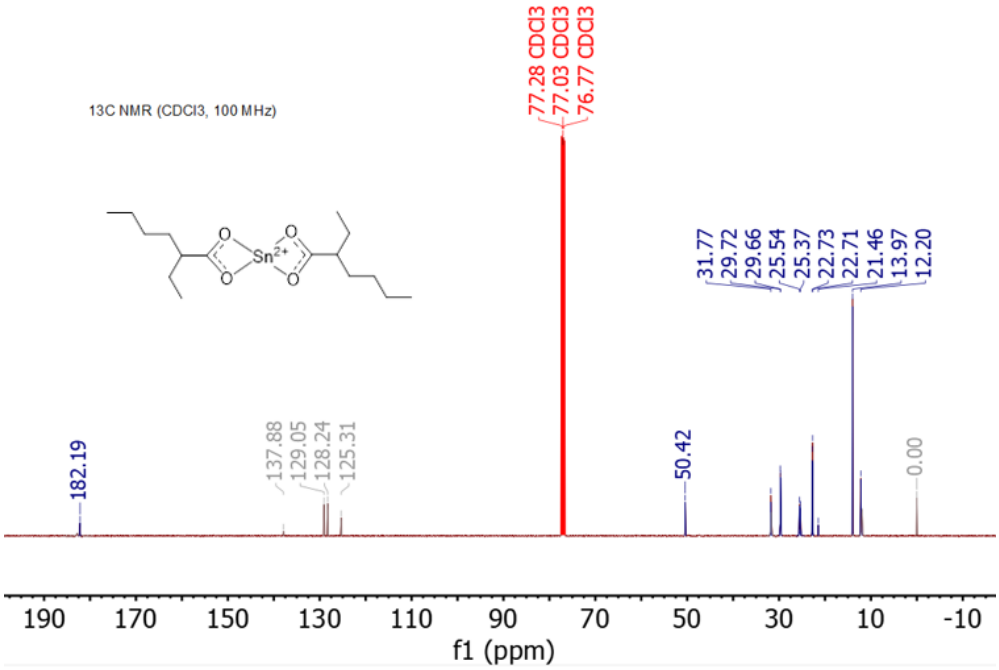

Figure A 2.2. ^{13}C NMR spectrum of SnOct. Grayed out signals in the 125-137 ppm region are due to toluene impurity from the provider.

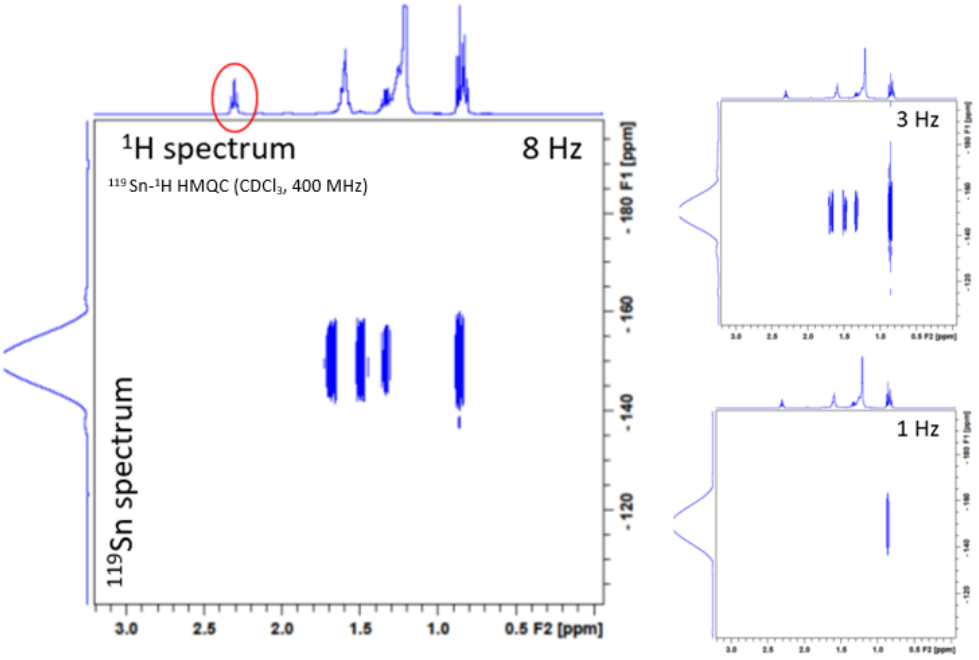

Figure A 2.3. ^{119}Sn-^{1}H HMQC NMR spectra of DBTDL. Optimized coupling constant in top right of spectra. Shows no SnH correlations are seen to laurate α-CH_2.

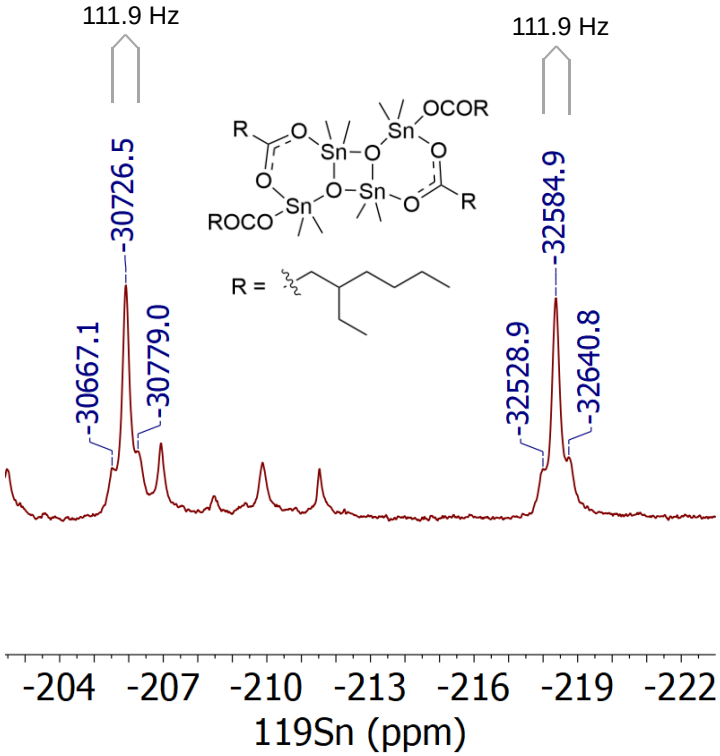

Figure A 2.4. ^{119}Sn NMR spectrum of TBT:2DBTDL after hydrolysis/aging indicating distannoxane Sn_4 formation.[2] Structure is literature suggested structure of analogous distannoxane with R = CH_3. Sn-butyl groups have been shortened to methyl to simplify the drawn structure.

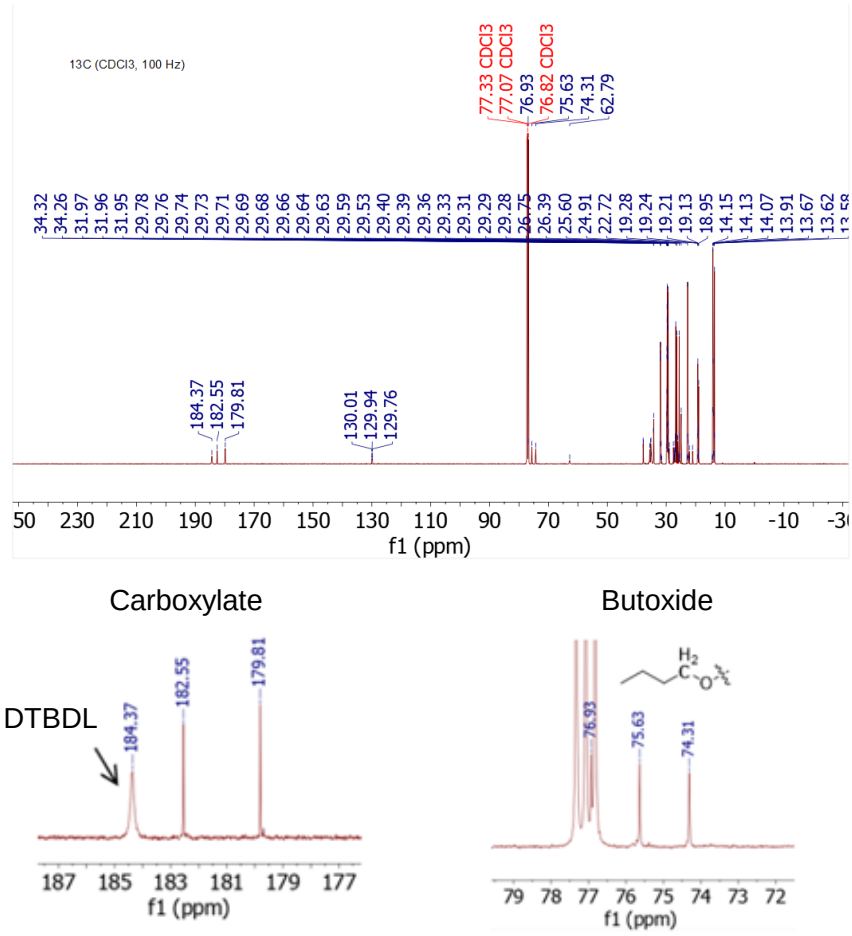

Figure A 2.5. ^{13}C NMR spectrum of TBT:2DBTDL.

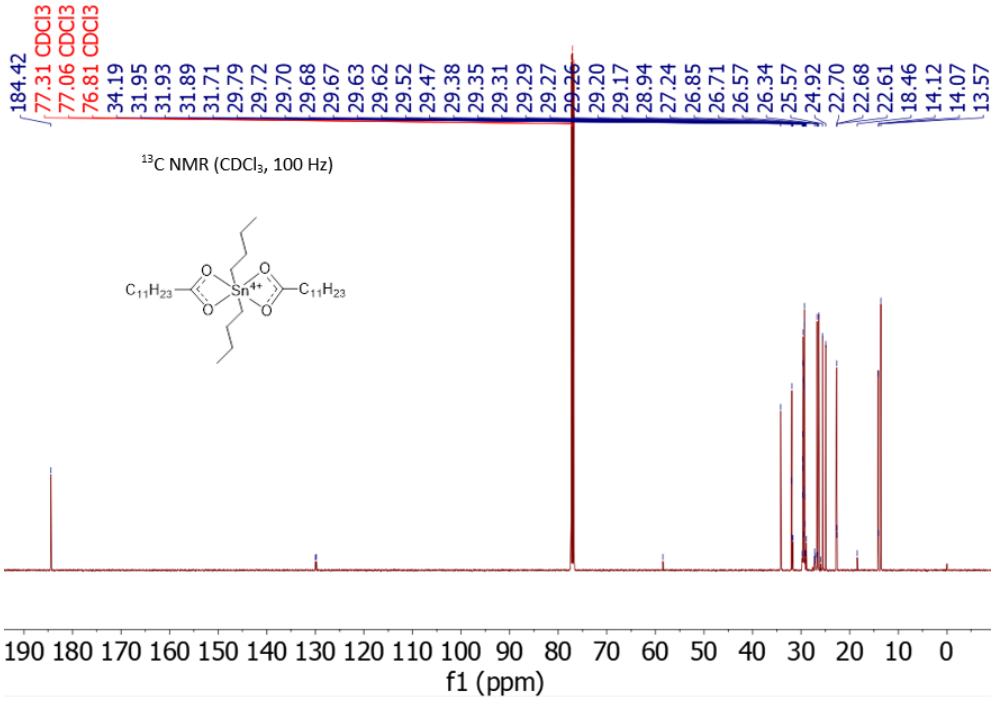

Figure A 2.6. ^{13}C NMR spectrum of DBTDL.

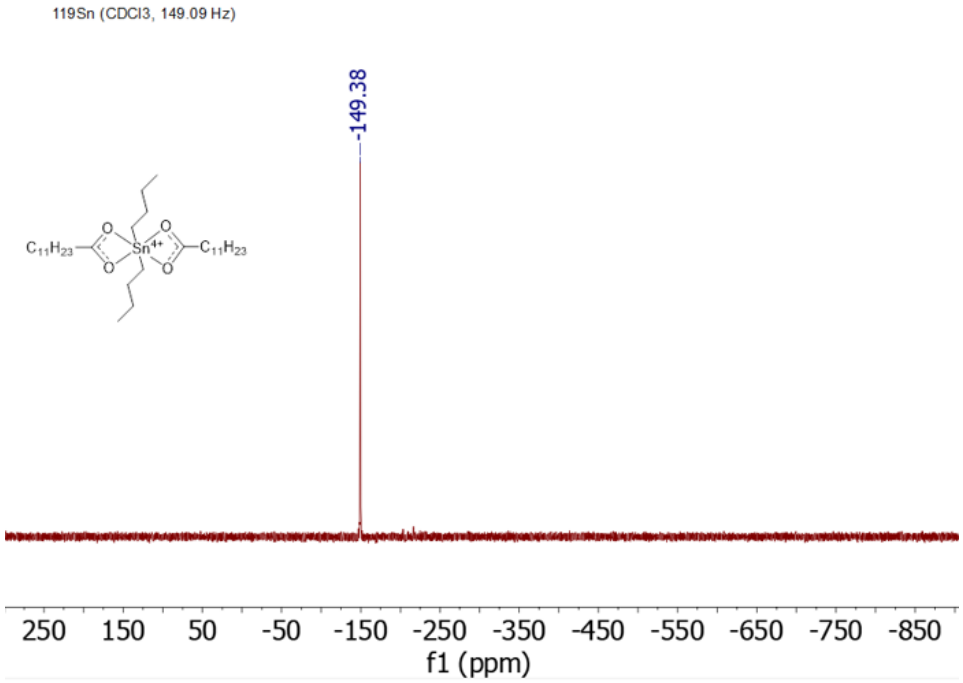

Figure A 2.7. ^{119}Sn NMR spectrum of DBTDL.

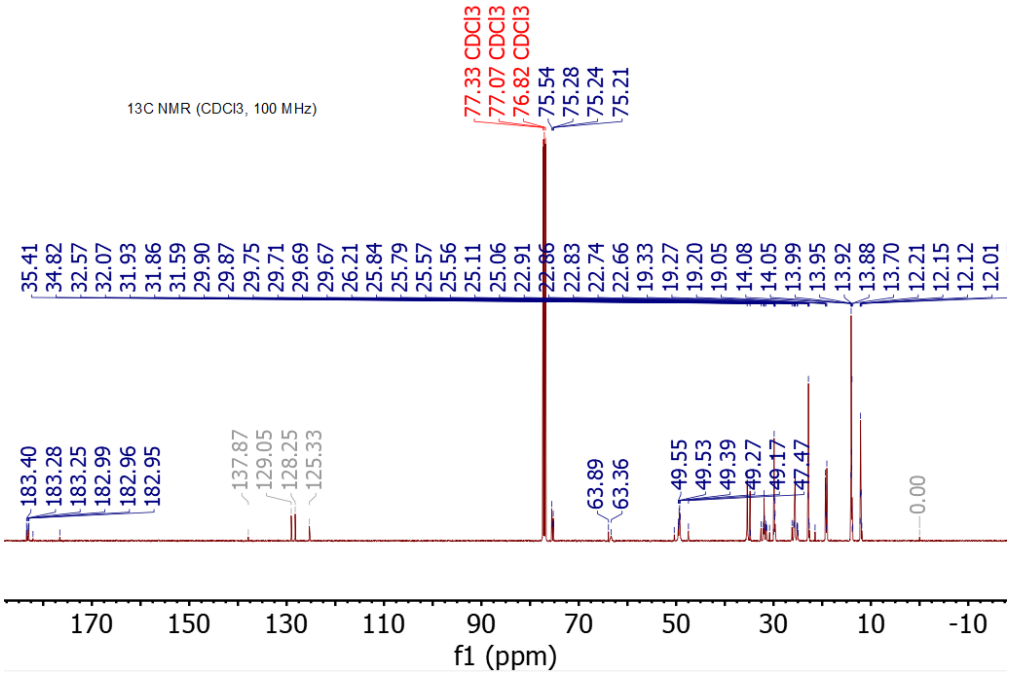

Figure A 2.8. ^{13}C NMR of TBT:2SnOct. Grayed out signals in the 125-137 ppm region are due to a toluene impurity from the provider.

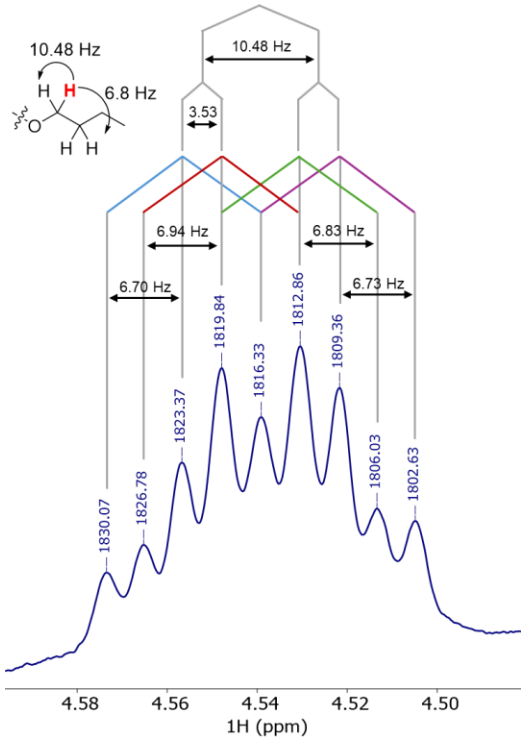

Figure A 2.9. Coupling tree for multiplet from TBT:2SnOct and hypothesized source of coupling.

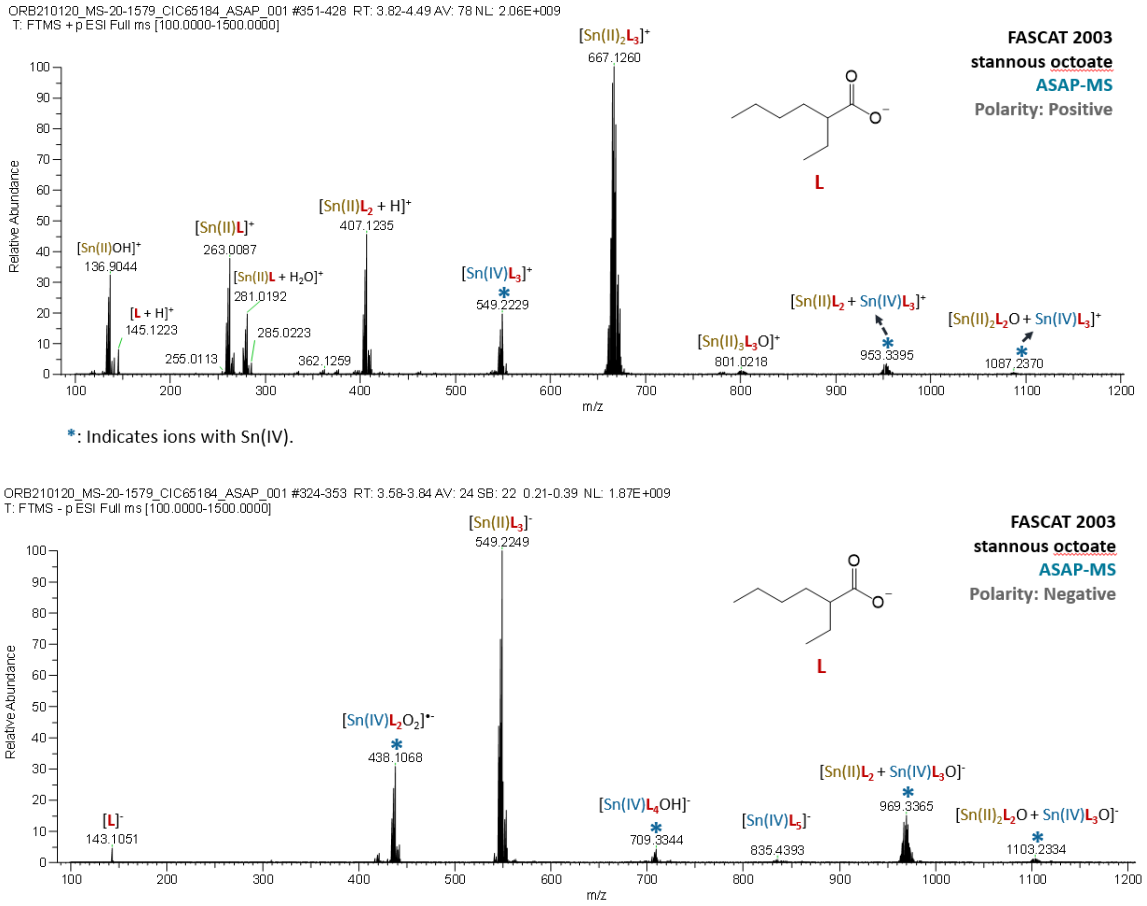

Figure A 2.10. ASAP-MS spectrum of stannous octoate in positive and negative polarity. The positive polarity mode shows Sn(II) dimers are the most abundant species, but this can be dismissed as the results of in-source cluster formation as DOSY NMR predicts monomers in solution. Sn(IV) may be from hydrolysis product or from oxidation during ionization.

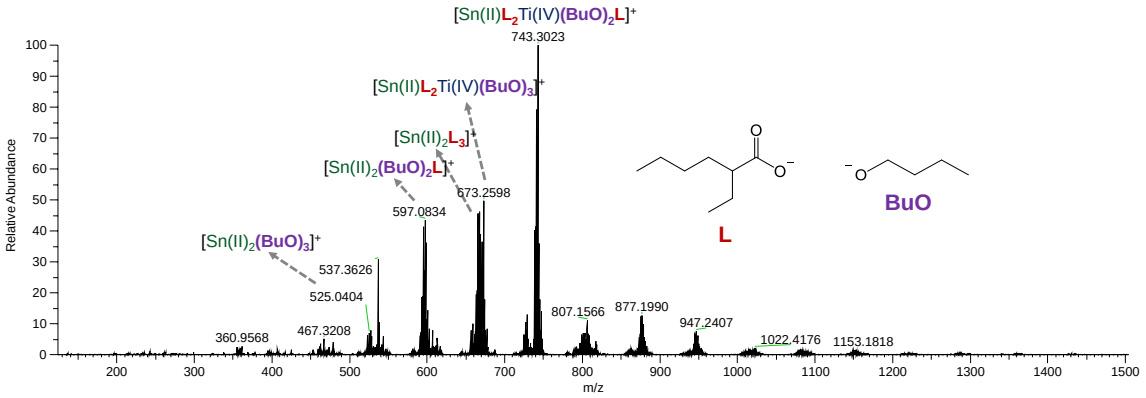

Figure A 2.11. ASAP-MS spectrum of TBT:2SnOct. Over-representation of Sn_2 dimers demonstrated by ASAP-MS of pure SnOct in positive polarity mode in Figure S27.

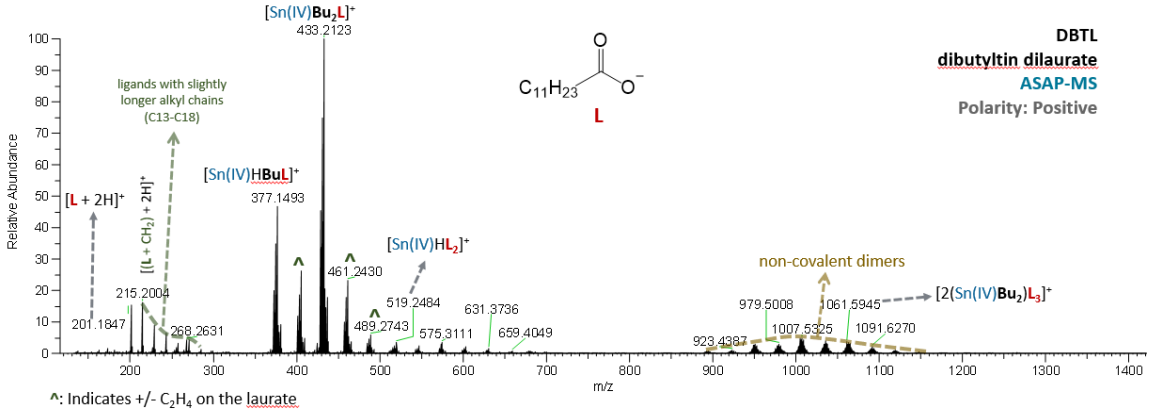

Figure A 2.12. ASAP-MS of DBTDL. Hat symbols represent laurate ligand impurities +/- C_2H_4.

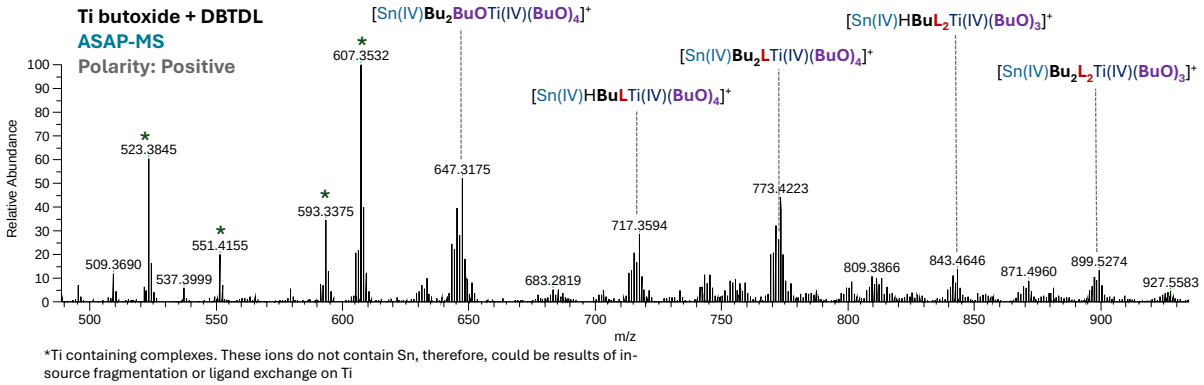

Figure A 2.13. ASAP-MS of TBT:2DBTDL.

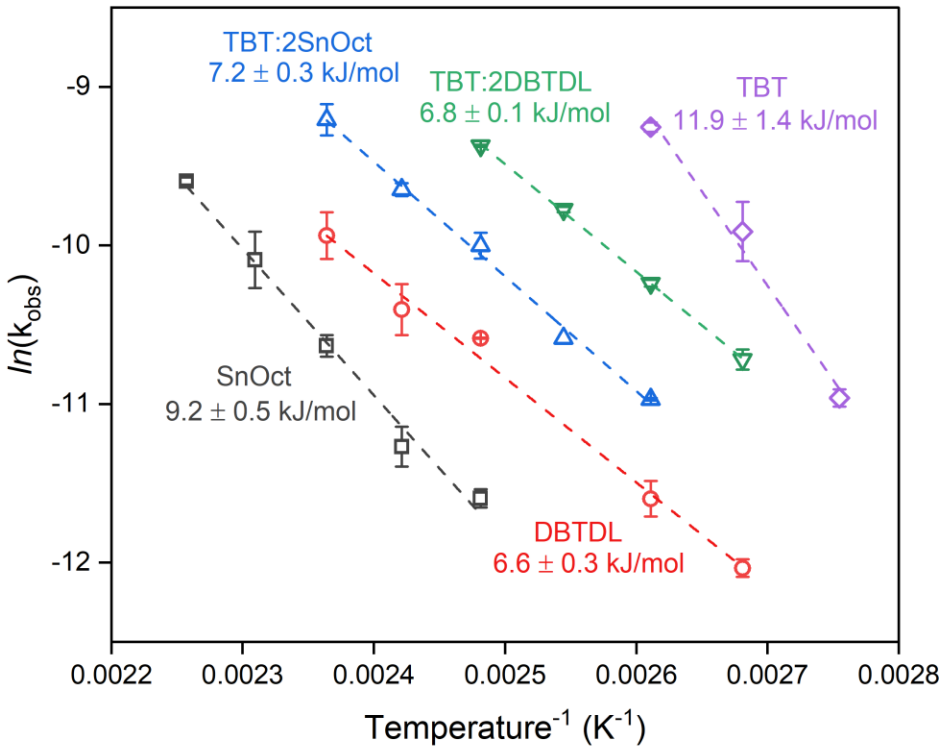

Figure A 2.14. Arrhenius Plots for different tested catalysts. Initial rates collected at <10% conversion at a 0.01 mol% catalyst loading by total metal. Error bars represent 2 standard deviations based off independent triplicate runs. Dotted line is a least-squares fit of the experimental data.

A3. Chapter 3 Appendix

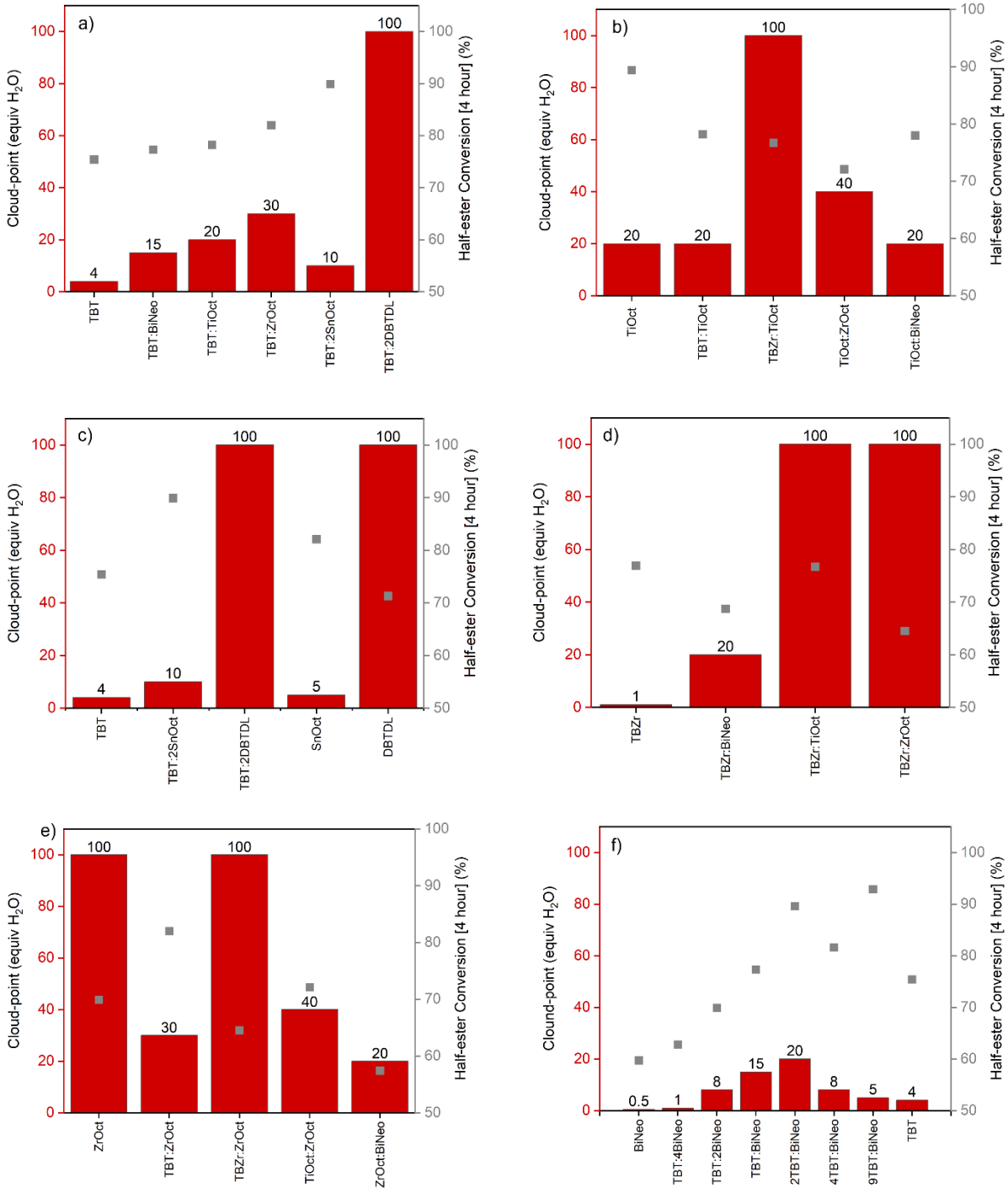

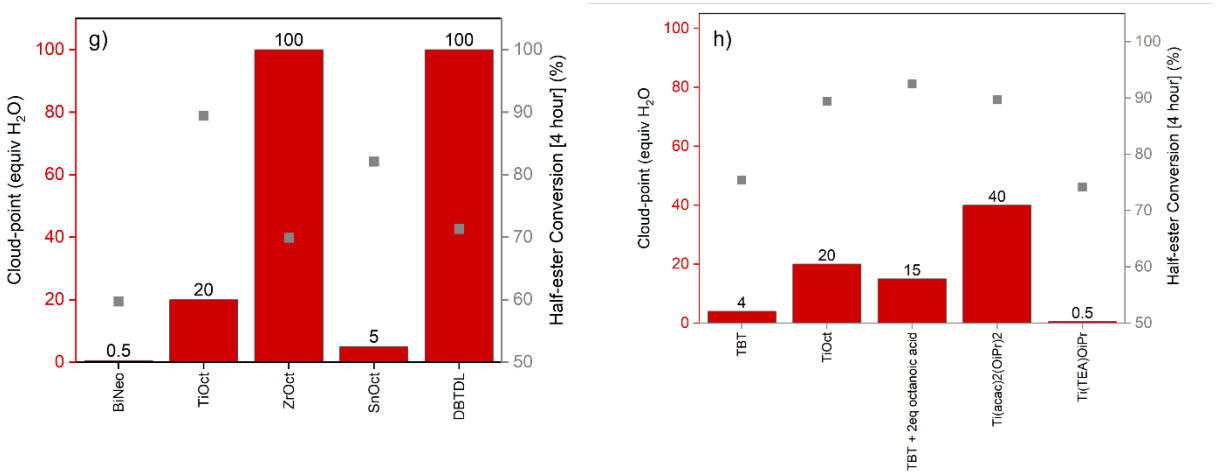

Figure A 3.1. Stability and reactivity data for mixed metal catalysts. (a) Tetrabutyl titanate (TBT) mixes with metal carboxylates, (b) mixtures with titanium octoate (TiOct), (c) tin carboxylates and mixtures with TBT, (d) tetrabutyl zirconate (TBZr) mixes with metal carboxylates, (e) mixtures with zirconium octoate (ZrOct), (f) TBT mixtures with bismuth neodecanoate (BiNeo), (g) metal carboxylates, and (h) titanium catalysts. Conversion data after 4 hours was chosen as an intermediate time-point that shows contributions of both high initial activity and robustness of the catalysts.

Table A 3.1. Cloud-point and reactivity summary for mixed and unmixed catalysts.

Catalyst	Cloud-point (equiv H_2O)	Half-ester conversion [4 hour] (%)
9TBT:BiNeo	5	92.9
TBT + 2eq octanoic acid	15	92.5
TBT:2SnOct	10	89.9
$Ti(acac)_2(O^iPr)_2$	40	89.7
2TBT:BiNeo	20	89.6
TiOct	20	89.4
SnOct	5	82.1
TBT:ZrOct	30	82.0
4TBT:BiNeo	8	81.6
TBT:TiOct	20	78.2
TiOct:BiNeo	20	78.0
TBT:BiNeo	15	77.3
TBZr	1	76.9
TBZr:TiOct	100	76.7
TBT	4	75.4
$Ti(TEA)O^iPr$	0.5	74.2
TiOct:ZrOct	40	72.1
DBTDL	100	71.3
ZrOct	100	69.9
TBT:2BiNeo	8	69.9
TBZr:BiNeo	20	68.7
TBZr:ZrOct	100	64.5
TBT:4BiNeo	1	62.8
BiNeo	0.5	59.7
ZrOct:BiNeo	20	57.4
No Catalyst	N/A	61.7

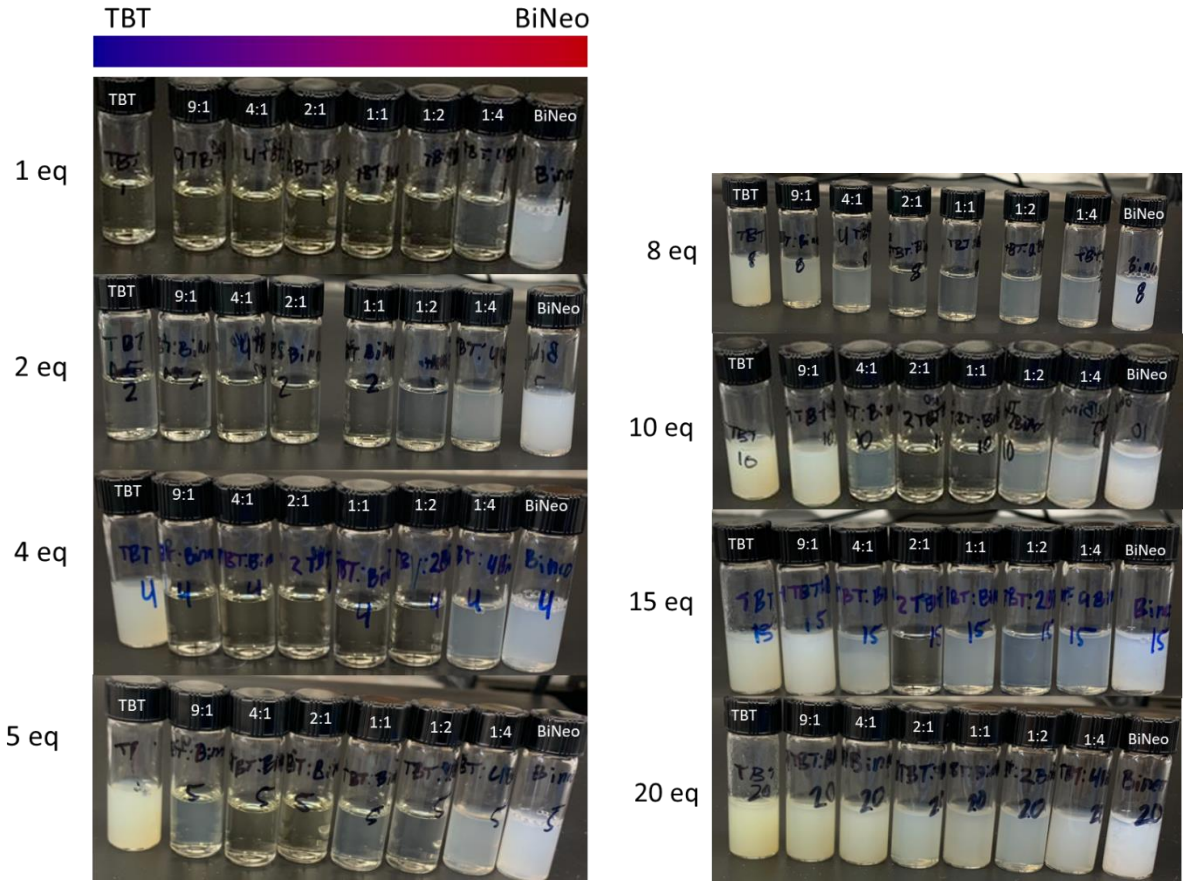

Figure A 3.2. Example photos of cloud-point measurement for TBT/BiNeo mixed metal catalysts. Vials are each 0.1 M by metal of the indicated catalyst mixing ratio in a total of 2 mL of liquid (THF + H_2O). Note the yellowing in TBT predominant catalysts. This is an additional disadvantage to using pure titanates as catalysts as the anatase phase of TiO_2 is known to be yellow in color and can discolor polymers made using titanate.

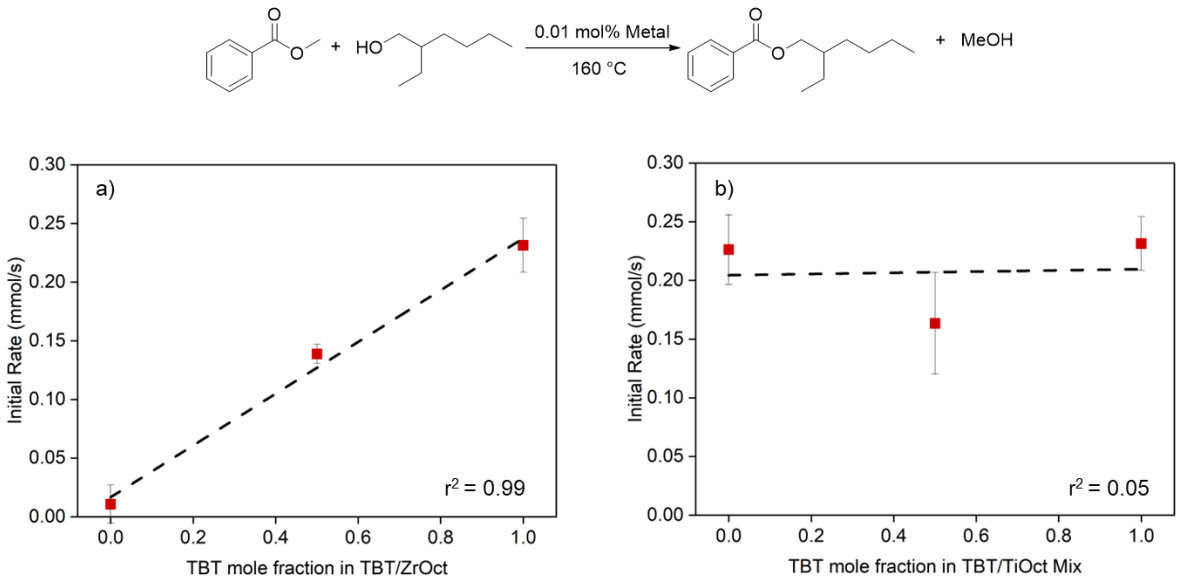

Figure A 3.3. Initial rates of reaction of methyl benzoate with 2-ethylhexanol for different TBT mixed catalysts with various metal carboxylates. (a) TBT:ZrOct, (b) TBT:TiOct. Dashed lines are least-squares fits of the three points. Error bars are two standard deviations based on independent duplicate runs. Reactions were all run with conversions less than 10% to remain in the differential regime with 0.01 mol% metal loading at 160 °C.

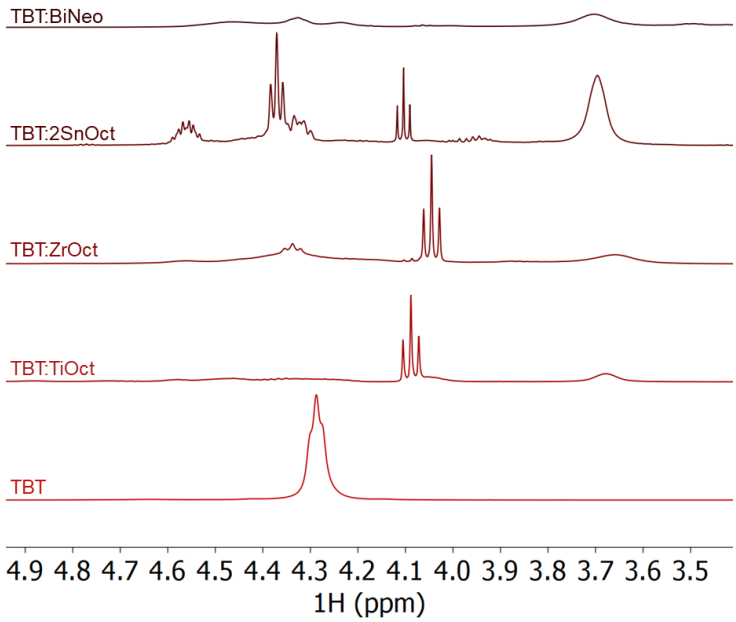

Figure A 3.4. ^{1}H NMR spectra zoomed into butoxy-region of mixed catalysts with metal carboxylates. Note the sharp signals in all but the TBT:BiNeo spectra.

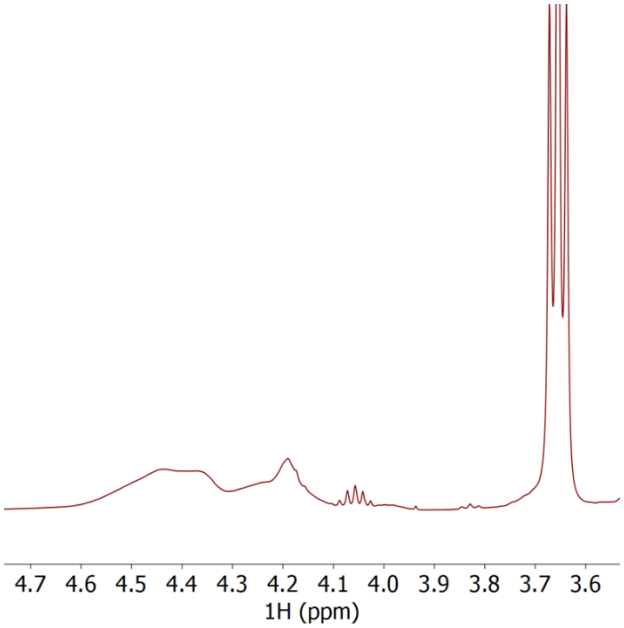

Figure A 3.5. ^{1}H NMR spectra of TBT:BiNeo collected at -30 °C. Where the butanol signal sharpens significantly into a clear triplet, the M-O^{n}Bu signals from 4.1 to 4.6 ppm are still unresolved indicating that rapid exchange is still present at decreased temperatures.

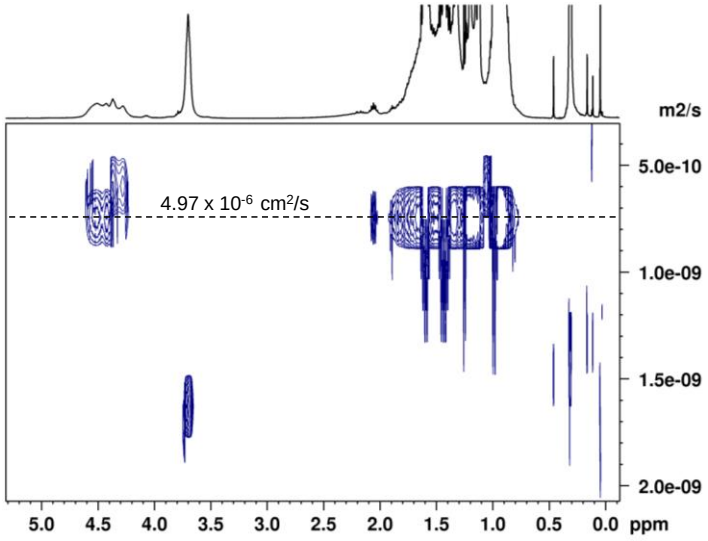

Figure A 3.6. DOSY plot of TBT:BiNeo. Dotted lines indicate the shared diffusion constant of the major compound.

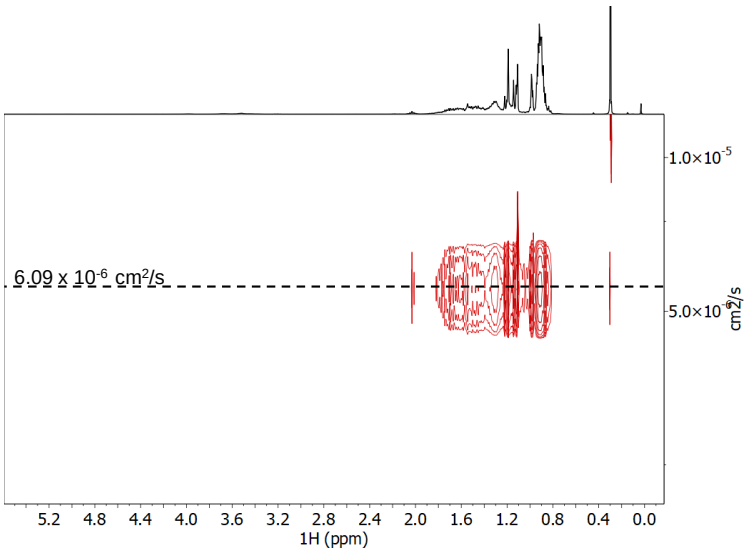

Figure A 3.7. DOSY plot of BiNeo. Dotted lines indicate the shared diffusion constant of the major compound.

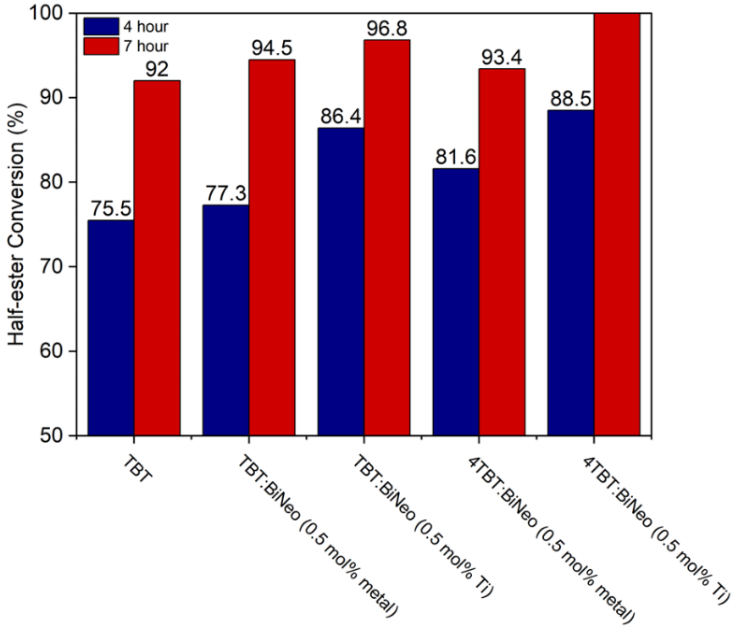

Figure A 3.8. Phthalic anhydride probe reactivity of mixed-metal catalysts at 0.5 mol% titanium loading compared to 0.5 mol% metal loading.

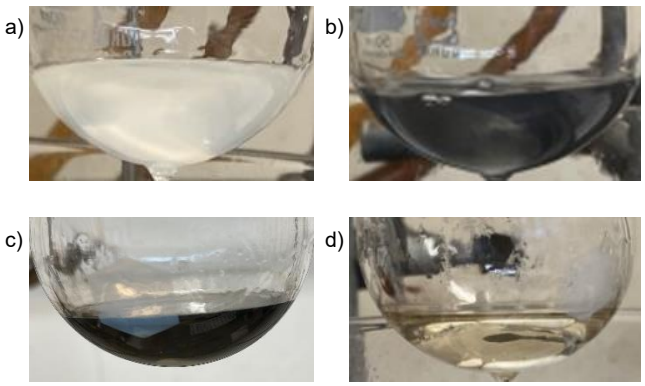

Figure A 3.9. Photo of reaction flasks after 24 hours of esterification reactivity of phthalic anhydride with 2-ethylhexanol at 180 °C for (a) TBT, (b) BiNeo, (c) TBT with BiNeo added separately, and (d) 2TBT:BiNeo premixed.

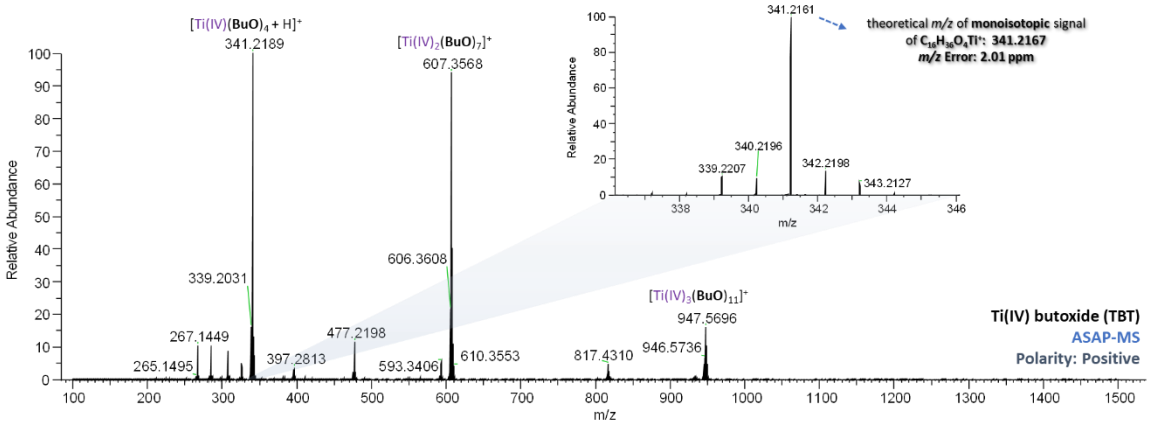

Figure A 3.10. ASAP-MS spectra of tetrabutyl titanate (TBT) with selected labelled peaks with matched molecular formulas. Zoomed in window showing major peak for TBT-generated ions.

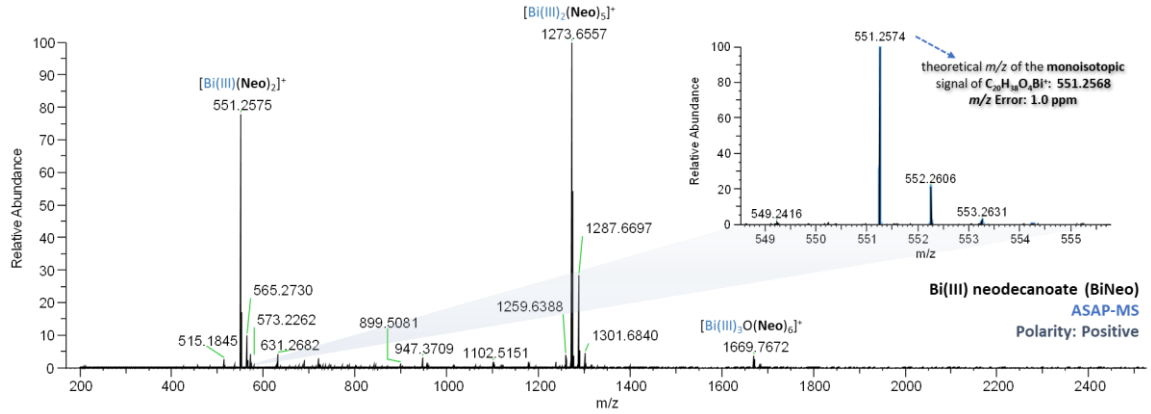

Figure A 3.11. ASAP-MS spectra of bismuth neodecanoate (BiNeo) with selected labelled peaks with matched molecular formulas. Zoomed in window showing major peak for BiNeo-generated ions.

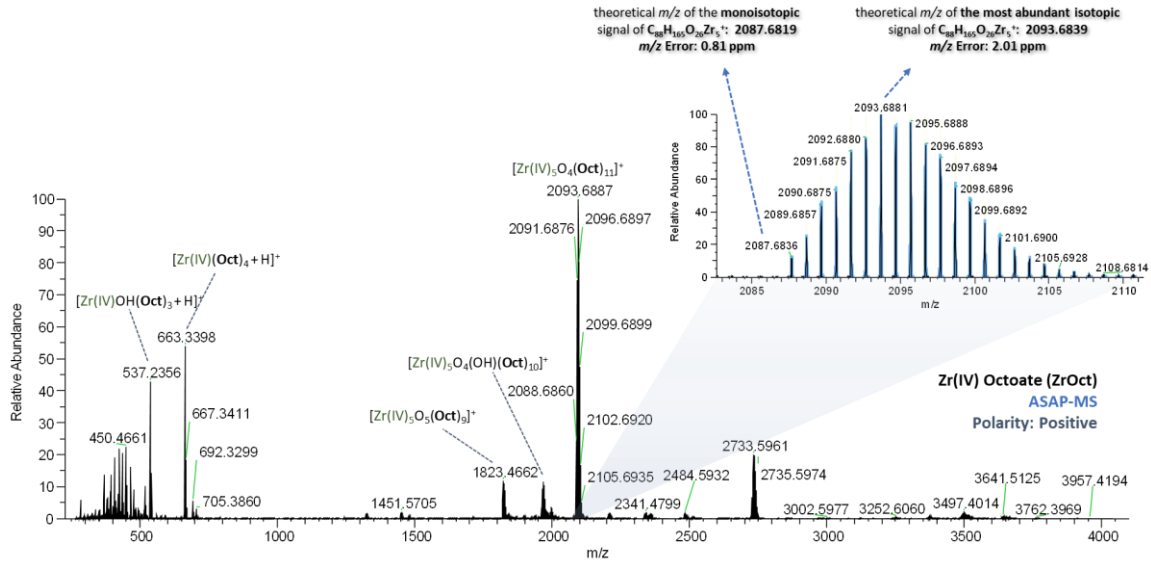

Figure A 3.12. ASAP-MS spectra of zirconium octoate (ZrOct) with selected labelled peaks with matched molecular formulas. Zoomed in window showing major peak for ZrOct-generated ions.

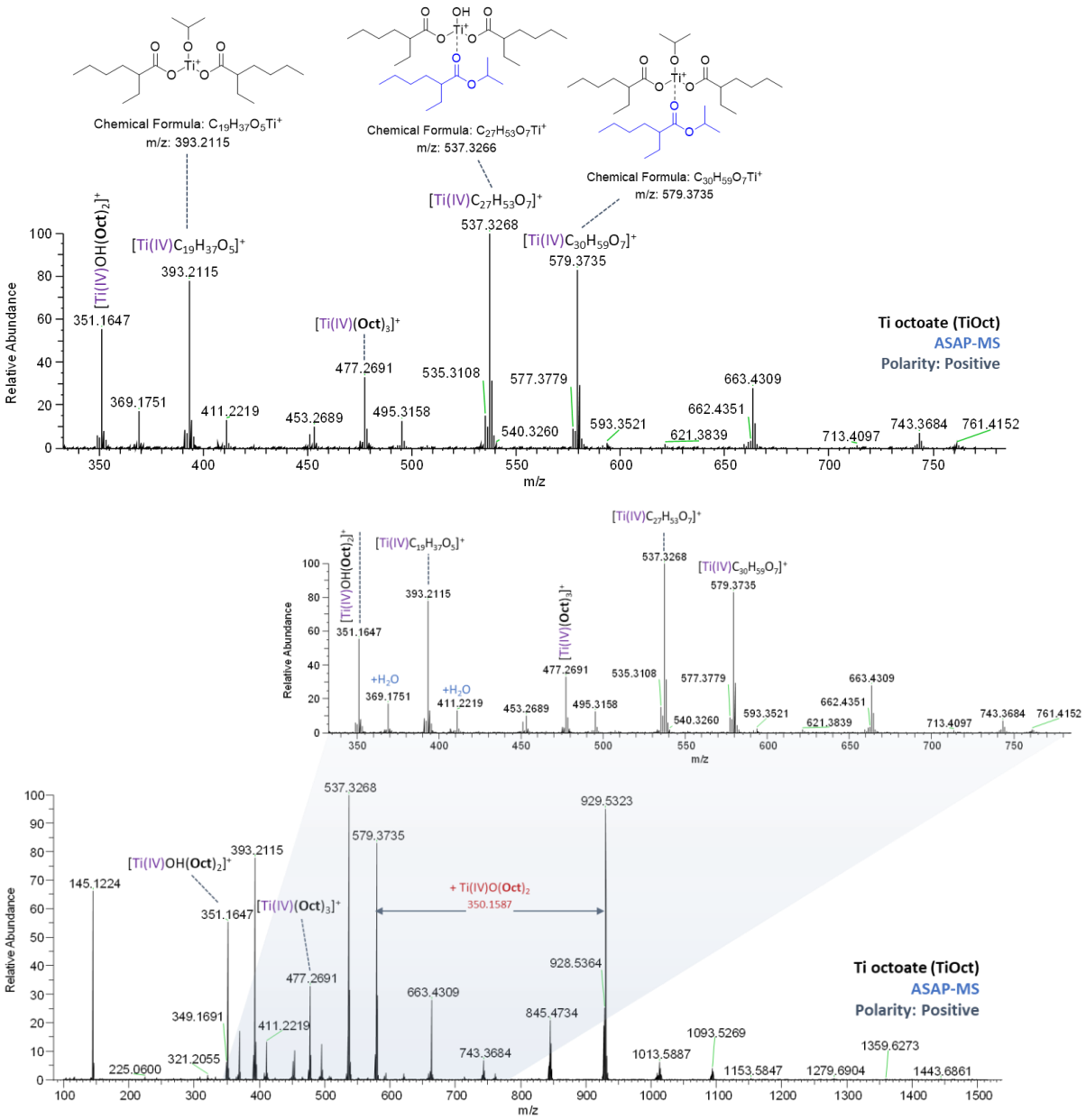

Figure A 3.13. a) ASAP-MS spectra of titanium octoate (TiOct) with selected labelled peaks with matched molecular formulas. Zoomed in window showing major peak for TiOct-generated ions. b) Zoomed in spectra for TiOct with molecular structures assigned to show the products of the esterification of ligands have occurred as well as isopropyl impurities from the manufacturer.

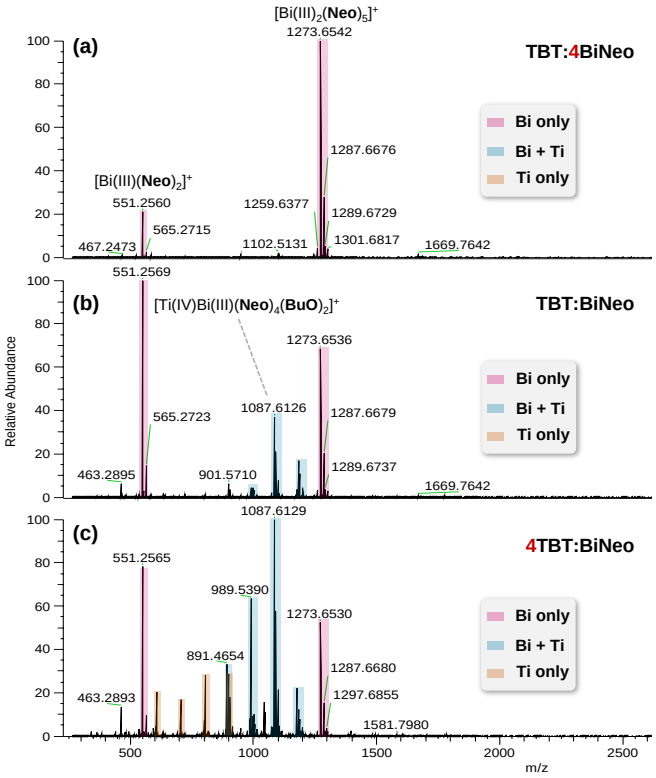

Figure A 3.14. ASAP-MS spectra of different ratios of TBT and BiNeo. Peaks with only Bi, Bi + Ti, and only Ti are highlighted, showing more Bi + Ti clusters are present in 4TBT:BiNeo than other mixing ratios.

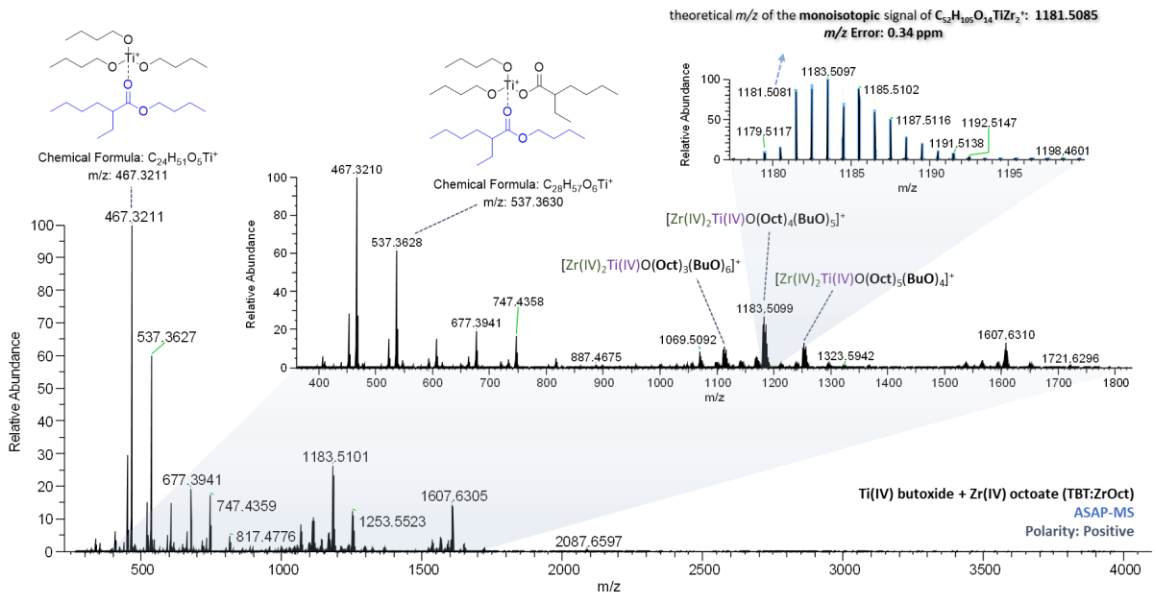

Figure A 3.15. ASAP-MS spectra of tetrabutyl titanate with zirconium octoate (TBT:ZrOct) with selected labelled peaks with matched molecular formulas. Zoomed in window showing major peak for TBT:ZrOct-generated ions. Molecular structures are provided for species formed via esterification of ligands prior to reaching the mass analyzer.

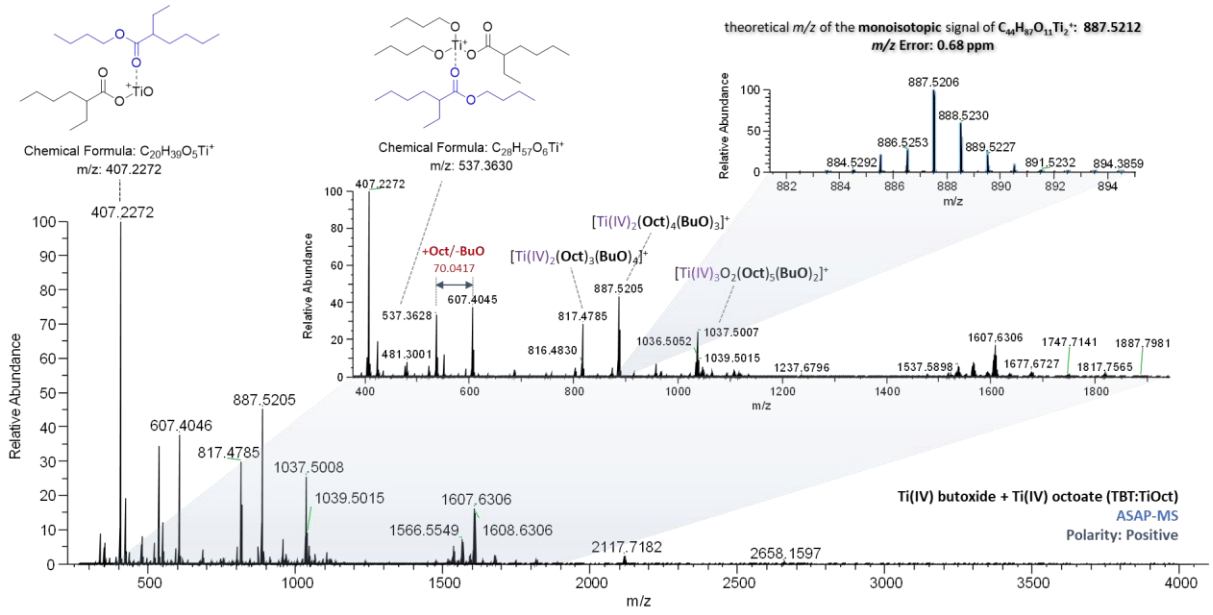

Figure A 3.16. ASAP-MS spectra of tetrabutyl titanate with titanium octoate (TBT:TiOct) with selected labelled peaks with matched molecular formulas. Zoomed in window showing major peak for TBT:TiOct-generated ions. Molecular structures are provided for species formed via esterification of ligands prior to reaching the mass analyzer.

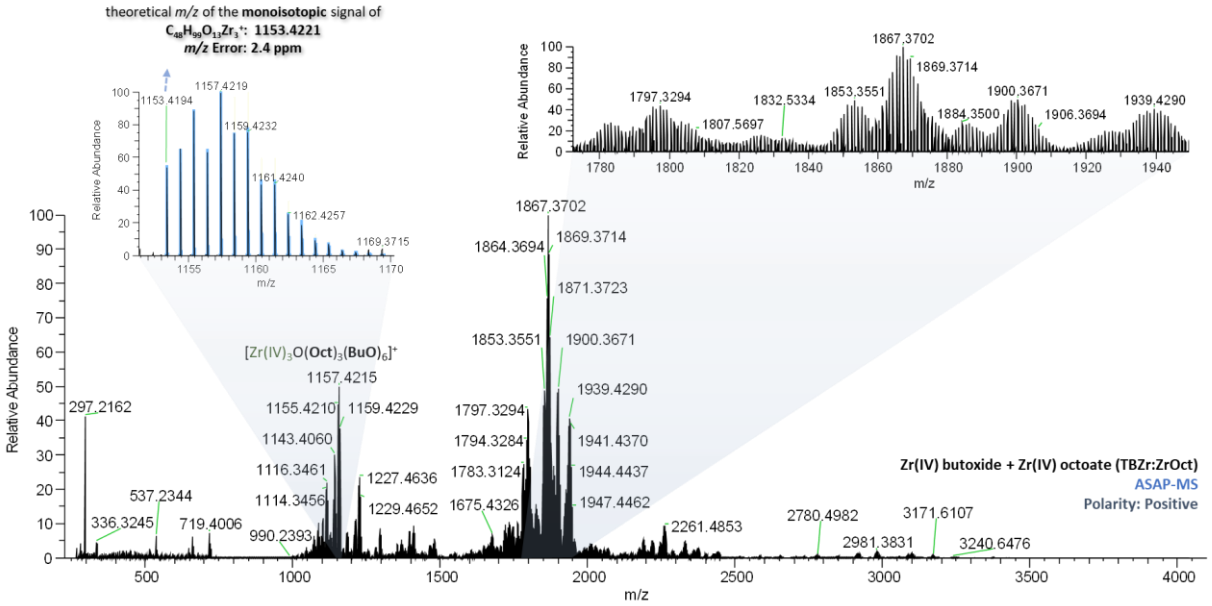

Figure A 3.17. ASAP-MS spectra of tetrabutyl zirconate with zirconium octoate (TBZr:ZrOct) with selected labelled peaks with matched molecular formulas. Zoomed in window showing major peak region for TBZr:ZrOct-generated ions.

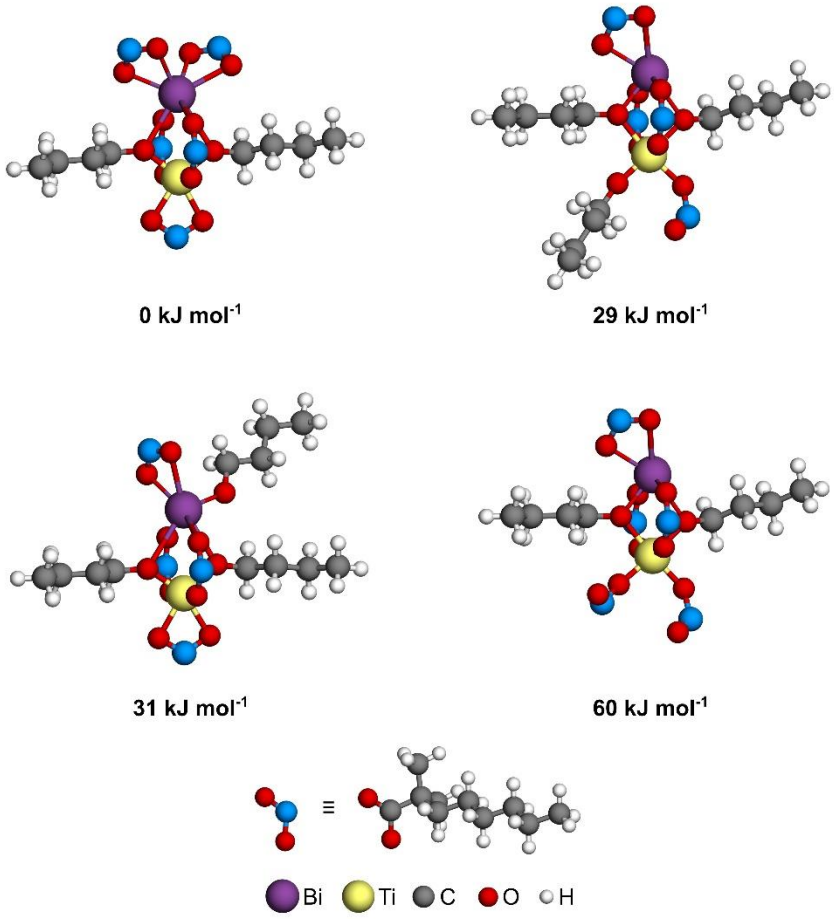

Figure A 3.18. DFT computed energies of different ligand arrangements around predicted catalyst composition.

A4. Chapter 4 Appendix

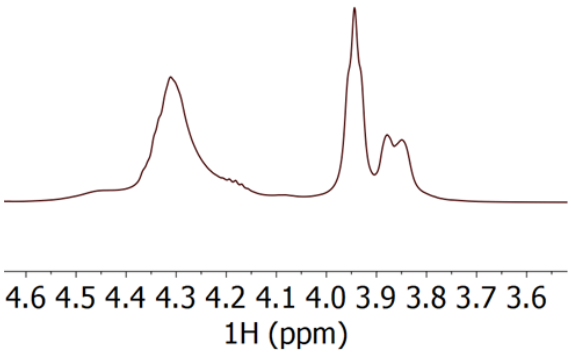

Figure A 4.1. VT ^{1}H NMR spectrum of 1:1 mixture of 2-ethylhexanol and TBT collected at -20 °C zoomed into α-CH_2 region. Triplet at 3.95 ppm is butoxy-based, doublet at 3.87 ppm is 2-ethylhexyl-based.

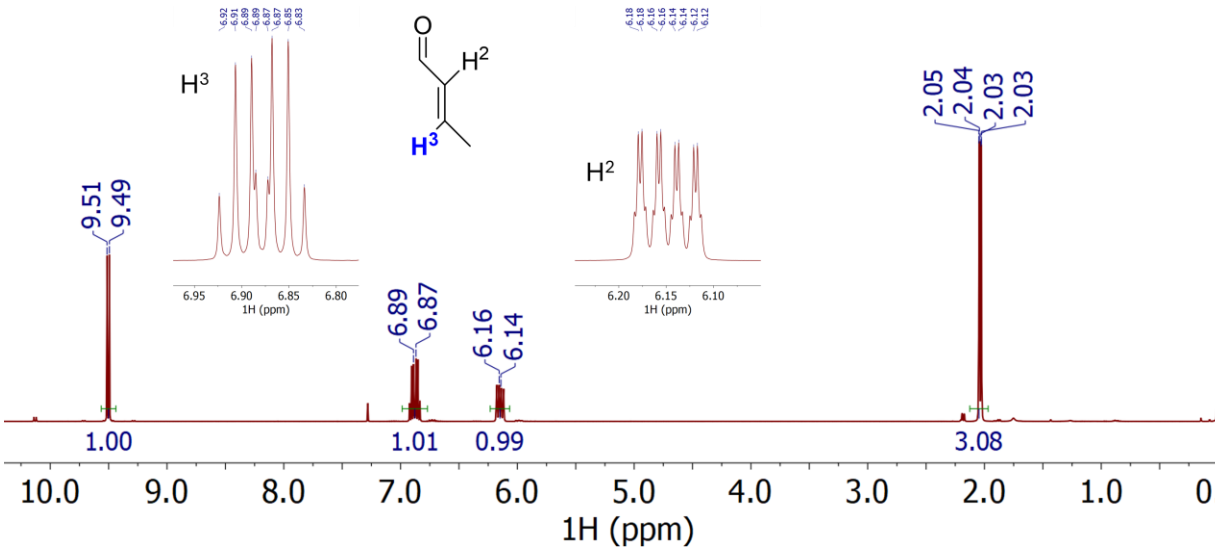

Figure A 4.2. ^{1}H NMR spectrum of trans-crotonaldehyde. Signal labelled H^3 is signal of interest for Child's method measurements.

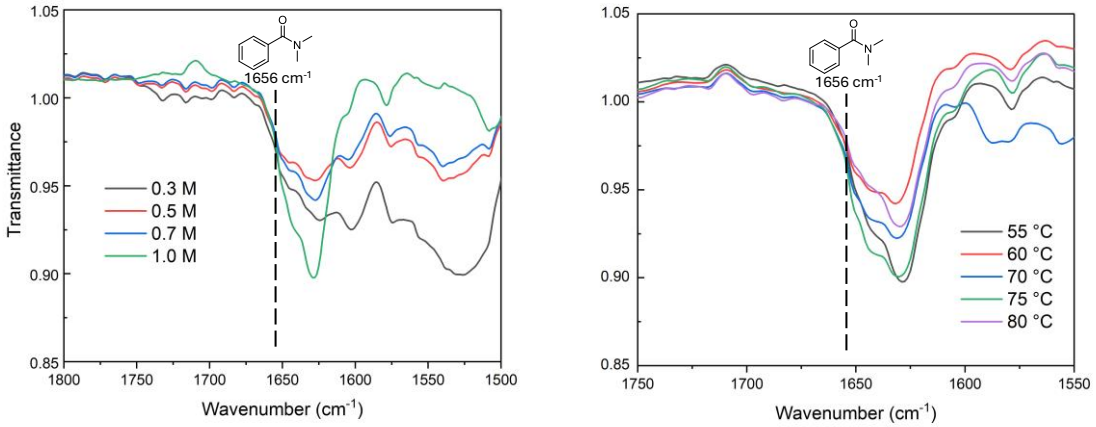

Figure A 4.3. ATR-FTIR spectra of TBT mixed with N,N'-dimethylbenzamide. Dotted line indicates peak wavelength of only NNDMB ν(C=O). (a) concentration dependence, (b) premixing temperature.

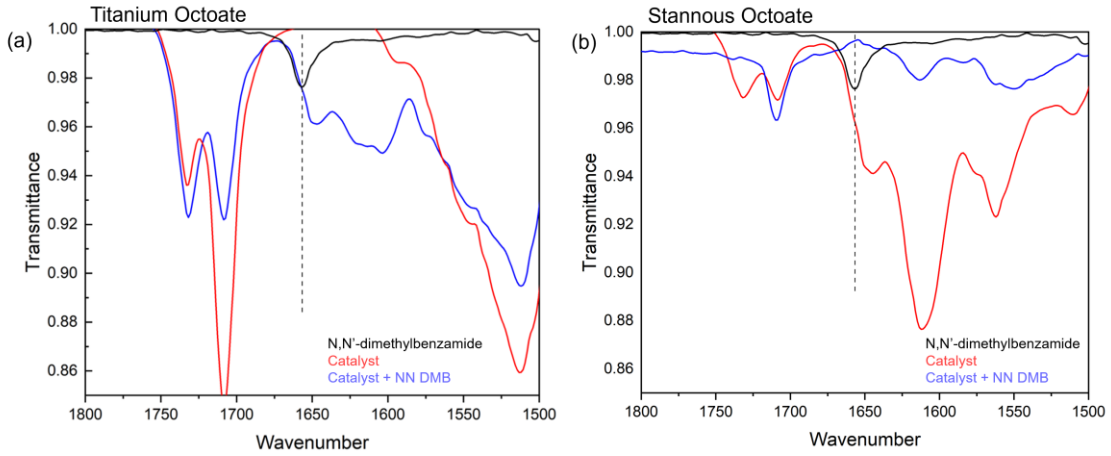

Figure A 4.4. ATR-FTIR spectra of 1.0 M a) TiOct or b) SnOct catalysts with 1.0 M N,N'-dimethylbenzamide dissolved in hexanes. Dotted line indicates peak wavelength of only NNDMB *ν*(C=O). Mixture premixed for 10 minutes at 50 °C.

A5. Chapter 5 Appendix

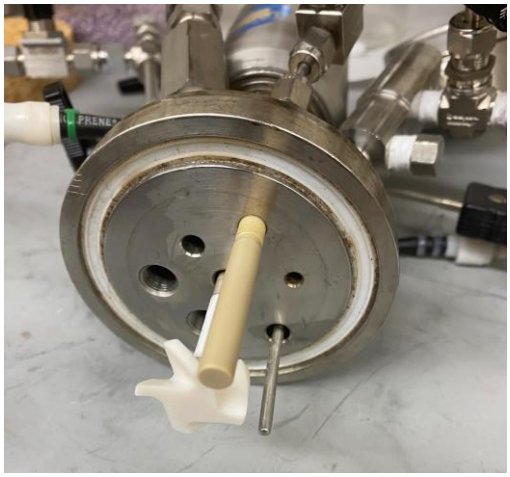

Figure A 5.1. Picture of top part of autoclave reactor (left) showing Teflon stirrer, thermocouple, and optional Teflon sampling/dip tube with pinhole sampling port. Right picture shows autoclave reactor mounted in heating mantel. The top attachments include pressure gauge with gas addition/removal quick connect needle valve, thermocouple plug, catalyst addition (under pressure) valving, sampling (under pressure) tube, and stirrer magnet going counterclockwise from the left. For ambient pressure experiments the catalyst addition valving is replaced by a 11 mm septum fitted into 1/2” tubing connected via SwageLok fittings.

A6. Journal Cover Images

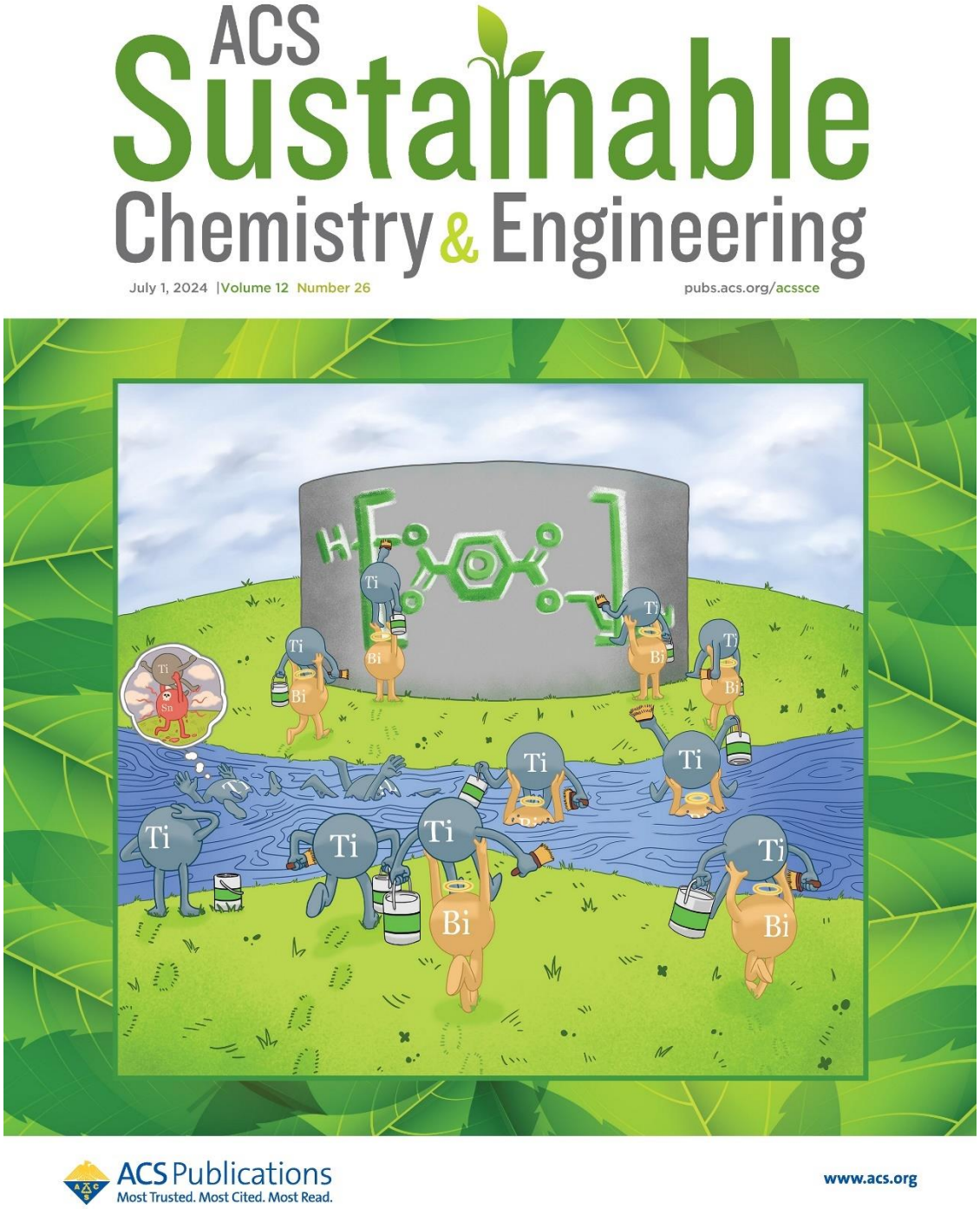

A7. List of Works from this Thesis

Published Works:

1. **Jacob H. Jansen**, Destiny Mathews, Alexander Marrione, Jalianet Román-Matías, Abdullah Al Abdulghani, Adam B. Powell, Sarah E. Specht, William Keown, Selim Garislioglu, Ive Hermans. "Sustainable and Stable Esterification Catalysts Made from Titanium-Bismuth Clusters" *ACS Sustainable Chemistry & Engineering,* **2024**, 12, 26, 9612-9619. *(In Collaboration with PPG)*

2. Son Dong, Taekyung Ryu, Collin Oi, Jiayang Wu, Natalie R. Altvater, Ryan Hagmann, Zahra Alikhani, Edgard A. Lebrón-Rodríguez, **Jacob H. Jansen**, et. al. "Catalytic Conversion of Post-Consumer Recycled High-Density Polyethylene Oil over Zn-impregnated ZSM-5 Catalysts" *Chemical Engineering Journal*, **2024**, 482, 148889.

3. Abdullah Al Abdulghani, Edgar Turizo-Pinilla, Maria Fabregas-Angulo, Ryan Hagmann, Faysal Ibrahim, **Jacob H. Jansen**, et. al. "Realizing Synergy Between Cu, Ga, and Zr for Selective CO_2 Hydrogenation to Methanol" *Applied Catalysis B: Environment and Energy,* **2024**, 355, 124198.

4. Melissa C. Cendejas, Oscar A. Paredes Mellone, Unni Kurumbail, Zisheng Zhang, **Jacob H. Jansen**, et. al. "Tracking Active Phase Behavior on Boron Nitride during the Oxidative Dehydrogenation of Propane Using Operando X-ray Raman Spectroscopy" *Journal of the American Chemical Society*, **2023**, 145, 47, 25686-25695.

5. **Jacob H. Jansen**, Adam B. Powell, Sarah E. Specht, Selim Garislioglu, Ive Hermans. "Understanding the Structure and Reactivity of Mixed Titanium(IV) Alkoxides and Tin(II)/(IV) Carboxylates as Esterification Catalysts" *ACS Sustainable Chemistry & Engineering,* **2022**, 10, 7, 2484-2493. *(In Collaboration with PPG)*

6. Lesli O. Mark, Rick W. Dorn, William P. McDermott, Theodore O. Agbi, Natalie R. Altvater, **Jacob H. Jansen,** et. al. "Highly Selective Carbon-Supported Boron for Oxidative Dehydrogenation of Propane" *ChemCatChem*, **2021**, 13, 16, 3611-3618.

Unpublished Works:

1. **Jacob H. Jansen**, Jose Yamil Adorno, Arianna Alirez, Alexander Marrione, Oscar Li, Ive Hermans. "Binuclear Titanium-Bismuth Catalyst for Polyethylene terephthalate Glycolysis". (To be submitted)

Submitted Patents:

1. **Jacob H. Jansen**, Adam B. Powell, Sarah E. Specht, Ive Hermans. A Catalyst Composition for Improving Time to Reach High Esterification Conversion of Carboxylic Acids/Anhydrides. December 21, 2023. (PCT/US23/85382). *Pending.*